

(NASA-TM-81295) SIMULATION STUDY OF TWO  
VTOL CONTROL/DISPLAY SYSTEMS IN IMC APPROACH  
AND LANDING (NASA) 90 p HC A05/MF A01

N81-30136

CSCD 01C

Unclass

63/08

27225

---

# Simulation Study of Two VTOL Control/Display Systems in IMC Approach and Landing

---

Vernon K. Merrick

---

August 1981



---

# **Simulation Study of Two VTOL Control/Display Systems in IMC Approach and Landing**

---

Vernon K. Merrick, Ames Research Center, Moffett Field, California



National Aeronautics and  
Space Administration

**Ames Research Center**  
Moffett Field, California 94035

---

# TABLE OF CONTENTS

	<u>Page</u>
SUMMARY . . . . .	1
INTRODUCTION . . . . .	1
APPROACH AND LANDING TASK . . . . .	2
TYPE 1 CONTROL/DISPLAY SYSTEM . . . . .	3
TYPE 2 CONTROL/DISPLAY SYSTEM . . . . .	9
Longitudinal (Thrust-Vector-Angle) Flight Director . . . . .	13
Vertical (Throttle) Flight Director . . . . .	19
Hover Flight Director . . . . .	22
Lateral Flight Director . . . . .	24
OPERATIONAL DESCRIPTION OF CONTROL/DISPLAY SYSTEMS . . . . .	24
Typical Landing Using Type 1 System . . . . .	24
Typical Landing Using Type 2 System . . . . .	28
SIMULATION . . . . .	29
Simulation Models . . . . .	29
Scope of the Simulation . . . . .	30
Simulation Equipment . . . . .	36
Pilot Experience . . . . .	36
SIMULATION RESULTS AND DISCUSSION . . . . .	40
Operational Acceptability of the Task . . . . .	40
Pilots' Evaluations . . . . .	41
Transition (Type 1 system; AV-8A Harrier) . . . . .	41
Transition (Type 2 system; AV-8A Harrier) . . . . .	41
Landing (Type 1 system; lift-fan transport) . . . . .	43
Landing (Type 1 system; AV-8A Harrier) . . . . .	43
Landing (Type 2 system; AV-8A Harrier) . . . . .	46
Task Performance Parameters . . . . .	47
Transition . . . . .	47
Landing . . . . .	51
Evaluation of the HUD Format . . . . .	54
Attitudes . . . . .	56
Position . . . . .	56
Velocity and acceleration . . . . .	57
Evaluation of Pilot Control Modes . . . . .	57
Evaluation of the Flight Directors . . . . .	58
Evaluation of the Pilot's Controls . . . . .	59
Simulation Equipment Limitations . . . . .	60
Modeling Fidelity . . . . .	67
CONCLUSIONS . . . . .	67

	<u>Page</u>
APPENDIX A - REFERENCE HOVER POINT EQUATIONS . . . . .	69
APPENDIX B - AV-8A HARRIER CONTROL SYSTEM MODIFICATIONS . . . . .	74
APPENDIX C - FSAA MOTION DRIVE LOGIC . . . . .	81
REFERENCES . . . . .	86

SIMULATION STUDY OF TWO VTOL CONTROL/DISPLAY  
SYSTEMS IN IMC APPROACH AND LANDING

Vernon K. Merrick

Ames Research Center

SUMMARY

Two control/display systems, differing in overall complexity but both designed expressly for VTOL approaches to and landings on ships in IMC were tested using the Ames Flight Simulator for Advanced Aircraft (FSAA). Both systems had full attitude command; the more complex system (Type 1) also had translational velocity command. The systems were applied to existing models of a VTOL lift-fan transport and the AV-8A Harrier. Simulated landings were made on a model of a DD963 Spruance-class destroyer. It was concluded that acceptable transitions and vertical landings can be performed, using the Type 1 system, in free-air turbulence up to 2.25 m/sec and sea state 6 and, using the Type 2 system, in free-air turbulence up to 1.5 m/sec and sea state 4.

INTRODUCTION

An important component in the assessment of the cost and maintainability of VTOL aircraft requires at least a broad answer to the question: What is the degree of flight control and display complexity necessary to meet specific operational requirements? Contributions toward answering this question, for requirements relevant to the task of instrument meteorological conditions (IMC) approach and vertical landing on both fixed and moving platforms, have already been made. Of note are the design and simulation of advanced VTOL flight controllers at Ames Research Center (refs. 1, 2) and the flight test and simulation work sponsored by the U.S. Navy (refs. 3-5).

Because of the vast number of variables involved, a complete answer to the above question, even in the form restricted to the approach and landing, would be a formidable task involving large resources. A less complete answer, and one that would require fewer resources, may be obtained through the straightforward approach of (1) designing a series of control and display systems, each consistent with a different level of complexity; (2) applying those systems, in turn, to one or more VTOL models; and (3) testing the results on a piloted simulator. The term "level of complexity" used here relates to the number and type of the major control and display features that influence the degree of stability and control and, therefore, the handling qualities. The ordering judgment is qualitative, based on what is perceived to be a consensus on the number and type of instruments, electronics, and mechanisms required to implement each control and display system. This simple approach is the one currently adopted at Ames. Because it omits many detailed

considerations associated with variations within a given control and display system concept, however, it can provide only a broad answer. The approach also runs the risk of missing important results. Nonetheless, the exploratory nature of the approach is appropriate at the present stage of VTOL development.

In this paper two control/display designs are considered. The first, designated Type 1, is that described and tested in references 1 and 2. This system employs full-authority attitude and flightpath flight controllers to control all degrees of freedom; by today's standards, it is a complex system. A simulation evaluation (ref. 2) indicated that an aircraft equipped with a Type 1 system could be landed, in zero visibility conditions, on a small ship operating in sea state 4. The pilot rating for the task was 3.5; however, it should be noted that potentially important aerodynamic effects of the ship on the aircraft were not represented in the tests. The second system, designated Type 2, is derived from the first by removing the flightpath flight controller and reverting to power and thrust vector angle for longitudinal flightpath control. In complexity, this system may be regarded as being about midway between the Type 1 system and a system employing a minimum of stability augmentation (typified by that used on the Harrier AV-8A).

This paper starts with a definition of the approach and landing task, followed by a brief review of the Type 1 system and a more detailed technical description of the Type 2 system. To provide a more complete understanding of how the various elements of control and display work together during the various segments of the approach and landing, a description of both systems is given from an operational viewpoint.

Both types of control/display systems have been incorporated into models of the AV-8A Harrier (ref. 6) and the MCAIR Model 253 lift-fan V/STOL transport (ref. 1). A piloted simulation has been carried out on the Ames FSAA to obtain a performance comparison for IMC approach to and landing on a destroyer operating in various sea states. An important difference between these tests and those reported in reference 2 is the inclusion of a model of ship air-wake turbulence (ref. 7). The simulation is described and the primary results are given and discussed.

## APPROACH AND LANDING TASK

The approach and landing may be regarded as taking place in three distinct phases: transition, hover maneuvers, and final descent. The beginning and end of each of these phases are clearly defined.

The transition starts at the point where conversion from conventional flight to powered-lift flight is complete. For some aircraft (Dornier Do 31, VAK 191) the conversion process involves starting additional lift propulsion units. The point at which all the propulsion units are in operation and ganged together is defined as the start of transition. For aircraft that do not use additional lift-propulsion units (Harrier), the start of transition is defined as the point where the thrust is first deflected on the approach. The

transition ends at the initial station-keeping point, which is a point at rest relative to the mean ship position (position when the ship roll, pitch, yaw, heave, surge, and sway are all zero). The initial station-keeping point is usually located such that some degree of overshoot is allowed without danger of colliding with the ship.

The approach path and velocity schedule during the transition are not arbitrary. The control/display systems discussed in this report were designed to be most efficient for flying the approach paths and velocity schedules shown in figure 1. The longitudinal deceleration during these transitions is essentially constant. The regions AB and CH shown in figure 1, in which the pilot starts and ends the deceleration, are exaggerated; each takes place in only 4 sec in a total deceleration period of about 70 sec. The equations defining these reference approach paths and velocity schedules are given in appendix E of reference 1.

The hover maneuvers take place at constant altitude and involve translating the aircraft from the initial station-keeping point to the final station-keeping point. The latter point is directly over the mean position of the desired touchdown point on the ship's deck. Since the Type 2 control/display system uses a hover flight director, a reference hover point must be defined that translates, in some predetermined way, from the initial to the final station-keeping points. The equations defining the kinematics of the reference hover point are given in appendix A.

The vertical descent phase starts at the final station-keeping point and ends at touchdown. Since the Type 2 control/display system uses a vertical flight director during this phase, a reference hover point must be defined that descends, in some predetermined way, from the final station-keeping point to the touchdown point. The equations defining the appropriate kinematics are also given in appendix A.

It is important to note that these various phases of the approach and landing have special significance in the control/display design in that each phase may involve different control, display, and flight director elements, with the switch from one to the next being made either automatically or manually.

#### TYPE 1 CONTROL/DISPLAY SYSTEM

The Type 1 system is described in detail in references 1 and 2, and a summary of the primary features of the system is given in figure 2. State rate feedback implicit model following (SRFIMF) flight controllers (ref. 1) are used throughout. The pilot control modes provided by the attitude and flightpath flight controllers are shown in tables 1 and 2, respectively, and the corresponding control sensitivities and second-order control characteristics are shown in tables 3 and 4. A breakdown of the head-up display (HUD) into the attitude, transition, and terminal subdisplays is shown in figure 3.

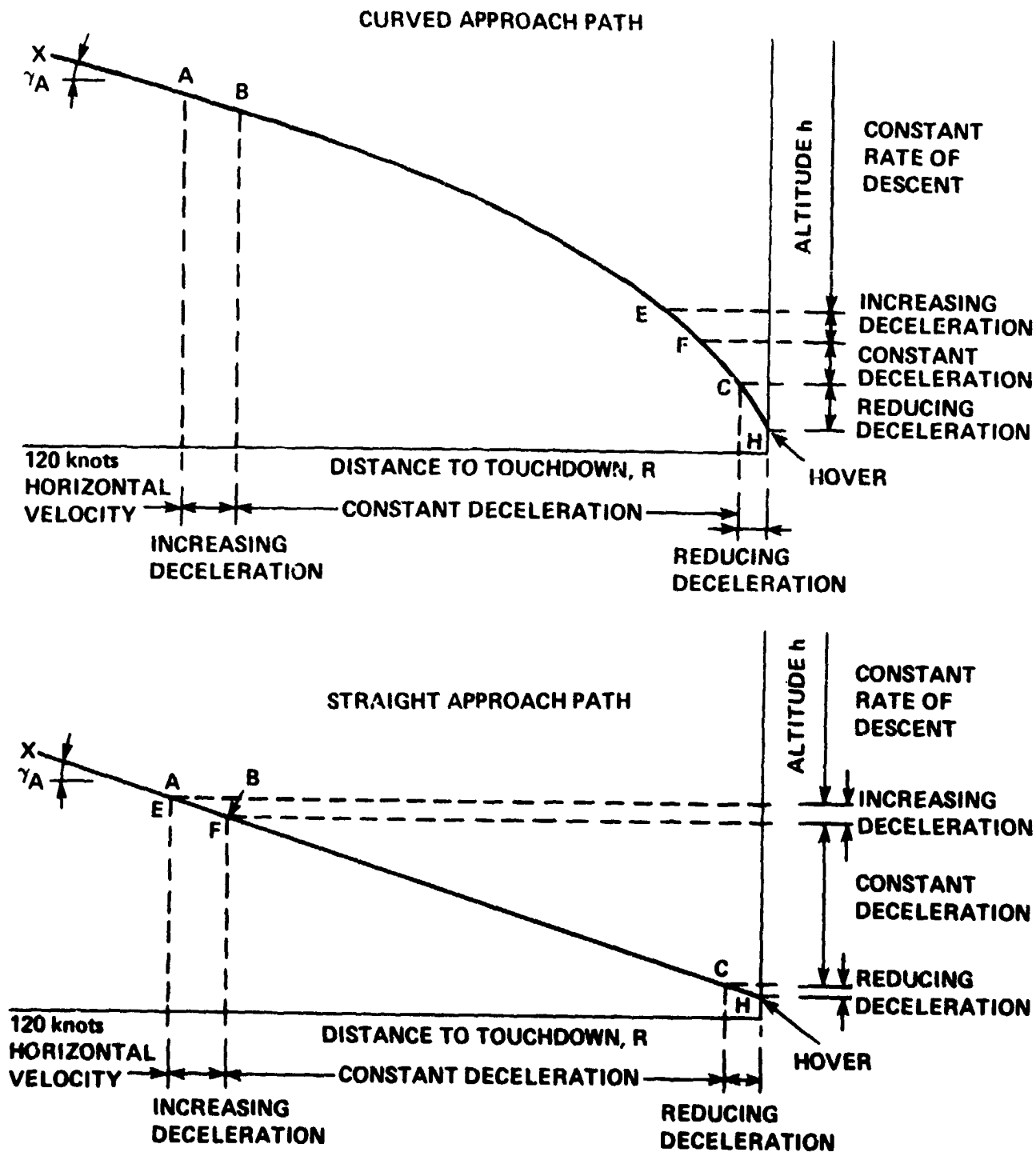
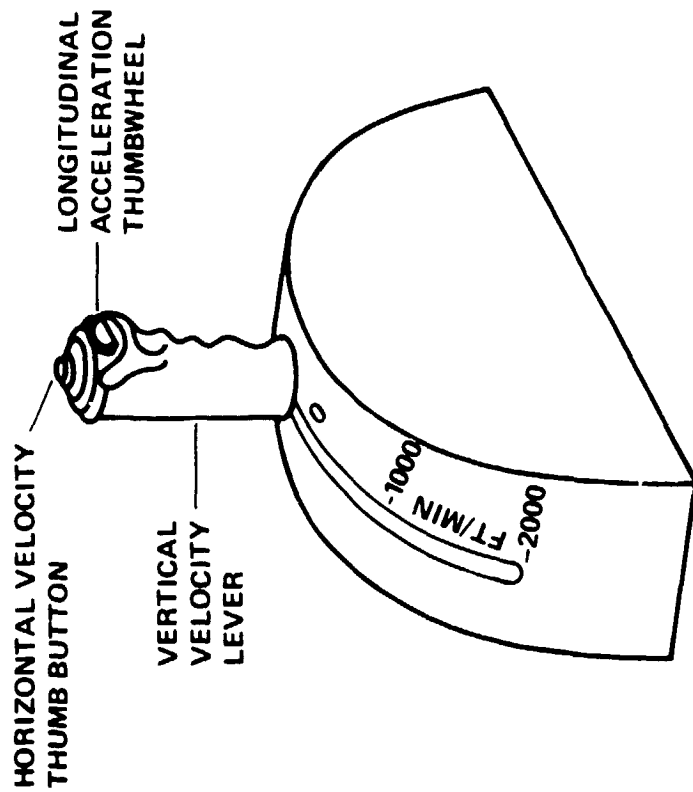
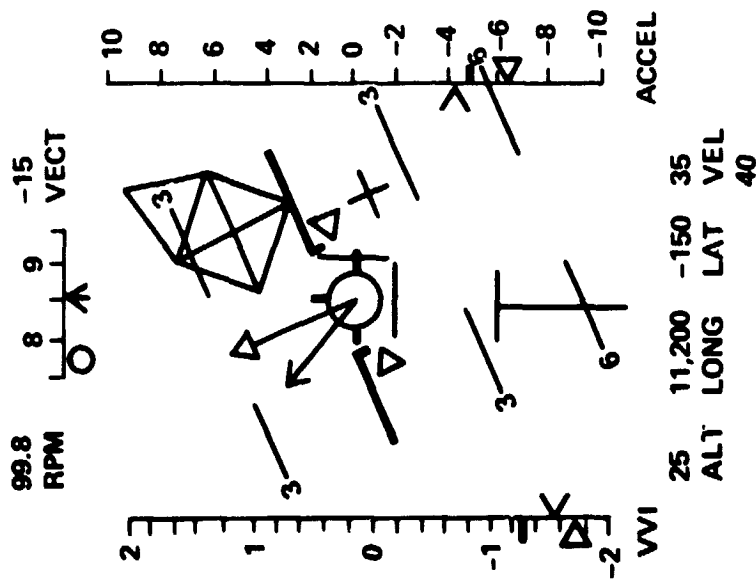


Figure 1.- Types of VTOL approach path.





### SYSTEM FEATURES

- ATTITUDE COMMAND
- LONGITUDINAL ACCELERATION AND VERTICAL VELOCITY COMMAND FOR TRANSITION
- HORIZONTAL AND VERTICAL VELOCITY COMMAND FOR HOVER AND TOUCHDOWN
- INTEGRATED ACCELERATION AND VELOCITY CONTROLS
- HUD WITH THREE-AXIS FLIGHT DIRECTOR FOR TRANSITION

Figure 2.- Velocity command system: Type 1 system.

TABLE 1.- PILOT CONTROL MODES: ATTITUDE FLIGHT CONTROLLER

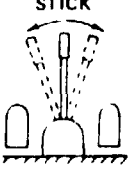

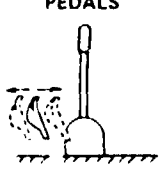
		ATTITUDE FLIGHT CONTROLLER (AFC)		
		ROLL	PITCH	YAW
				
SPEED REGIME	0-20 knots	ROLL ATTITUDE COMMAND	PITCH ATTITUDE COMMAND	YAW RATE COMMAND WITH HEADING HOLD
	20-30 knots	BLEND		BLEND
	30 knots CONVERSION SPEED (120 knots)	ROLL RATE COMMAND WITH BANK ANGLE HOLD		YAW RATE COMMAND WITH BANK ANGLE FEEDBACK

TABLE 2.- PILOT CONTROL MODES: FLIGHTPATH FLIGHT CONTROLLER

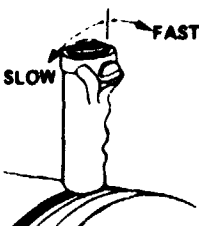
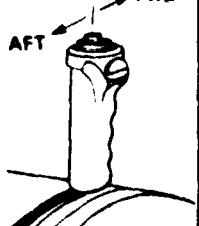
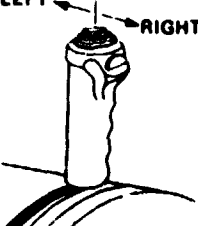
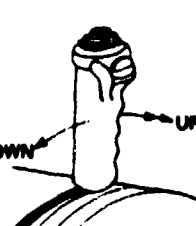
		FLIGHTPATH FLIGHT CONTROLLER (FPFC)			
		LONGITUDINAL		LATERAL	VERTICAL
					
SPEED REGIME	0-20 knots	ACCELERATION COMMAND WITH VELOCITY HOLD	VELOCITY COMMAND	VELOCITY COMMAND	VELOCITY COMMAND
	20-30 knots		PHASE OUT	PHASE OUT	
	30 knots CONVERSION SPEED (120 knots)		—	—	

TABLE 3.- ATTITUDE CONTROLLER CHARACTERISTICS

AXIS	LONGITUDINAL		LATERAL	VERTICAL
PILOT'S CONTROL	THUMB WHEEL VC LEVER	THUMB BUTTON VC LEVER	THUMB BUTTON VC LEVER	VC LEVER
	ACCELERATION COMMAND 0.043m/sec <sup>2</sup> / (0.14ft. sec <sup>2</sup> / )	VELOCITY COMMAND 0.66m. sec. N (9.7ft./sec./lb)		VELOCITY COMMAND 80m/sec/m (400ft./min./in.)
CONTROL SENSITIVITY				
CONTROL MODE FREQUENCY rad/sec		1.25		
CONTROL MODE DAMPING FACTOR		0.7		

TABLE 4.- FLIGHTPATH CONTROLLER CHARACTERISTICS

AXIS	ROLL	PITCH	YAW
PILOT'S CONTROL	STICK	STICK	PEDALS
CONTROL SENSITIVITY	ATTITUDE COMMAND 394°/m (10°/in.) RATE COMMAND 263°/sec/m (6.67°/sec/in.)	ATTITUDE COMMAND 175°/m (4.44°/in.) TRIM 4°/sec	RATE COMMAND 485°/sec/m (12.31°/sec/in.)
CONTROL MODE FREQUENCY rad/sec	2.0		
CONTROL MODE DAMPING FACTOR	0.75		

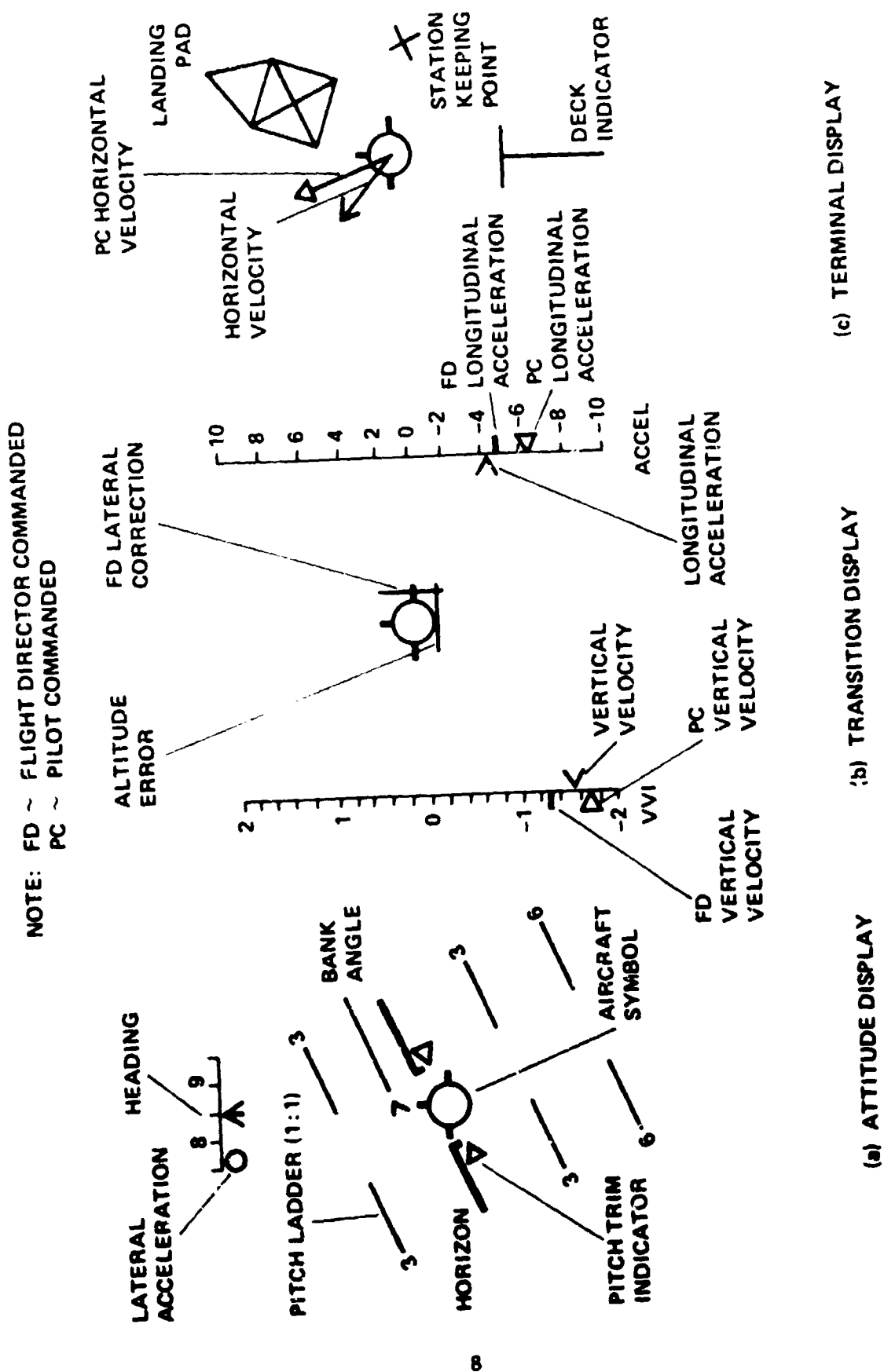


Figure 3.- HUD format breakdown for Type 1 system.

It is important to note that the Type 1 system contains a three-axis flight director (ref. 2) for the transition phase only. During the hover maneuvers and final descent phases, the HUD provides the pilot with situation information only. A flight director summary is shown in table 5.

## TYPE 2 CONTROL/DISPLAY SYSTEM

A summary of the primary features of the Type 2 system is given in figure 4. The same attitude flight controller is used in this control/display system as in the Type 1 system, with the same pilot control modes and control characteristics (tables 1 and 3). A flightpath flight controller is not provided in the Type 2 system, flightpath control being through the direct use of thrust magnitude and thrust vector angle. However, the management of flightpath control is integrated into a single lever arrangement (fig. 4). The thrust magnitude is controlled by the pilot with a conventional power lever and the thrust vector angle with a switch mounted on the side of the power lever. This switch enables the pilot to rotate the thrust vector forward or aft, at a fixed predetermined rate, depending on the scheduled transition deceleration.

In early development work on the Type 2 system, using a fixed-base simulator, the possibility of using a thumb-wheel control (similar to that on the Type 1 system flightpath control lever shown in fig. 3) for direct command of thrust vector angle, was investigated. This approach was soon abandoned, largely because it seemed unsafe to have such a powerful control on a small thumb wheel.

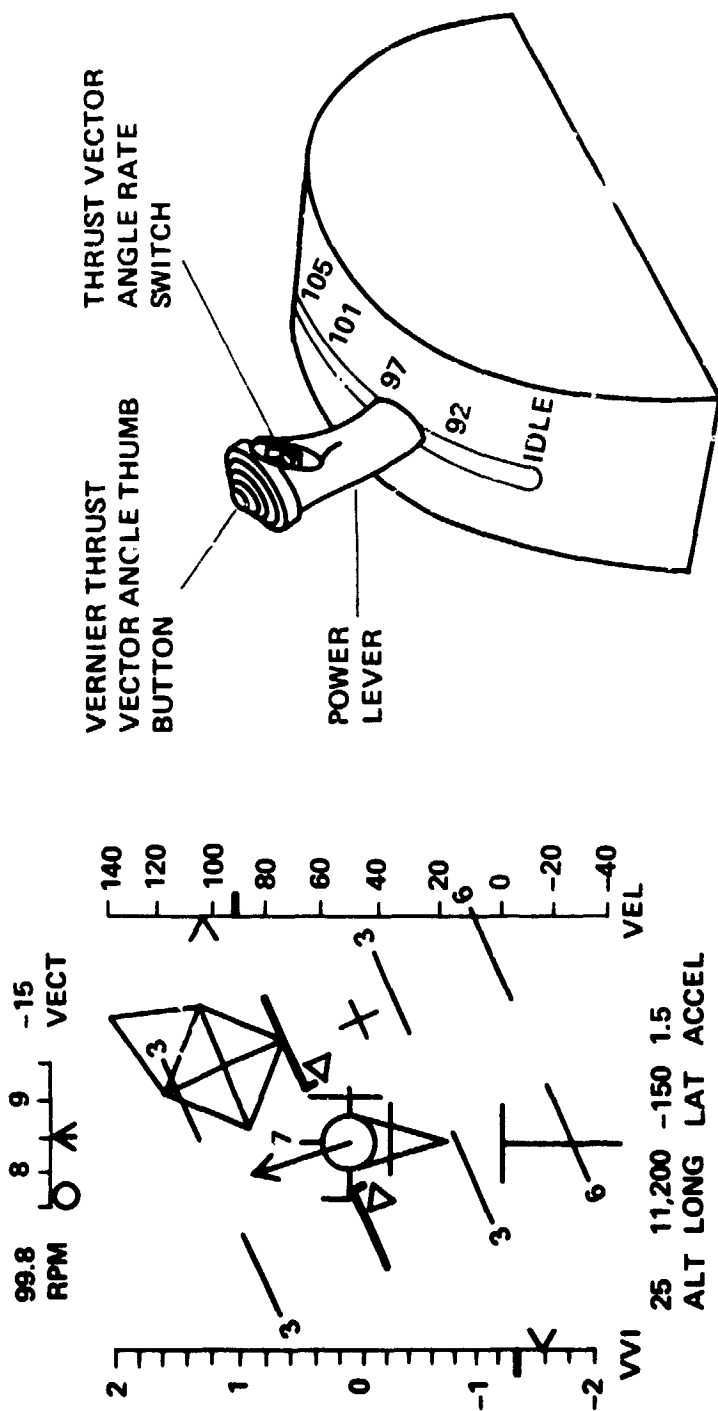
However, although the use of thrust-vector-angle rate command appears to be a safer approach, and from a pilot workload viewpoint may be even desirable during transition, it is decidedly inferior to the thrust-vector-angle command for precise longitudinal positioning in hover. This is why a thumb button was provided; it was located on top of the power lever, and was used by the pilot to command an incremental thrust vector angle (proportional to thumb pressure) up to limits of  $\pm 10^\circ$ . The use of thrust-vector-angle rate command during transition and thrust-vector-angle command during hover has certain similarities to use in the Type 1 system of longitudinal acceleration command in transition and longitudinal velocity command in hover.

The Type 2 system HUD format is shown in detail in figure 5. As with the Type 1 system HUD, this format is designed with close attention to the method of control used. The most notable difference between the Type 1 and Type 2 HUD formats is that the longitudinal acceleration scale, on the right-hand side of the Type 1 HUD, is replaced by a longitudinal velocity scale. Other, less significant differences will become evident during the discussion of the operational use of the two systems.

It can be seen from the flight director summary (table 5) that unlike the Type 1 system, the Type 2 system provides the pilot with a three-axis flight director for use in hover maneuvers and during final descent. The need for

TABLE 5.- FLIGHT DIRECTOR SUMMARY

Approach and landing phase	Translational degree of freedom	Type 1 system		Type 2 system	
		Flight director	Control method	Flight director	Control method
Transition	Longitudinal	Yes	Longitudinal acceleration	Yes	Constant vector-angle rate
	Lateral	Yes	Roll rate	Yes	Roll rate
	Vertical	Yes	Vertical velocity	Yes	Power
Hover maneuvers and final descent	Longitudinal	No	Longitudinal velocity	Yes	Pitch-attitude or thrust-vector angle
	Lateral	No	Lateral velocity	Yes	Roll attitude
	Vertical	No	Vertical velocity	Yes	Power



#### SYSTEM FEATURES

- ATTITUDE COMMAND
- THRUST AND THRUST VECTOR ANGLE RATE COMMAND
- INTEGRATED POWER AND THRUST VECTOR ANGLE RATE CONTROLS
- HUD WITH THREE-AXIS FLIGHT DIRECTORS FOR TRANSITION, HOVER MANEUVERS, AND FINAL DESCENT TO TOUCHDOWN

Figure 4.- Thrust and thrust-vector-angle rate command system: Type 2 system.

NOTE: FD ~ FLIGHT DIRECTOR COMMANDED

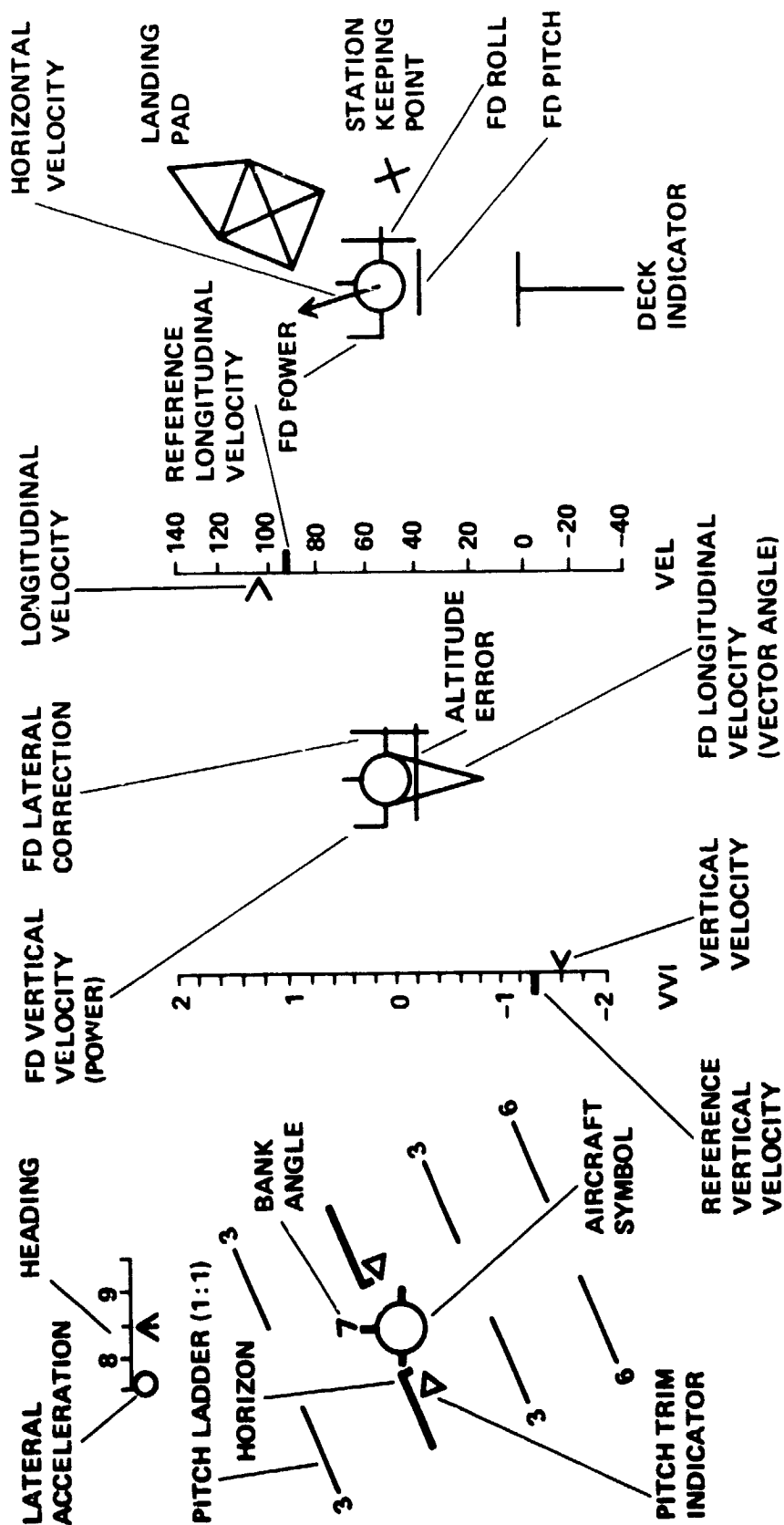


Figure 5.- HUD format breakdown for Type 2 system.



this director was established during Type 2 system development. This earlier work showed that without a suitable flight director the low translational damping of the aircraft, combined with the limited situation information provided by the HUD, made precise positioning in hover extremely difficult. Low translational damping, particularly in heave, also causes some piloting problems during transition. However, a more important problem in transition is caused by the coupling between the power and thrust-vector-angle controls (a change of vertical speed or horizontal speed, with the other held constant, requires a change of both power and thrust vector angle). This control coupling is eliminated and the translational damping augmented in the Type 1 system by the use of a flightpath flight controller. It follows that the problem of flight director design is much more critical for the Type 2 system than for the Type 1 system, because the director must provide, in addition to basic guidance information, a degree of compensation for some important handling-qualities deficiencies inherent in an aircraft equipped with a Type 2 system. In fact, the success of a Type 2 system in achieving an all-weather approach and landing capability rests largely on the effectiveness of the flight director design.

#### Longitudinal (Thrust-Vector-Angle) Flight Director

In the design of the Type 2 system it is assumed that the primary longitudinal velocity control is the thrust vector angle. Pitch attitude is not used specifically as a means of either speed or height control. Any changes of pitch attitude during transition are assumed to be for some other reason, such as improved visibility or to attain a good touchdown attitude. As stated earlier, the pilot changes the thrust vector angle, during transition, by depressing a thrust-vector-angle rate switch (TVRS) located on the power lever. The purpose of the transition longitudinal flight director is to inform the pilot when, and in which direction, to press the TVRS so that the aircraft's longitudinal velocity follows, acceptably closely, the preestablished reference velocity schedule.

Because the method employed to control velocity is discontinuous or "bang-bang," the relationship between the input - through the TVRS - and the output - as measured by aircraft velocity - is nonlinear, and it is not possible to synthesize a suitable flight director by linear theory. The problem of selecting a suitable flight director is closely related to the problem of control in relay servomechanisms. Following the lead established in relay servomechanisms, a fruitful design technique utilizes the phase plane, which, for velocity control, is defined by aircraft velocity and acceleration. The motion of the aircraft in the phase plane is simply a trajectory formed by pairs of values of velocity error and acceleration error, each pair being measured at the same instant. Time, therefore, is a parameter that varies along the phase-plane trajectory. The central problem in designing a satisfactory flight director is one of identifying suitable switching lines. These lines are defined in the phase plane and are usually, but not necessarily, independent of time. The crossing of the phase-plane trajectory and a switching line signifies a switching event that is registered on the HUD and used by the pilot as a cue for pressing the TVRS in the appropriate direction, or of releasing it.

The principal aim in selecting the switching lines is to minimize the number of times the pilot is directed to press the TVRS, while maintaining the velocity error within acceptable bounds ( $\pm 10$  knots). There appears to be no analytical technique available to achieve the desired aim. Fortunately, however, the selection of the switching lines does not appear to be too critical. The approach adopted here was to select a simple analytical form, for the switching lines, which is a function of a small number of parameters. The values of these parameters were then selected by trial and error, first using a simplified computer model representing the VTOL approach and pilot, and finally using the fixed-base piloted simulator.

The shape of the switching lines used for the Type 2 velocity flight director is shown in figure 6. The analytical form of these lines is given below.

$$\left. \begin{aligned} \text{Line AB: } \Delta V_X &= \Delta V_U - \frac{(\Delta \dot{V}_X)^2}{2g\dot{\zeta}} \\ \text{Line BC: } \Delta V_X &= \Delta V_U + \frac{(\Delta \dot{V}_X)^2}{2g\dot{\zeta}} \\ \text{Line DE: } \Delta V_X &= \Delta V_L - \frac{(\Delta \dot{V}_X)^2}{2g\dot{\zeta}} \\ \text{Line EF: } \Delta V_X &= \Delta V_L + \frac{(\Delta \dot{V}_X)^2}{2g\dot{\zeta}} \end{aligned} \right\} \quad (1)$$

where

$\Delta V_X$  longitudinal velocity error

$\Delta V_U$  upper longitudinal velocity error limit at zero acceleration error

$\Delta V_L$  lower longitudinal velocity error limit at zero acceleration error

$\Delta \dot{V}_X$  longitudinal acceleration error

$g$  acceleration due to gravity

$\dot{\zeta}$  thrust vector angle rate (fixed)

it is clear from this analytical form that there are three adjustable parameters,  $\Delta V_U$ ,  $\Delta V_L$ , and  $\dot{\zeta}$ . The switching zones are also shown in figure 6. A typical phase-plane trajectory is shown in figure 7, and the time variation of the variables involved is shown in figure 8. This trajectory was generated using a digital computer programmed to represent a model of the Harrier and a pilot. The trajectory corresponds to a decelerating transition along a

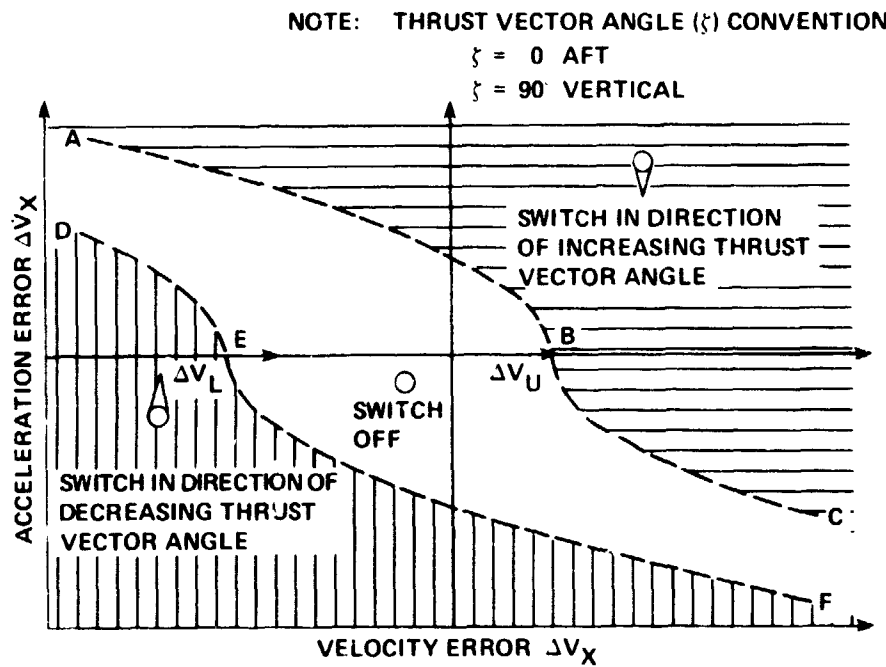


Figure 6.- Longitudinal velocity flight director switching diagram.

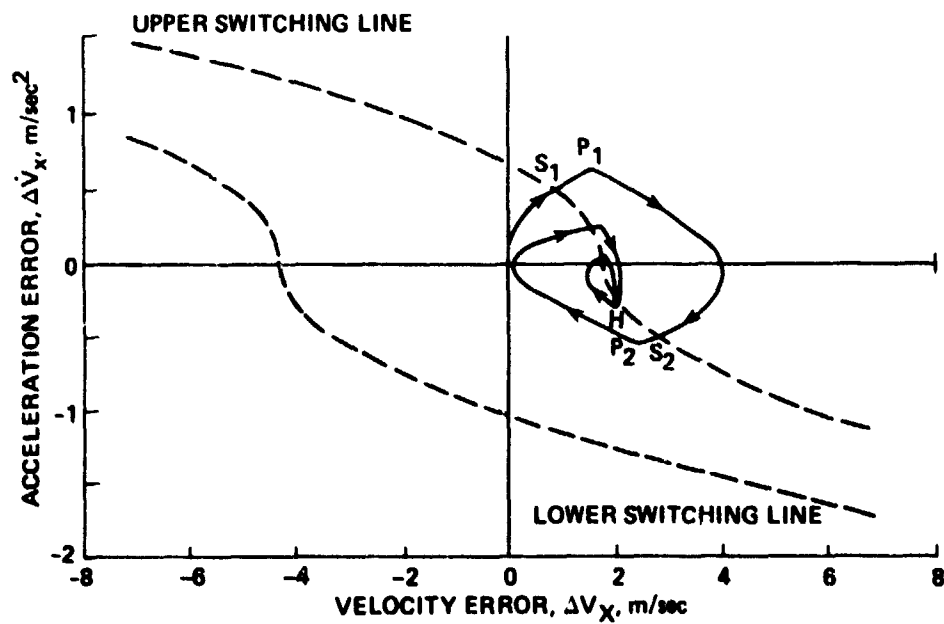


Figure 7.- Typical transition phase plane trajectory.

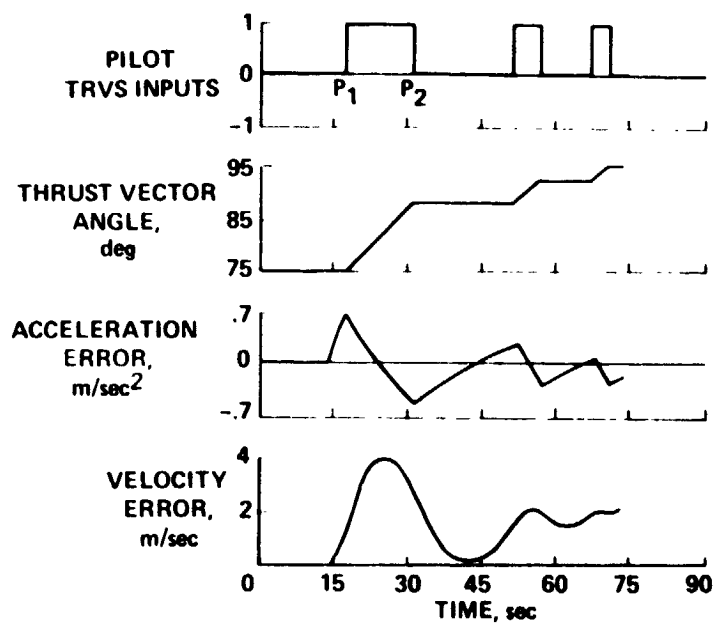


Figure 8.- Time variation of longitudinal parameters in typical transition.

straight,  $6^\circ$  approach path, starting at 120 knots and ending at hover. The aircraft was assumed to start on the glide slope, at a speed of 120 knots. This initial condition corresponds to the origin of figure 7. The phase-plane trajectory stays at the origin until the start of the scheduled deceleration of  $0.91 \text{ m/sec}^2$  ( $3 \text{ ft/sec}^2$ ). From this point, the acceleration and velocity errors start to increase until the trajectory crosses the switching line at  $S_1$  (fig. 7). In a piloted simulation this event would be shown on the HUD. The pilot model used here contains a time lag (0.2 sec) to represent the time needed by the pilot to interpret the HUD and press the TVRS (point  $P_1$ , fig. 7). With the TVRS pressed, the thrust vector angle increases at a fixed rate (in this example  $0.75^\circ/\text{sec}$ ) and, since the aircraft's deceleration exceeds the reference deceleration, the acceleration error is reduced (figs. 7, 8). However, since the acceleration error remains positive for some time after the TVRS is pressed, the velocity error increases and reaches a maximum of about  $4 \text{ m/sec}$  ( $13.1 \text{ ft/sec}$ ). Eventually the acceleration error becomes negative, the velocity error starts to reduce, and the trajectory crosses the switching line at  $S_2$ . At this point, the HUD would indicate that the TVRS should be released, which the pilot does at  $P_2$ . After release of the TVRS, the aircraft's deceleration becomes less than the reference deceleration and the acceleration error again begins to approach zero. In this example, two more switch-and-release cycles were required before the aircraft approached a hover at point H (fig. 7). For this example, the variation of longitudinal velocity with distance to hover is shown in figure 9.

By its very nature, the velocity flight director cannot, in general, provide sufficient information to enable the pilot to reduce the velocity and acceleration to zero at hover. In the example shown, the final velocity error is  $2 \text{ m/sec}$  ( $6.6 \text{ ft/sec}$ ) and the final acceleration error is  $-0.2 \text{ m/sec}^2$  ( $-0.66 \text{ ft/sec}^2$ ) (fig. 8). When the aircraft is in the vicinity of the initial station-keeping point, the pilot switches to the hover flight director and reduces the velocity and acceleration errors to zero using the hover control modes provided.

Two further points regarding the velocity flight director should be mentioned. First, the general shape of the switching line is an important factor in reducing the number of times the pilot must press the TVRS during transition. The slope of the switching line at any point is a measure of the amount of lead information, from acceleration, that is being used. When the errors are large, the pilot is given a relatively early indication of when to press the TVRS, and this tends to reduce these errors rapidly. On the other hand, when the errors are small, the lead is reduced; although the reduction in the errors is slower, this is less important than the fact that the number of switches required is also reduced. In other words, the form of the switching line provides tight control of large errors and loose control of small errors.

The second point concerns the use of the lower switching line (fig. 7). In the example shown, the lower switching line was never crossed and all the switching occurred in the direction of increasing thrust vector angle. Although ideal, this situation is attainable only if the pilot is reasonably quick (less than 0.5 sec) to respond to the flight director. If he is slow to respond, the errors may grow and the trajectory may eventually cross the

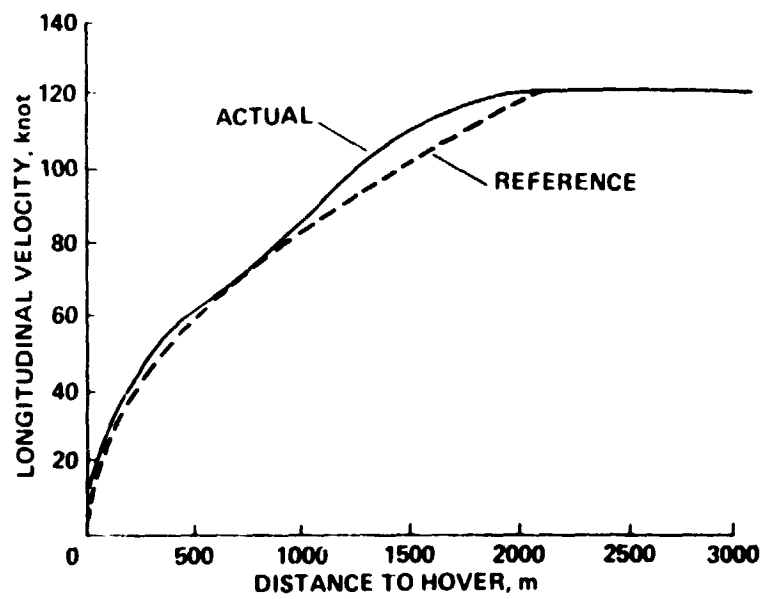


Figure 9.- Variation of longitudinal speed in typical transition.

lower switching line. This event means that the aircraft has been decelerated too much or that the speed is well below the reference speed or both. The pilot is therefore directed to reduce the deceleration, and in extreme cases to accelerate the aircraft, by reducing the thrust vector angle. This type of action, although not serious, increases the pilot workload.

A functional block diagram of the velocity flight director is shown in figure 10. To avoid false switching indication in turbulence, it was found necessary to filter the acceleration signal (fig. 10). The filter used here is a simple "moving-averages" design; it was a convenient design because the simulation of the system used a digital computer. If, in the real aircraft, the computation were analog, then an equivalent filter design would be required. Tests carried out with the fixed-base simulator resulted in the selection of a filter span of 0.5 sec. The equivalent filter-induced lag is therefore 0.25 sec. With this filter, false switching signals were apparent only in extremely high turbulence (greater than 2.5 m/sec (8.2 ft/sec) rms) and even then their short duration tended to make them recognizable to the pilot. These same tests also indicated that the first switch after the onset of the deceleration tended to be delayed too much, resulting in higher than desirable velocity errors. This problem was overcome by setting the upper velocity error limit,  $\Delta V_U$ , to half its nominal value until after the first switch had occurred.

The nominal values of  $\Delta V_U$  and  $\Delta V_L$  selected from the tests were 1.83 m/sec (6 ft/sec) and -4.27 m/sec (-14 ft/sec), respectively. The nominal value of the vector-angle rate depends on the particular aircraft being considered. However, the vector-rate value is strongly related to the difference between the steady-state vector angles for hover and for the approach conditions (prior to deceleration). The rate selected for the Harrier was 1.0°/sec; for the lift-fan transport the selected rate was 2.5°/sec.

#### Vertical (Throttle) Flight Director

In the design of the Type 2 system it is assumed that engine thrust is the primary means of altitude control. Throughout the entire approach and landing, the pilot maintains the preselected reference flightpath by adjusting the throttle setting to null the vertical flight director output given on the HUD (figs. 5(b) and 5(c)).

A block diagram of the vertical flight director is shown in figure 11. In terms of its feedback loops, this director is closely related to the SRFIMF flight controller (ref. 1). This similarity is superficial, since the pilot provides the inputs to the SRFIMF, whereas the flight director provides inputs to the pilot. Thus, the bandwidth requirements of a flight controller and flight director differ markedly.

The primary problem in flight director design is to obtain a satisfactory compromise between the magnitude of the aircraft's position errors and the pilot workload required to follow the flight director. If the director gains are high, then the errors will be low, but the pilot workload will be high.

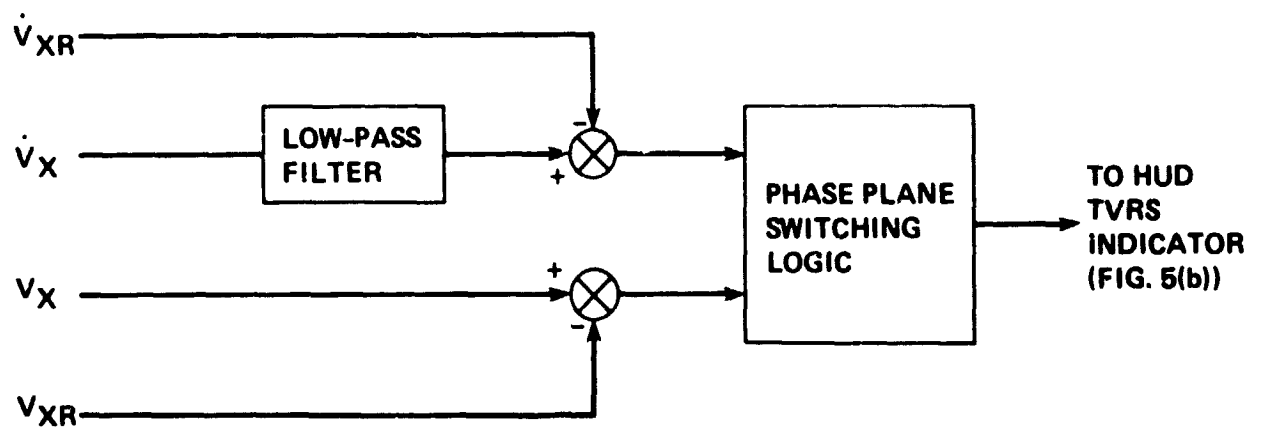


Figure 10.- Longitudinal (thrust-vector-angle) flight director.



# NOMINAL PARAMETER VALUES

PARAMETER	TRANSITION	HOVER MANEUVERS AND FINAL DESCENT
$k_h$	$0.0278 \text{ sec}^{-2}$	$0.01796 \text{ sec}^{-2}$
$k_h'$	$0.3333 \text{ sec}^{-1}$	$0.268 \text{ sec}^{-1}$
$k_{2h}$	$3.691 \text{ deg sec}^2/\text{m}$	$2.920 \text{ deg sec}^2 \text{ m}^{-1}$
$\tau_h$	$0.3333 \text{ sec}$	$0.3333 \text{ sec}$

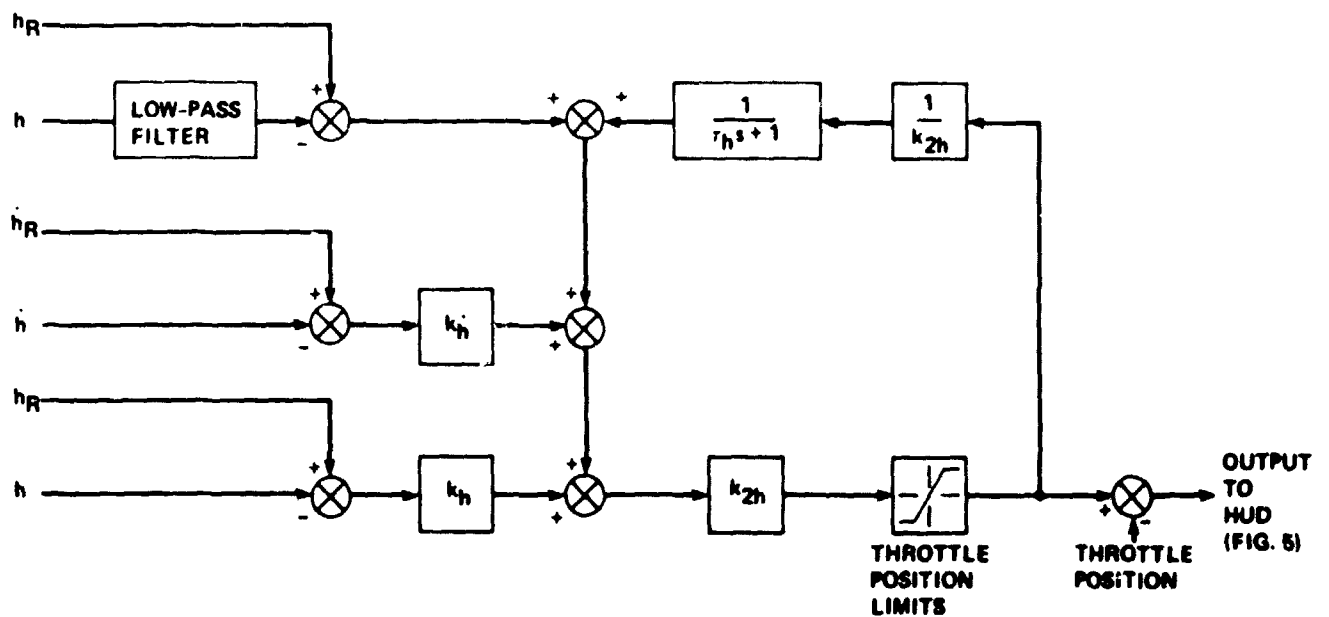


Figure 11.- Vertical (throttle) flight direction.

Unlike the constant-airspeed, constant-throttle approaches typical of conventional (CTOL) aircraft, VTOL aircraft approaches require a continuously varying throttle setting to counter the changing aerodynamic forces during transition. It follows that for comparable altitude errors, the VTOL flight director must have a higher bandwidth (larger gains) than a CTOL flight director. Therefore, the primary flight director design problem is more difficult for VTOL aircraft than for CTOL aircraft.

The vertical flight director (fig. 11) uses vertical acceleration to assist in providing lead information to the pilot to help him maintain acceptable altitude errors during the deceleration. The disadvantage of using vertical acceleration is that it produces a very active flight director indication in turbulence. This problem can be alleviated, to some extent, by filtering the acceleration signal (fig. 11). The filter used is similar to that used for the longitudinal flight director (fig. 10).

The nominal values for the vertical flight director parameters (fig. 11) were selected in the following way. First, with the flight director coupled directly to the throttle (no pilot), several sets of parameters were determined analytically, each corresponding to a different total system (aircraft plus flight director) damping level. Each of these parameter sets was then tried out in the previously mentioned simplified digital simulation to obtain the magnitude of the altitude errors during transition. A typical example of the results of this simulation, using the parameter values given in figure 11, is shown in figure 12. In addition to showing the maximum altitude error (-1.8 m), figure 12 shows the large increase of throttle required during transition. From the results of the simplified simulation, several candidate sets of parameter values were selected and tested, using the fixed-base piloted simulation, to evaluate the pilot workload required to follow the flight director signal. From these tests, two sets of parameter values were selected, one for transition, the other, with somewhat lower gains, for hover maneuvers and final descent. These parameter value sets correspond to coupled system (no pilot) time constants of 8 sec for transition and 10 sec for hover maneuvers and final descent.

#### Hover Flight Director

In the design of the Type 2 system it is assumed that during the hover maneuvers and final descent, control of aircraft position in the horizontal plane is primarily through pitch and roll attitudes. The pilot follows a pre-selected flightpath (appendix A) by varying the aircraft's altitude (using the stick) to null the hover flight director output given on the HUD (fig. 5(c)).

A block diagram of the hover flight director is shown in figure 13. Because the directors for both pitch and roll are identical, only roll is shown in figure 13. The method used to select the parameter values was similar to that used in the design of the vertical flight director. The design problems are similar, though somewhat less severe, than for the vertical flight director. An important requirement for the hover maneuvers and final

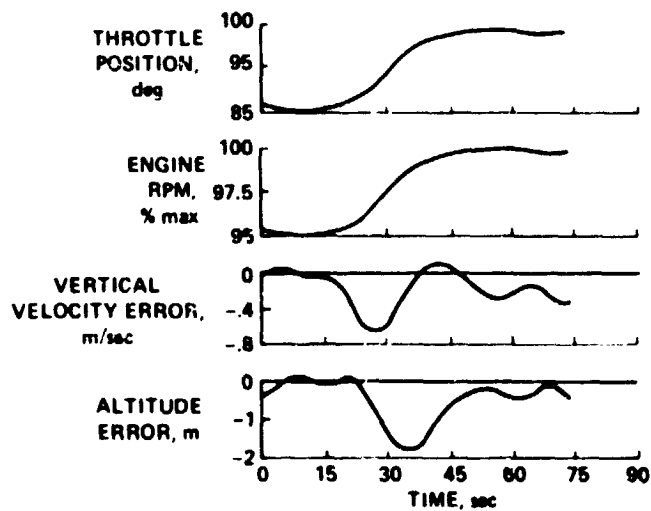


Figure 12.- Time variation of vertical parameters in typical transition.

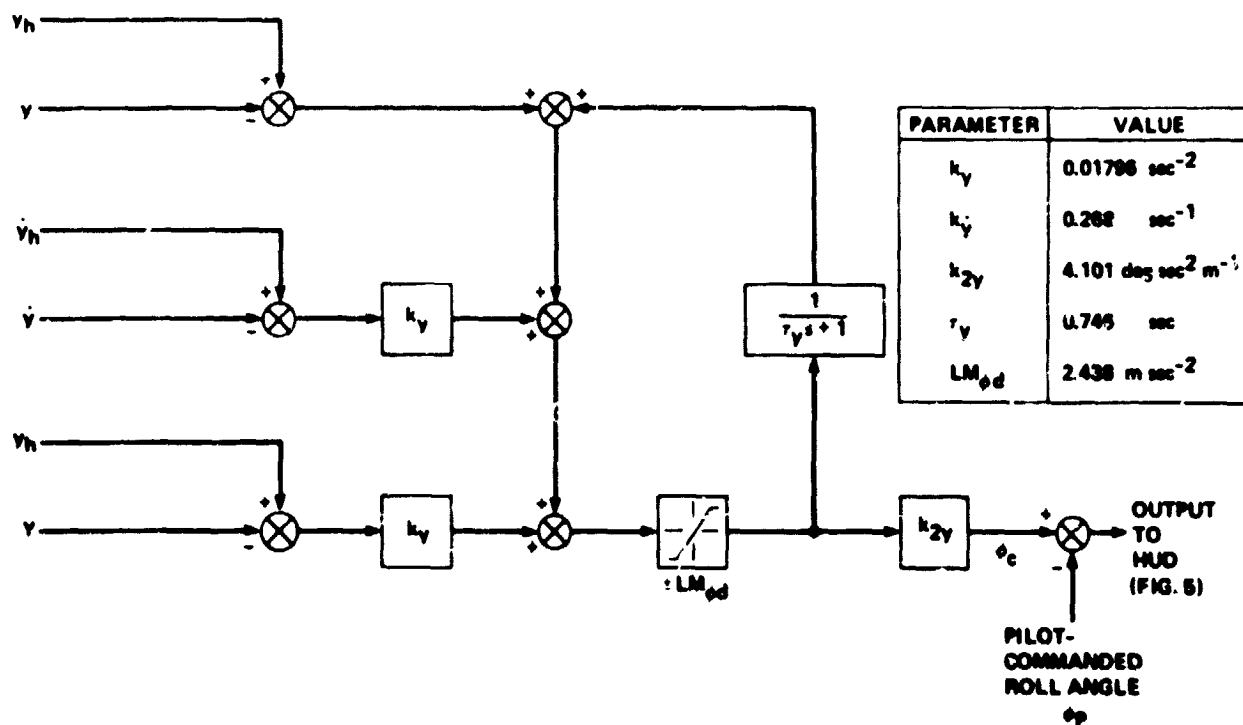


Figure 13.- Hover flight director (later. 1).

descent is that they be completed in the shortest possible time and this, together with the need for accurate station keeping during the final descent, forces consideration of relatively high flight director gains and the inclusion of acceleration feedback. The acceptability of these gains is largely dependent on the activity of the flight director output, particularly in turbulence. Since the effect of turbulence, in hover, is far less than in transition, the acceleration input to the director is not filtered (compare figs. 11 and 13). The selected parameter values (fig. 13) correspond to a direct-coupled (no pilot) minimum damping time constant of 10 sec. A Bode plot, showing the dynamic performance of the flight director/aircraft system is shown in figure 14. The response of the aircraft in position  $y$  to a pilot roll angle command  $\phi_p$  behaves, as expected, like a double integrator (phase lag of  $180^\circ$ ) at low frequencies. At frequencies higher than 0.5 rad/sec, the combined flight controller and aircraft roll dynamics introduce additional lags which become pronounced at frequencies greater than the 2-rad/sec break frequency designed into the SRFIMF roll controller "implicit" model. The response of the flight director output  $\phi_c$  to pilot roll-angle command  $\phi_p$  shows a significant phase lead over the response of the displacement  $y$  to the pilot command. Figure 14 shows a phase lead of  $90^\circ$  at low frequency rising to  $290^\circ$  at a frequency of 1 rad/sec. This lead compensation eases the piloting task of acquiring and maintaining the station-keeping point.

#### Lateral Flight Director

The transition lateral flight director is used to acquire the localizer. The same director feedback loops and gains are used for both the Type 1 and Type 2 systems (fig. 33 in ref. 1). Because the localizer is a vertical plane and no commanded maneuvering is involved, the lateral flight director gains are lower than for the vertical or hover flight directors and no acceleration feedback is required. The lower gains are reflected in the fact that the direct-coupled (no-pilot) minimum damping time constant is 20 sec.

### OPERATIONAL DESCRIPTION OF CONTROL/DISPLAY SYSTEMS

Any control/display system functions can be understood best by following, step by step, the intended piloting operation during a typical approach and landing. Such an operational description is given for each of the two types of systems. Both systems require the pilot to perform certain switching operations for control mode and flight director selection. These switches are located on the stick grip (fig. 15).

#### Typical Landing Using Type 1 System

It is assumed that at the start of the approach, the aircraft is on the glide slope with the scheduled speed and rate of descent, but is displaced laterally from the localizer and trimmed at a pitch attitude that is different from that required at touchdown. With these conditions the pilot will have

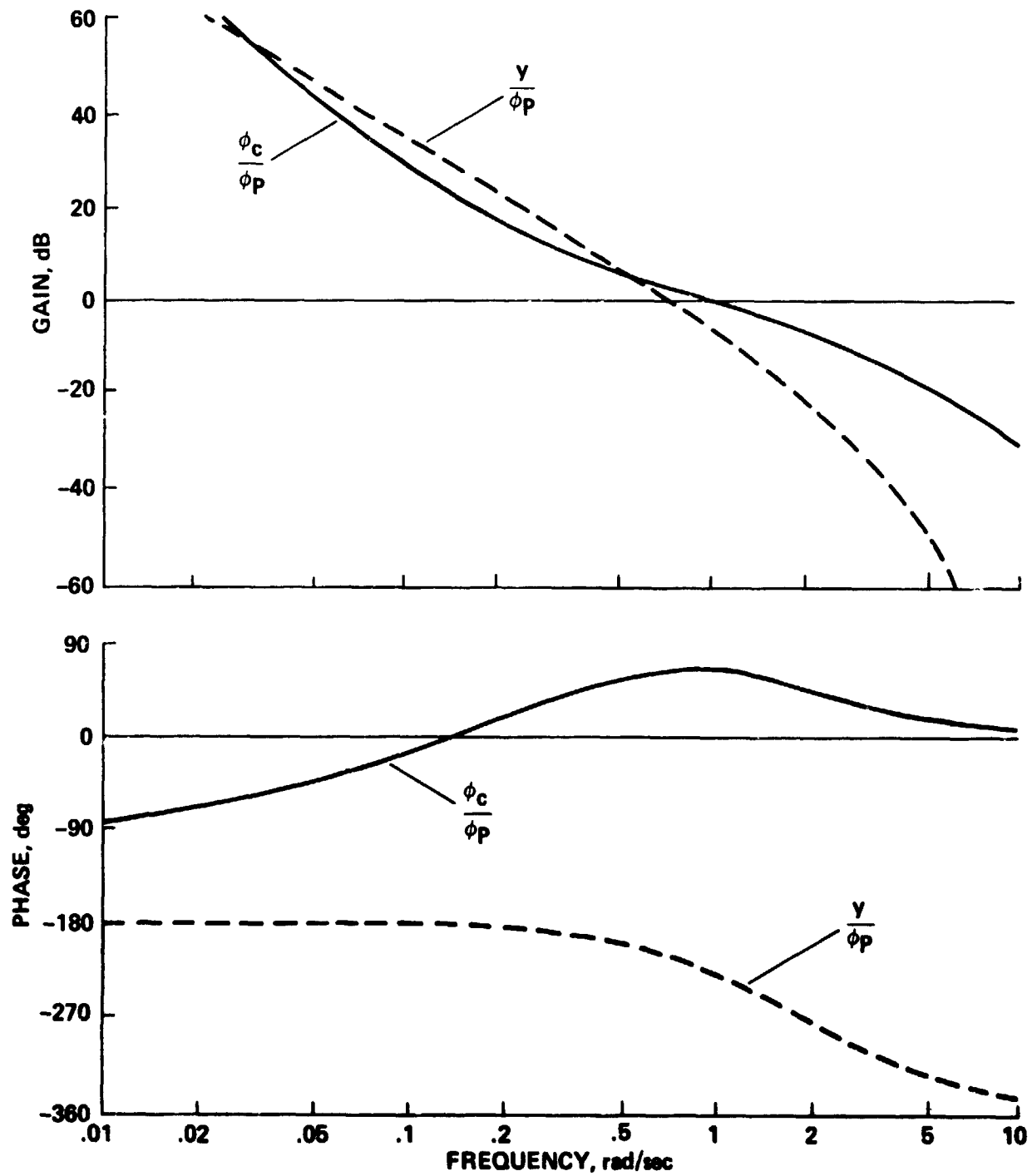


Figure 14.- Bode plots for hover flight director (lateral control).

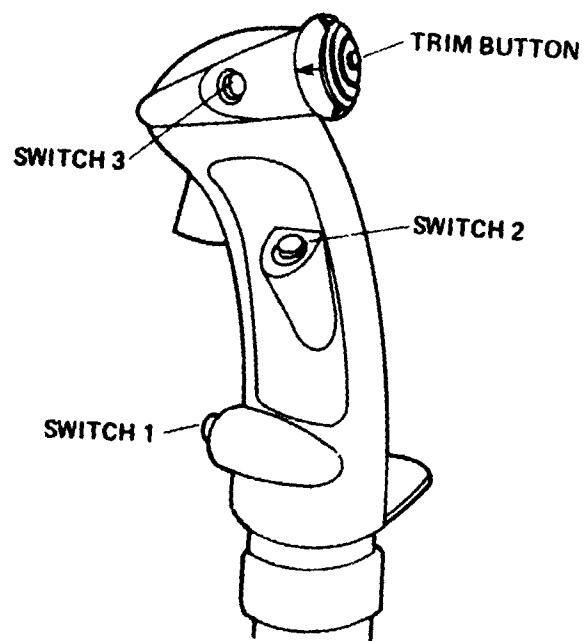


Figure 15.- Stick grip.

the vertical velocity lever and longitudinal acceleration thumb wheel (fig. 2) positioned so that the two pilot command symbols on the left and right scales of figure 3(b) match the corresponding flight director symbols.

The actions taken by the pilot during the approach and landing are detailed below.

1. Lateral stick in conjunction with the lateral flight director (fig. 3(b)) is used to acquire the localizer.
2. At a predetermined distance from the initial station-keeping point (this distance depends on the preselected level of longitudinal deceleration during transition), the acceleration flight director (right scale of fig. 3(b)) moves, from zero, to indicate the required deceleration. The pilot then moves the thumb wheel (fig. 2) until the pilot acceleration command symbol matches the acceleration flight director symbol.
3. Assuming that the predetermined flightpath is straight, the vertical velocity flight director will indicate a gradually reducing rate-of-descent requirement as the aircraft decelerates. The pilot moves his vertical velocity level so that the associated command symbol matches that of the flight director.
4. At about 100 knots, the pilot retrim the aircraft, in pitch, to the touchdown attitude. He may retrim in either of two ways. He can use the trim button (fig. 15), which changes the pitch attitude at  $4^\circ/\text{sec}$ , or he can press the trim reset button (switch No. 3 in fig. 15) and the control system will automatically retrim at  $4^\circ/\text{sec}$  to the preset touchdown attitude. Using either technique, the final trimmed pitch attitude is indicated on the display (fig. 3(a)).
5. The transition continues with the pilot following the three flight director symbols (lateral, longitudinal, and vertical) with the appropriate controls, while using the pedals to keep the lateral acceleration symbol (fig. 3(a)) centered.
6. At 100 m (328 ft) from the initial station-keeping point, the symbol representing the initial station-keeping point appears on the HUD, and, when the aircraft's speed relative to the station-keeping point is less than 10 m/sec (32.8 ft/sec), the horizontal relative velocity arrow appears on the HUD (fig. 3(c)). This arrow is the projection of the relative velocity vector in the horizontal plane. Assuming that the pilot has followed the flight directors reasonably closely, the initial station-keeping point will approach the fixed aircraft symbol with reducing relative velocity. Eventually, the vertical velocity and horizontal acceleration flight directors will both indicate zero, the relative velocity vector will be small, and the pilot will have both his vertical velocity lever and the longitudinal acceleration thumb wheel in their respective detents.
7. At this point in the landing, the pilot changes control modes by pressing switch No. 1 on the stick (fig. 15). This action changes the control

mode from longitudinal acceleration to longitudinal velocity (table 2) and activates the direct-force lateral velocity controller, if one is available. Both the longitudinal and lateral velocities are controlled through the horizontal velocity thumb button (fig. 2). The pressing of switch No. 1 also commands the longitudinal velocity of the aircraft, relative to the initial station-keeping point, to be zero (this is apparent to the pilot from the velocity arrow), and introduces a pilot horizontal velocity command arrow on the HUD (fig. 3(c)). In a system such as that of the Harrier, in which a direct-force lateral control is not provided, the technique of laterally acquiring the initial station-keeping point is similar to that described when using the Type 2 system.

8. Still keeping the vertical velocity lever in the detent, the pilot then presses the horizontal-velocity command thumb button so that the corresponding pilot-command arrow on the HUD points toward the initial station-keeping point. In this manner, the pilot brings the aircraft symbol and initial station-keeping point symbol roughly into coincidence.

9. The pilot then presses switch No. 2 on the stick (fig. 15) and the station-keeping point symbol on the HUD jumps to the center of the landing pad.

10. The pilot uses his thumb button to bring the aircraft symbol and station-keeping symbol (now in its final position) into coincidence.

11. When the altitude is less than 30 m (100 ft) above the deck, the deck altitude indicator symbol (T bar) appears on the HUD (fig. 3(c)). The distance between the bottom of the aircraft symbol and the horizontal arm of the deck indicator is a measure of the height of the wheels above the deck. If the ship is moving in pitch and heave, this motion is apparent from the deck indicator. The pilot uses his vertical velocity lever to establish a suitable rate of descent (relative to mean sea level) until the aircraft settles onto the deck, at which point he pulls back the vertical velocity lever to reduce the engine speed to idle.

#### Typical Landing Using Type 2 System

The aircraft state, at the start of the approach, is assumed to be the same as that in the description of the use of the Type 1 system. The pilot is assumed to have the power and thrust-vector-angle levers positioned correctly for the start of approach conditions.

The actions taken by the pilot during the approach and landing are detailed below.

1. The lateral control, in conjunction with the lateral flight director (fig. 5(b)) is used to acquire the localizer.

2. At a predetermined point, the longitudinal (thrust-vector-angle) flight director indicates the start of deceleration (on the HUD) by a broad



arrow pointing in the downward direction (fig. 5(b)). The pilot has the option of pressing the TVRS or, if a nose-up trim change is required to reach the landing attitude, he can make the trim change. Both options have the effect of decelerating the aircraft. Eventually the arrow symbol will disappear, indicating that the speed/acceleration error criterion is satisfied. At the same time that he starts the deceleration, the pilot must follow the vertical (power) flight director to maintain position on the glide slope.

3. The transition continues with the pilot following the lateral, longitudinal, and vertical flight directors, using the stick, power lever, and TVRS, respectively. The longitudinal flight director will indicate a downward pointing arrow (increase the thrust vector angle) three or four times and may, under some circumstances, indicate an up arrow (decrease the thrust vector angle).

4. When the aircraft is close to the initial station-keeping point, the relative speed, as indicated by the velocity arrow (fig. 5(c)), should be low (less than 10 knots). The pilot then presses switch No. 1 on the stick grip to activate the hover flight director (cross bar on fig. 5(c)). This switch also declutches the thrust-vector-angle lever.

5. The pilot commands the appropriate pitch and roll attitudes to center the cross bars of the hover flight director until he is satisfied that the aircraft's position is stabilized acceptably close to the initial station-keeping point.

6. The pilot then presses switch No. 2 on the stick grip. This action starts the station-keeping point translating toward the ship. The pilot continues to use the hover flight director, and the aircraft follows the station-keeping point reasonably closely.

7. Eventually, the station-keeping point reaches its final point over the desired touchdown point and, shortly thereafter, the aircraft also reaches the same point. Throughout the translation, the pilot has maintained a constant altitude by following the vertical flight director.

8. When the pilot is satisfied with the location of the aircraft over the deck, he presses switch No. 2 a second time. This action starts the vertical flight director to indicate the power required for a fixed rate of descent. If the pilot follows this director, the aircraft will descend to touchdown.

## SIMULATION

### Simulation Models

Models of a conceptual V/STOL lift-fan transport and an AV-8A Harrier were used in the simulation. The V/STOL lift-fan transport model, including the advanced SRFIMF flight controller, is described in reference 1. The model

of the basic AV-8A Harrier is described in reference 6. Modifications to the Harrier control system to include an SRFIMF flight controller are given in appendix B.

A Spruance-class destroyer (DD-963) model was used in the simulation. A model to provide representative motion of the ship in various sea conditions was obtained using the method given in reference 7. The general method for generating time histories of ship motion from the power spectra uses a decomposition of the spectra into a series of discrete sinusoids, with each component sinusoid weighted by the spectrum power in the frequency band it represents. Generally, 15 to 20 sinusoid components are recommended. This number provides an optimum trade-off between accuracy and computational time. However, a comparison between 6 and 32 component approximations, reported in reference 8, showed differences of less than 5% in most cases. Therefore, following the lead established in reference 3, the six-component sinusoid model was used for this simulation.

The ship air-wake model was again similar to that used in reference 3. This model was developed from test data from a 1/50-scale model of an FF-1052 class destroyer. These basic data were adapted to the DD-963 by Strouhal-number scaling.

Isotropic turbulence, outside the ship's air wake, was modeled using a standard Dryden representation (ref. 9).

#### Scope of the Simulation

The basis for evaluation and comparison of the Type 1 and Type 2 control/display systems is summarized in the following:

1. Operational acceptability of the task
2. Assessment of pilot workload
3. Task performance parameters
4. Evaluation of the HUD format
5. Evaluation of the pilot control modes and mode switching
6. Evaluation of the flight directors
7. Evaluation of the pilot controls (inceptors)
8. Modeling fidelity
9. Simulation equipment limitations

To help reduce the testing time, and to improve the flexibility of the test procedure, the approach and landing task was divided into two parts.

One part was the approach transition, starting at 120 knots and ending at the initial station-keeping point; the other was the hover maneuver and final descent, starting at the initial station-keeping point and ending at touchdown. These two parts will be termed "transition" and "landing," respectively.

The reference approach path used throughout the transition tests was a straight  $-3^\circ$  glidepath starting 3,660 m (12,000 ft) from the initial station-keeping point, at an altitude of 217 m (712 ft), and ending at the initial station-keeping altitude of 25 m (82 ft) above sea level. A longitudinal deceleration of  $0.91 \text{ m/sec}^2$  ( $3 \text{ ft/sec}^2$ ) was used for most of the tests, although a few comparison tests were made using decelerations of  $1.82 \text{ m/sec}^2$  ( $6 \text{ ft/sec}^2$ ) and  $2.73 \text{ m/sec}^2$  ( $9 \text{ ft/sec}^2$ ). The rate of descent variation with altitude for these types of approach transition is given in figure 16. The prime environmental variable in the approach transition tests was the turbulence level, and this was varied up to a maximum of  $2.9 \text{ m/sec}$  ( $7.5 \text{ ft/sec}$ ) rms. Visibility conditions approximated a ceiling of 30 m (100 ft) and a runway visual range (RVR) of 213 m (700 ft). With the approach path chosen, the ship became visible at a range of about 152 m (500 ft). All approaches were started with the aircraft on the glidepath but displaced 46 m (150 ft) laterally from the localizer.

The horizontal location of the initial station-keeping point was maintained constant throughout the tests at 30 m (100 ft) to starboard and 30 m (100 ft) aft of the touchdown point (fig. 17).

The geometry of the landing is shown in figure 17. A variety of environmental conditions (table 6) was assumed. These conditions corresponded to a wind-over-deck (WOD) variation from 15 to 43.3 knots and sea states from 0 (calm) to 6. These same conditions were assumed in tests reported in reference 3. The angle of the WOD relative to the longitudinal axis of the ship was either  $0^\circ$  or  $-30^\circ$ ; in either case, the landing from the initial station-keeping point to touchdown was within the ship's air wake. An important difference between these tests and those reported in reference 3 is that the path through the air wake to the final station-keeping point was about 9.75 m (32 ft) higher in the former (25 m vs 15.25 m). The higher altitude means that with the assumed air-wake model, the aircraft experiences rms turbulence levels about 40% less than in the tests reported in reference 3.

Most of the tests were carried out using the AV-8A Harrier model. The lift-fan V/STOL transport model was used only when it was desired to evaluate lateral thrust deflection. The free-air, hovering, maximum thrust/weight ratios of both aircraft were maintained at 1:1 throughout the tests.

Before recording data for each major test phase, the pilots were given some time, in the simulator, to familiarize themselves with the control system and the task. All the pilot ratings for the various tests were based on the Cooper-Harper handling qualities rating scale given in figure 18.

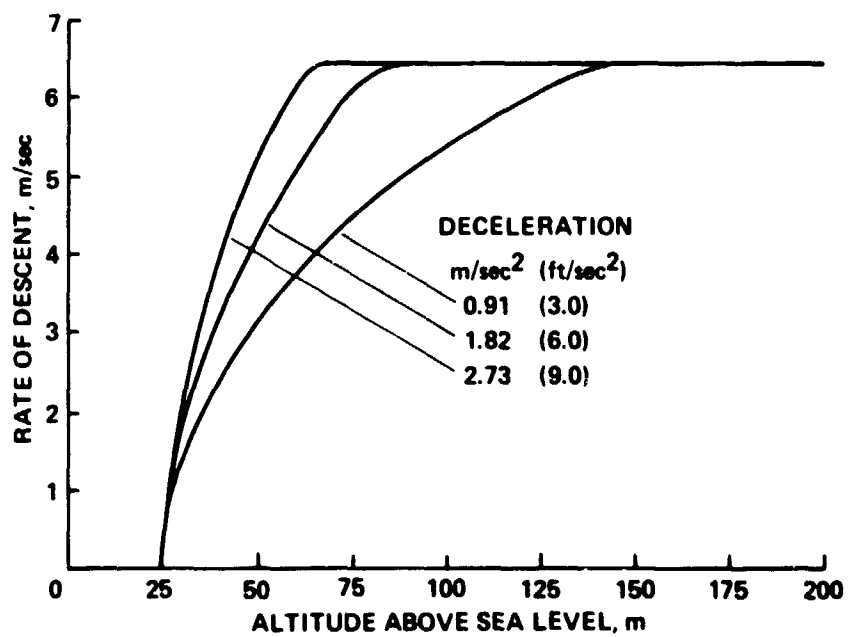


Figure 16.- Reference descent rates in transition.

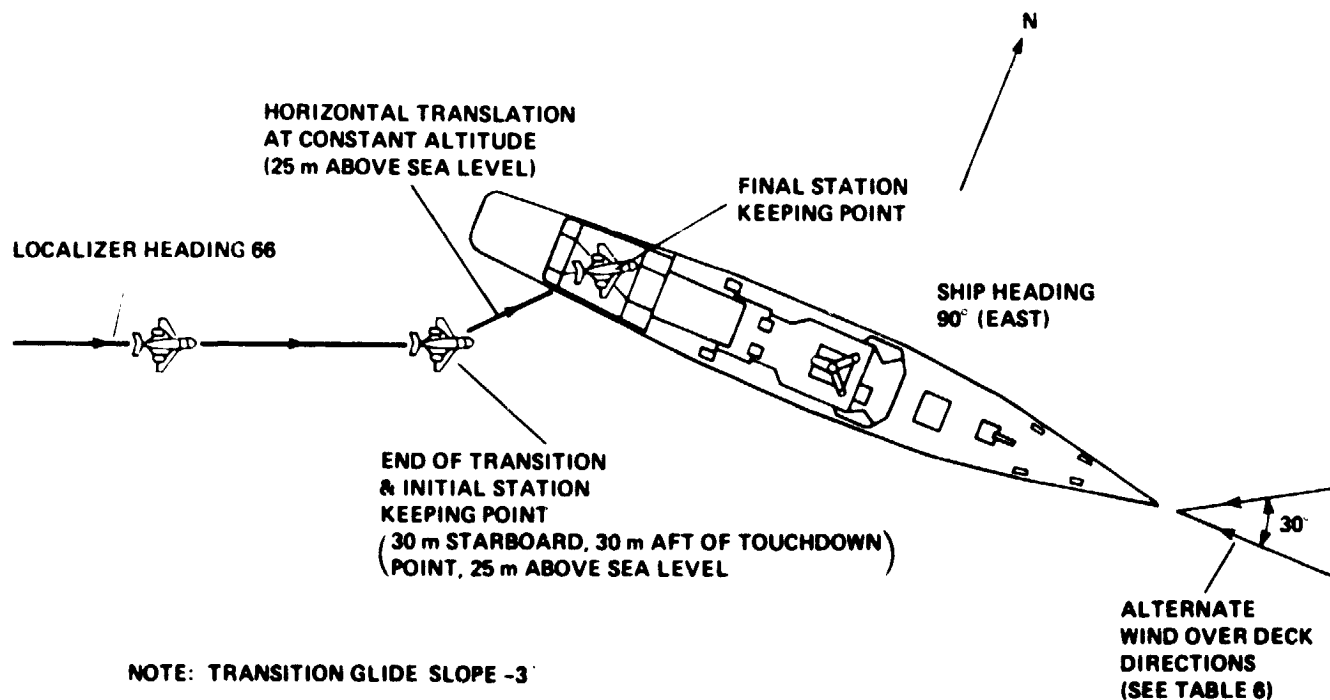


Figure 17.- Geometry of final approach

TABLE 6.- SIMULATION ENVIRONMENTAL CONDITIONS

Condition	Sea state	V <sub>S</sub> knots	μ <sub>S</sub> deg	V <sub>WIND</sub> deg	ψ <sub>WOD</sub> deg	V <sub>WIND</sub> knots	V <sub>WOD</sub> knots	H <sub>S</sub> ft	T <sub>0</sub> sec	σ <sub>φ<sub>S</sub></sub> <sup>a</sup> deg	σ <sub>θ<sub>S</sub></sub> <sup>a</sup> deg	σ <sub>z<sub>S</sub></sub> <sup>a</sup> ft
1	6	25	120	-60	-30	25.00	43.30	18	15.13	3.1	1.05	4.9
2	5	25	120	-60	-30	25.00	43.30	12	13.50	2.0	0.77	3.4
3	5	20	120	-60	-30	20.00	34.64	12	13.50	2.4	0.80	3.1
4	5	10	135	-45	-30	19.32	27.32	12	13.07	2.9	0.97	2.4
5	5	25	180	0	0	20.00	45.00	12	12.07	0	0.93	2.7
6	5	5	180	0	0	20.00	25.00	12	11.51	0	0.90	1.4
7	4	25	105	-75	-30	17.68	34.15	6.9	10.6	1.1	0.34	2.0
8	3	25	105	-75	-30	17.68	34.15	4.6	8.8	0.6	0.24	1.3
9	3	20	105	-75	-30	14.14	27.32	4.6	8.8	0.6	0.26	1.2
10	3	25	90	-90	-30	14.43	28.87	4.6	8.8	0.6	0.09	1.2
11	3	15	120	-60	-30	15.00	25.98	4.6	8.8	0.6	0.35	1.0
12	3	25	180	0	0	14.00	39.00	4.6	8.8	0	0.21	0.6
13	3	5	180	0	0	14.00	19.00	4.6	8.8	0	0.24	0.3
14	0 <sup>b</sup>	10	-	-68.26	-30	8.07	15.00	0 <sup>b</sup>	-	0	0	0

<sup>a</sup>Statistics for six sine wave approximations.<sup>b</sup>No ship motion.

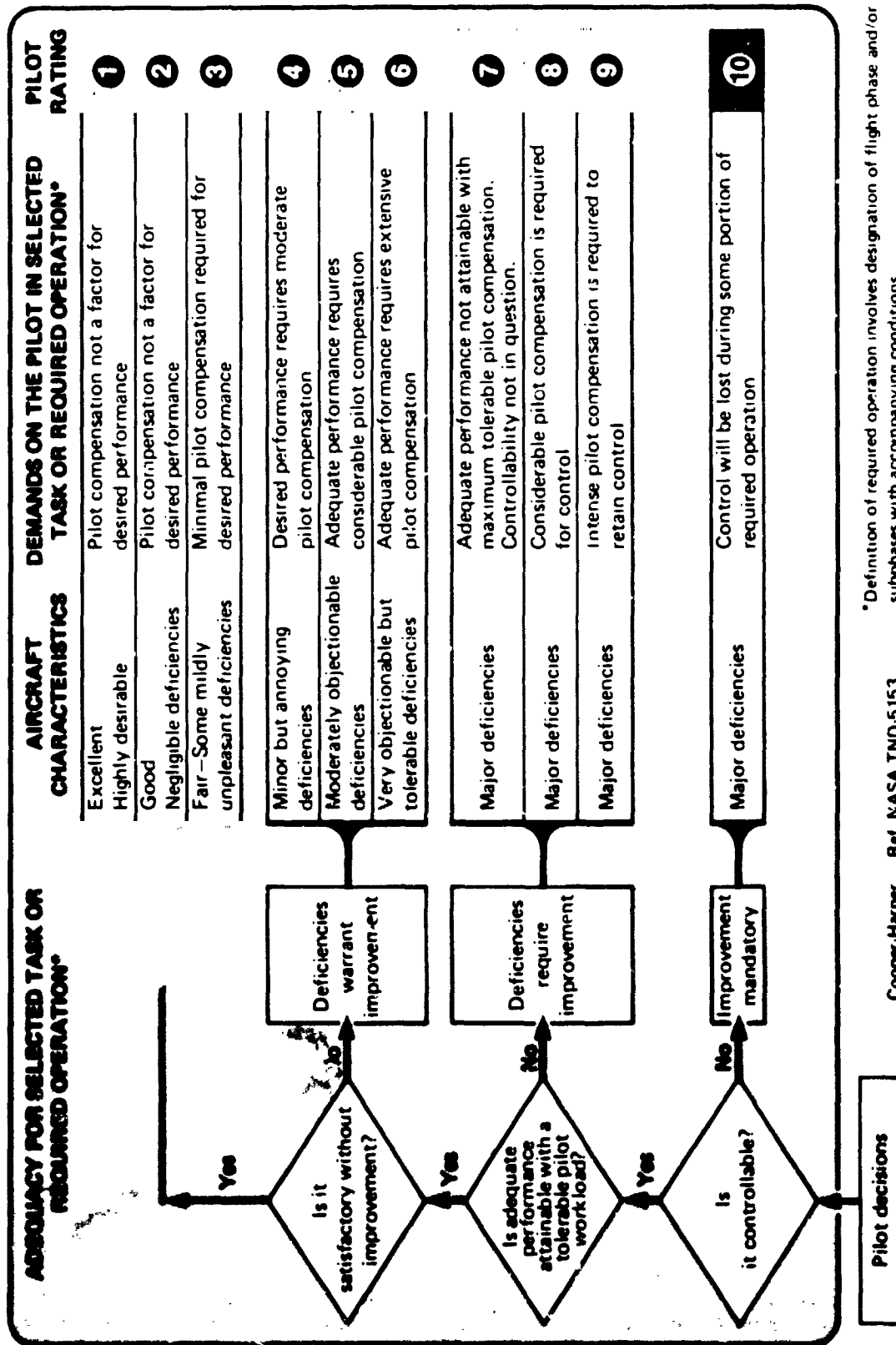


Figure 18.- Handling-Qualities rating scale.

### Simulation Equipment

The tests were conducted using the Ames Flight Simulator for Advanced Aircraft (FSAA). A full description of this simulator, including its dynamic performance, is given in reference 10. Details of the simulator motion drive washout logic used in the tests is given in appendix C.

The cockpit layout closely resembled that used in the tests reported in reference 3. Major differences were that the "Navy high-roll" stick (fig. 3-1 in ref. 3) was replaced by a stick with a low roll center, similar to that of an AV-8A Harrier, and the side arm controller shown in figure 3-1 of reference 3 was removed. Force/displacement characteristics of the stick and pedals are given in table 7.

The pilot was provided with a collimated colored television picture of a terrain model representing part land and part sea. The scenic features of interest were a 1/250-scale model of a DD963 destroyer, three runways of various lengths, and a land-based VTOL port. A picture of the scene is shown in figure 4.1.1-1 of reference 10 (VFA-07 Terrain Model - Details). The field of view relative to the pilot's eye was  $48^\circ$  horizontally and  $37^\circ$  vertically. The HUD picture was generated by a separate television monitor and combined optically with the picture of the scene (ref. 10). The field of view of the HUD was  $17^\circ$  both horizontally and vertically. The scale of the pitch ladder was 1:1 with the visual scene. The motion limits and dynamic performance of the "visual flight attachment" (VFA-07) are given in reference 10. All the tests were conducted using a model scale of 250:1.

The scale model of the Spruance-class destroyer DD963 was servo driven to provide the required motion in pitch, roll, and heave. Motion was restricted to these three primary degrees of freedom to simplify the ship-motion-producing device (see Simulation Equipment Limitations). The pilot's views of the ship from various points during the planned hover maneuvers and final descent to touchdown, for two aircraft headings, are shown in figures 19 and 20. These headings are roughly the two alternative WOD directions shown in figure 17 and table 6.

A Xerox Corporation Xigma 8 computer was used for overall simulation control and for calculation of aircraft and ship motion and simulation equipment drive signals. The digital frame time used was 55 msec. A Digital Equipment Corporation PDP-11/55 was used to generate the HUD format.

### Pilot Experience

Three pilots participated in the test: one from Ames Research Center, one from RAE Bedford (U.K.), and one from RAE Farnborough (U.K.). These pilots had a cumulative total of over 2000 hr flying fixed-wing VTOL aircraft. Both RAE pilots had extensive experience test-flying Harriers. One of the RAE pilots had been involved in a sea trial concerned with developing HUD symbology and flight profiles for poor weather and night recovery of the Royal Navy Sea Harrier to Invincible class ships - an activity directly related to this



TABLE 7.- CHARACTERISTICS OF COCKPIT CONTROLS

	Center stick		Pedals
	Pitch	Roll	Yaw
Breakout force, N (lb)	2.22 (0.5)	2.22 (0.5)	13.34 (3.0)
Force gradient, N/m (lb/in.)	245 (1.4)	289 (1.65)	2452 (14)
Travel, m (in.)	$\pm 0.0953$ ( $\pm 3.75$ )	$\pm 0.108$ ( $\pm 4.25$ )	$\pm 0.0533$ ( $\pm 2.1$ )

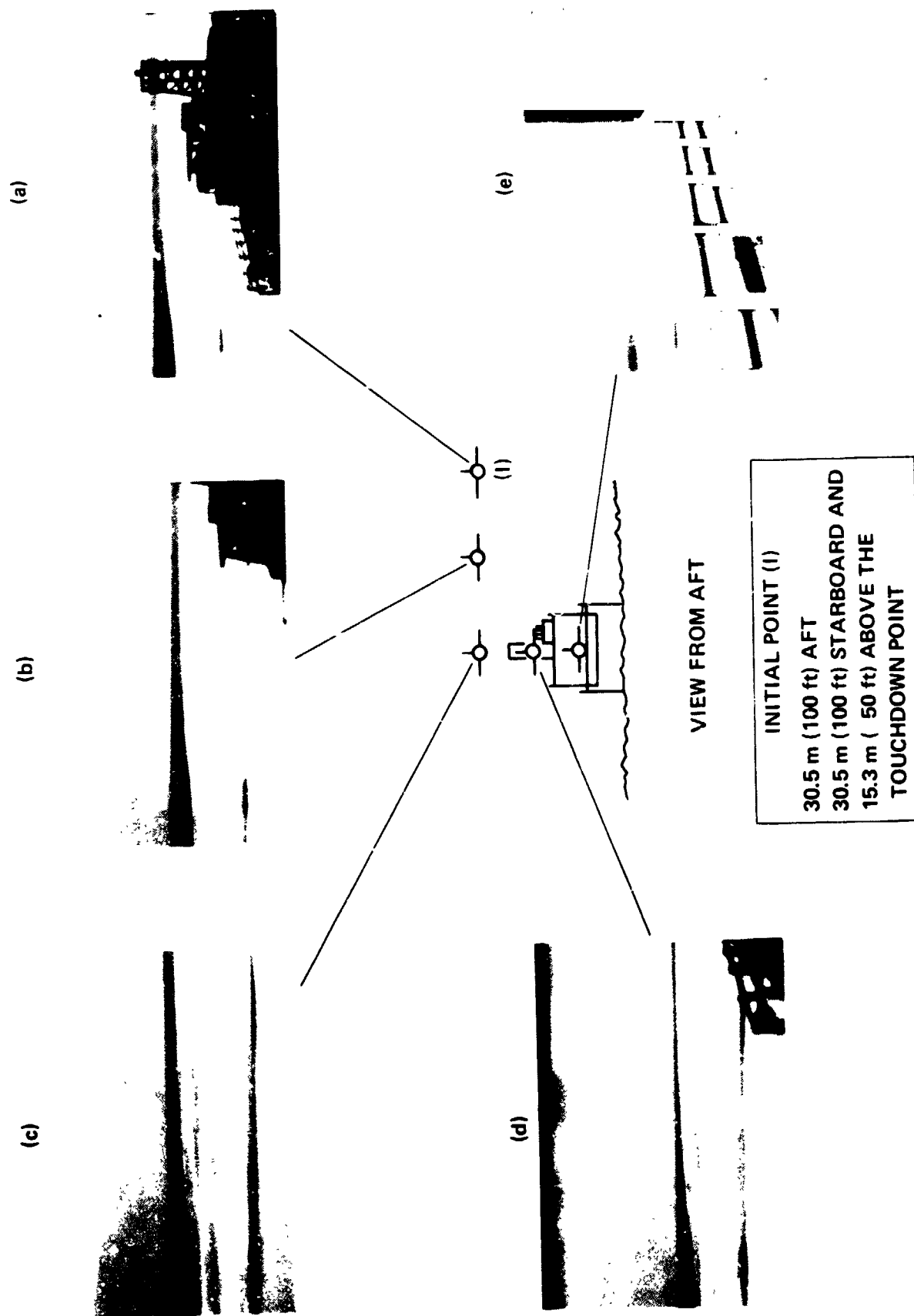


Figure 19:- Pilot's views of ship (ship heading 90°, aircraft heading 67°).

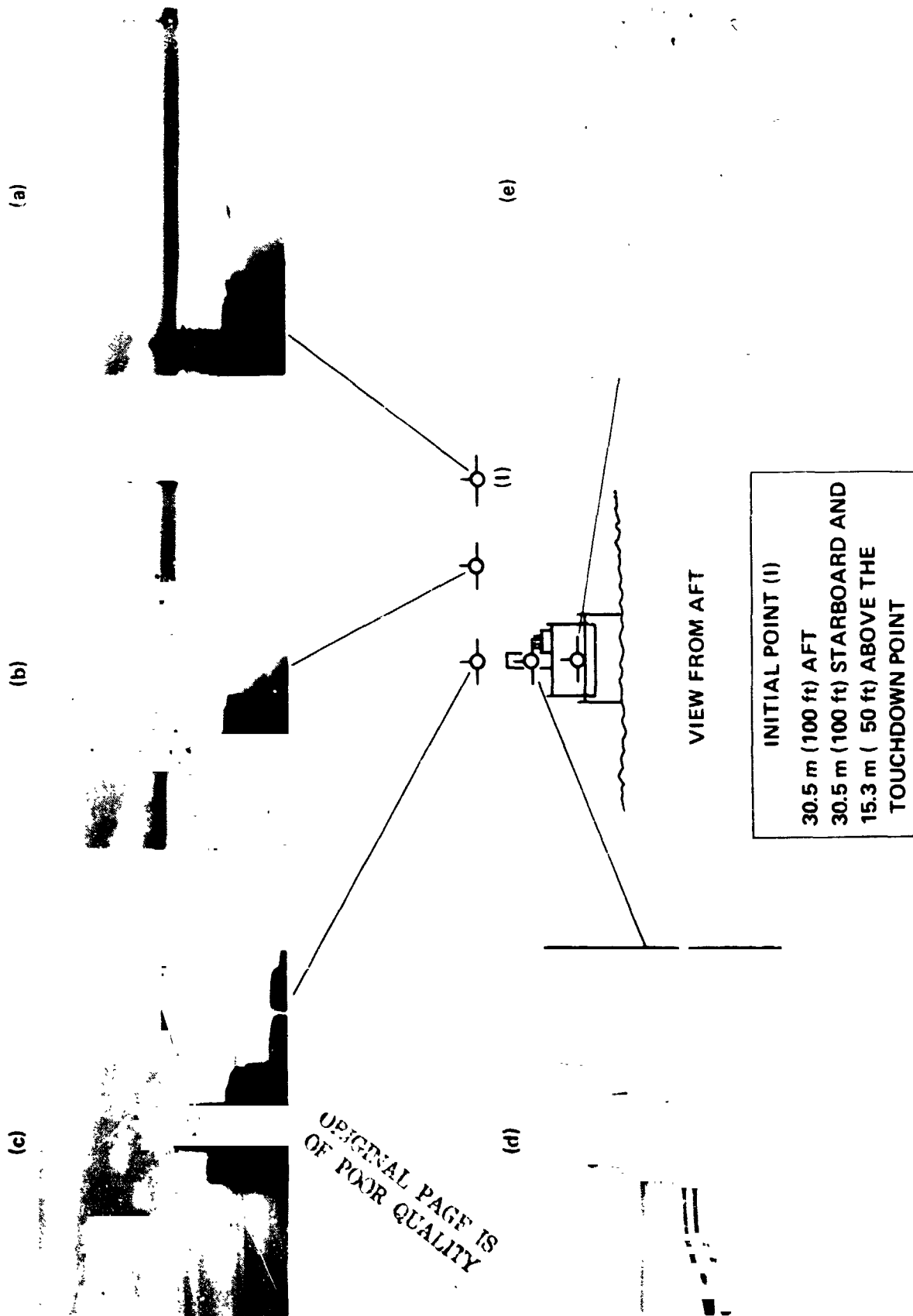


Figure 20.- Pilot's views of ship (ship heading 90°, aircraft heading 90°).

simulation study. The NASA pilot had extensive experience flying the XV-5B lift-fan VTOL aircraft and the X-14B VTOL in-flight simulator. The NASA pilot also had wide simulator experience flying the Type 1 system (refs. 1, 2).

In the results section of the report the pilots are identified by their initials: PB and RS are the RAE pilots; RG is the NASA pilot.

## SIMULATION RESULTS AND DISCUSSION

Pilot evaluation of transition and landing with Type 1 and Type 2 control/display systems are discussed below. (Comments of the RAE pilots are also presented in ref. 11.)

### Operational Acceptability of the Task

A major criticism of the simulator task used in this study had to do with the horizontal position of the initial station-keeping point and the localizer heading relative to the ship. The selected initial station-keeping point was located in the ship's air wake for both WOD directions considered. The pilots felt that it would have been better had the initial station-keeping point been located outside the air wake to minimize the work of initial acquisition. The combined localizer heading and initial station-keeping point position was such that if the pilot overshot the mark, the aircraft could hit the ship's superstructure. The pilots considered this to be a dangerous situation, especially if the visibility was poor or the field of view restricted.

The altitude selected for the hover maneuvers was acceptable, and the effects of the ship air wake were tolerable. The latter result contrasts strongly with that reported in reference 3, where pilots considered the air-wake turbulence effects severe. These severe wake turbulence effects were due to the fact, noted earlier, that the final approach altitude used in the tests reported in reference 3 were about 9.75 m (32 ft) lower than in these tests. It must be concluded that (1) either the wake turbulence model or its assumed mode of interacting with the aircraft is unrealistic at low altitudes or (2) if there is a compelling reason for traversing the ship's wake at length, the higher altitude is preferable.

The pilots considered the commanded reduction of deceleration at the end of transition to be too sudden, especially in the high deceleration tests; the reason was the sudden increase in workload caused by the need to arrest both the vertical and horizontal speeds more or less simultaneously. It is possible that this situation could be improved by providing a short horizontal segment just prior to reaching the initial station-keeping point. There would then be a time separation between the arresting of the vertical and horizontal velocities.

## Pilots' Evaluations

*Transition (Type 1 system; AV-8A Harrier)*- The variation of pilot ratings with isotropic turbulence level is shown in figure 21. These results show an increase in pilot rating from about 3 in low turbulence to about 4 in high turbulence. For 1.5 m/sec (5 ft/sec) turbulence the average pilot rating is about one-half unit higher than the 3 shown in reference 2. One reason for this difference is that the Harrier uses the Type 2 system of lateral control (no lateral side force generation), namely, bank-angle command with flight director information, to acquire the initial station-keeping point. This technique requires greater effort than the lateral velocity command system used for the lift-fan transport; also, the process of controlling lateral position with the stick and longitudinal position with the throttle-mounted thumb button results in poor control harmony.

All the pilots noted the need to continually move the vertical velocity command lever to maintain a straight approach path during deceleration and regarded this as a primary workload item during this phase of transition. Pilot PB (RAE pilot) was particularly concerned about this point and suggested that there may be more appropriate control modes (see Evaluation of Pilot Control Modes). The other primary workload item, namely, the acquisition and maintenance of the localizer, was regarded as satisfactory by all the pilots.

The effect on pilot ratings of increasing the reference deceleration is shown in figure 22. The primary effect is to compress the time available to make final control adjustments to remove the deceleration just prior to acquiring the initial station-keeping point (see Operational Acceptability of the Task). A secondary problem, which probably accentuated the pilots' feeling of time compression and urgency, was caused by exceeding the performance limits of the visual attachment (see Simulation Equipment Limitations). Because of this equipment limitation, the results shown in figure 22 may be pessimistic.

*Transition (Type 2 system; AV-8A Harrier)*- Pilot ratings for various levels of turbulence are shown in figure 23. At low turbulence levels the system worked reasonably well and was given pilot ratings about one-half unit higher (worse) than the Type 1 system (fig. 21). However, as the turbulence was increased, the pilot ratings also increased rapidly and the system became unacceptable for turbulence levels higher than about 2 m/sec (6.6 ft/sec).

The problems with the Type 2 system, for transition, were largely due to deficiencies in the flight director laws. From the pilot's viewpoint these deficiencies appeared as excessive sensitivity of the vertical flight director to altitude errors and turbulence, particularly at the higher speeds during the approach, and difficulty in judging when to switch to the hover flight director. In the early phases of testing it was found that pressing the stick switch when the initial station-keeping point was first observed on the HUD made the task easier. The results of figure 23 were obtained using this technique. However, toward the end of the tests, the wind condition and, therefore, the initial trim thrust vector angle were changed. As a result, the technique adopted earlier no longer worked. The aircraft repeatedly either

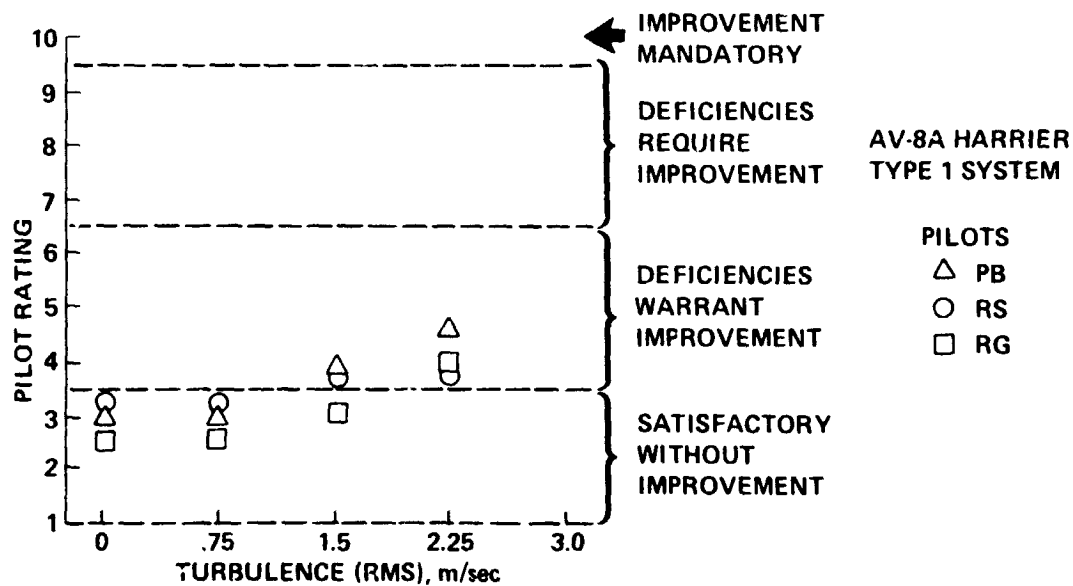


Figure 21.- Pilot ratings for transition (various turbulence levels).

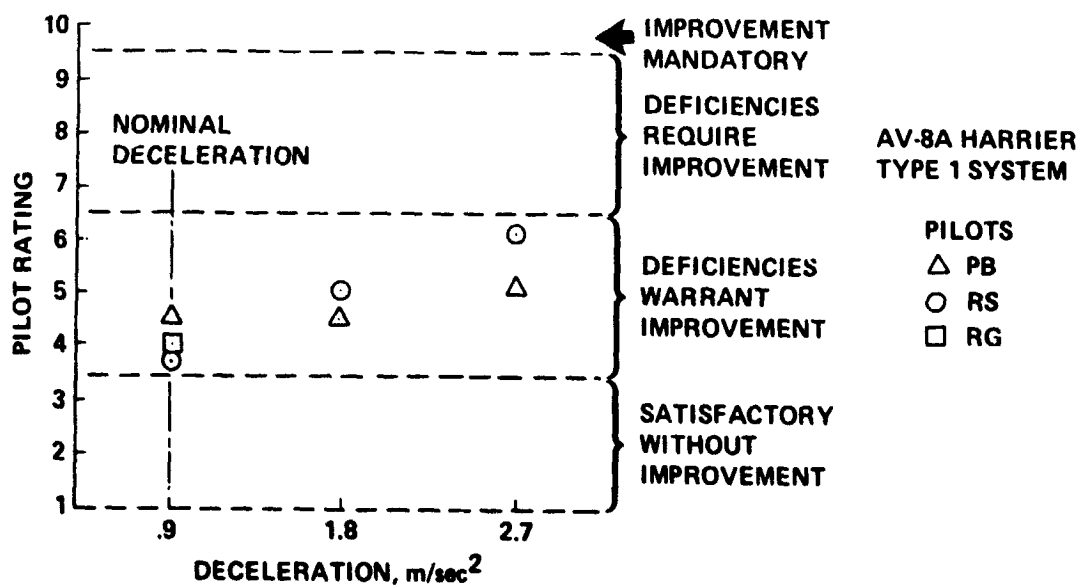


Figure 22.- Effect of transition deceleration on pilot ratings.

overshot or ended up short of the initial station-keeping point, which made it very difficult for the pilot to get back into the neighborhood of that point. The fact that the appropriate technique was dependent on the initial conditions is not represented in figure 23, and these results are therefore optimistic. A more detailed discussion of the flight director problems is given in a following subsection (Evaluation of the Flight Directors).

*Landing (Type 1 system; lift-fan transport)*- Pilot ratings for landings made in the various environmental conditions specified in table 6 are shown in figure 24. These ratings increase progressively with increasing sea state, going from about 2.5 to 3 in calm conditions, through 3.5 in sea state 4, to about 6 to 6.5 in sea state 6. The ratings of all three pilots were consistent. The tests reported in reference 2 gave a pilot rating of about 3 in sea state 4; however, these tests did not include a ship air-wake turbulence model. The pilots gave as the principal reason for the increase of workload with sea state the increasing difficulty of matching the aircraft and ship motion at touchdown. The ship air-wake turbulence became more noticeable as the WOD increased, but the additional workload to cope with it was always relatively small. This result differs from that of reference 3, which indicated that ship air-wake turbulence was the principal determinant of pilot rating during landing. These differing results are most probably due to the different altitude of approach to the final station-keeping point. However, it could be that known deficiencies in the landing gear model used in tests reported in reference 3 may have led to less emphasis on the actual touchdown than in the tests reported here, and thus have been a factor in the results.

The technique adopted by the pilots to perform the descent is of interest. After stabilizing the aircraft at the final station-keeping point, a rate of descent of about 1 m/sec (220 ft/min) was commanded and maintained until the top of the hangar came into view (figs. 19(d) and 20(d)). At this point the rate of descent was arrested. Attention was then focused almost entirely on the position of the deck indicator on the HUD, and a few cycles of the ship motion were observed. When the time was judged to be appropriate, the aircraft was again commanded to descend at 0.5 to 1.0 m/sec (1.6 to 3.3 ft/sec) to touchdown when the ship was at its maximum upward amplitude (zero vertical velocity). No attempt was made to match the aircraft attitude to that of the ship. The judgment of when to make the final rate-of-descent command was clearly crucial. The touchdown rates of descent, using this technique, were surprisingly consistent, as will be seen later.

It was clear, from these tests, that very little effort was required of the pilot to maintain the horizontal position of the aircraft, even in the highest turbulence levels. This was because of the good disturbance rejection characteristics of the SRFIMF and was a major contributor to keeping the overall task workload within reasonable bounds.

*Landing (Type 1 system; AV-8A Harrier)*- Pilot ratings for the AV-8A Harrier landings are given in figure 25. These results are comparable to those of figure 24 for the lift-fan transport. The only difference between the Type 1 systems assumed for the two aircraft was that the AV-8A Harrier used stick-commanded angle of bank and a lateral flight director for lateral

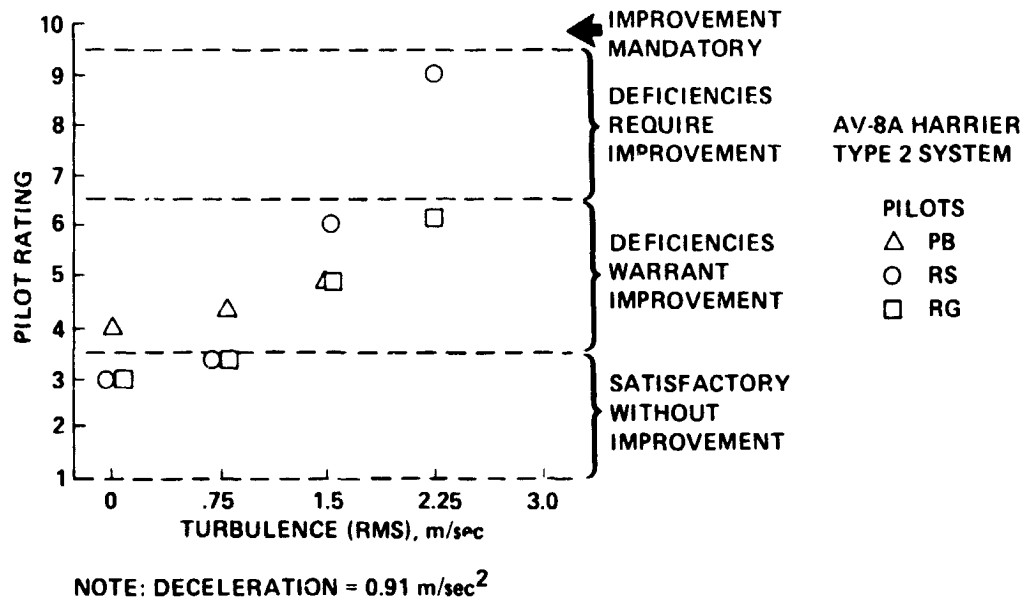


Figure 23.- Pilot ratings for transition (various turbulence levels).

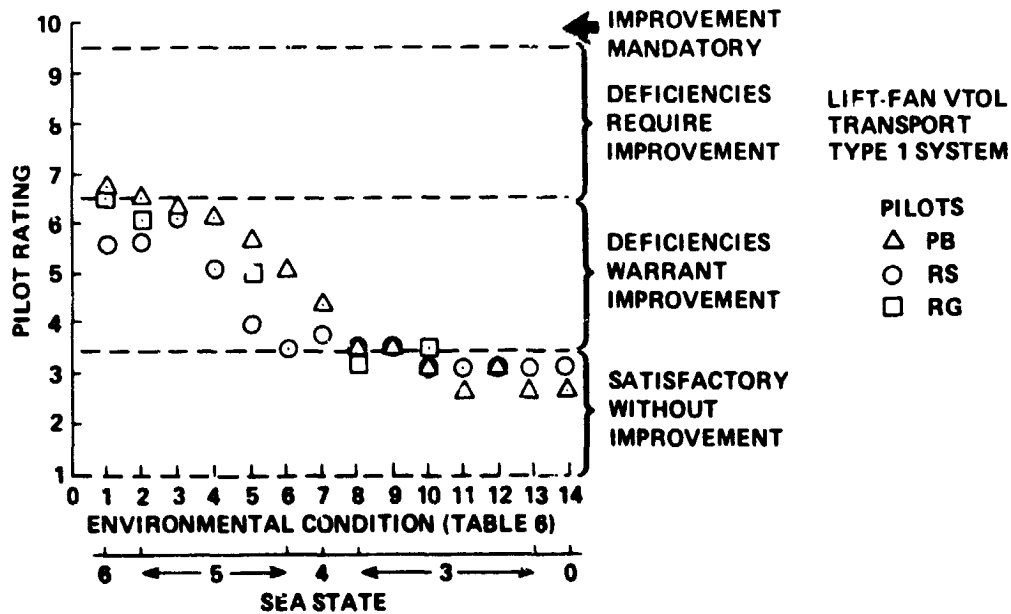


Figure 24.- Pilot ratings for landing from initial station-keeping point: lift-fan VTOL transport; Type 1 system.



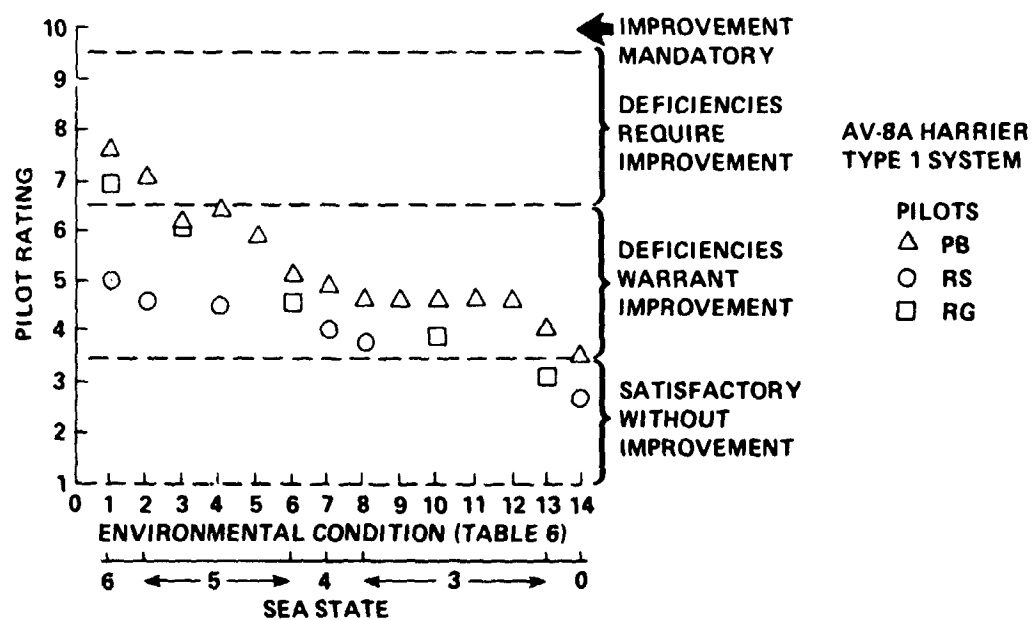


Figure 25.- Pilot ratings for landing from initial station-keeping point:  
AV-8A Harrier; Type 1 system.

positioning, rather than thumb-button commanded lateral velocity (through thrust deflection). The landing technique used with the Harrier differed somewhat from that used with the lift-fan transport. The Harrier pilots knew from experience that the time during which the aircraft was close to the ground must be minimized to avoid serious thrust loss as a result of hot-gas ingestion. Therefore, rather than arresting the rate of descent close to the deck, as with the lift-fan transport, they made a continuous final descent to touchdown. This technique naturally required better judgment of when to start the descent. In addition, extra work was required to keep the lateral flight director centered, a task rendered more difficult by the poor harmony between the two horizontal positioning controls (left hand operating the thumb button for longitudinal positioning and right hand operating the stick for lateral positioning).

Considering the previously stated differences between the Type 1 system as applied to the lift-fan transport and the AV-8A, it is surprising that the pilot ratings shown in figures 24 and 25 differ by only about 1 to 2 units and then mostly at the lower sea states. These results tend to mask the fact that the pilots stated that it was markedly easier to control lateral position using a lateral-velocity command than with bank-angle command.

During these tests it was noted that, in high turbulence, there was a tendency for the aircraft to lose altitude slowly. This effect was due to the flight controller occasionally commanding a thrust greater than that available. The effect had not been noticed in the tests using the lift-fan transport, even though the thrust/weight ratios of the two aircraft were the same (i.e., 1:1). The most probable reason for this is that the time required to make landings with the Harrier averaged 20 sec longer than with the lift-fan transport (see the following subsection, Task Performance Parameters), thus affording more time for the phenomenon to be observed. The pilots had no difficulty correcting for the altitude loss but the necessity to do so added to an already rather high workload.

*Landing (Type 2 system; AV-8A Harrier)*- At the start of these tests it was quickly determined that the use of pitch attitude to control longitudinal translation was undesirable (the pilots were unanimous on this point). The problem was caused by the relatively high sensitivity of the pitch flight director to velocity and acceleration errors. This sensitivity was due, in large measure, to the design techniques used (see the previous discussion of the hover flight director). To maintain the pitch flight director roughly centered the pilots commanded quite large ( $\pm 5^\circ$ ) pitch attitude changes. The corresponding HUD pitch ladder activity distracted and occasionally disoriented the pilot, who was trying to concentrate on the part of the HUD format representing the horizontal projection of the landing pad. To overcome this problem, longitudinal translation control was obtained by small (within  $\pm 10^\circ$ ) changes in the thrust vector angle ("nozzle nudging") keeping pitch attitude constant. The pilot's control for this function was located on top of the power lever (fig. 4). Both "bang-bang" and proportional systems were tried, with the proportional system being finally adopted for the tests. This proportional nozzle nudger was operated in conjunction with the existing hover

flight director and resulted in a more satisfactory system, even though the flight director had not been designed for this type of control.

The pilot rating results shown in figure 26 were obtained for landings using the proportional nozzle-nudger system. These ratings should be compared with those given in figures 24 and 25. It can be seen from figure 26 that the workload using the Type 2 system was 2 to 4 rating units worse than the best Type 1 system (fig. 24). In fact, for sea states higher than 4, the Type 2 system was unacceptable (pilot ratings greater than 6.5) and even in calm conditions the workload was quite high.

The main difficulty with the Type 2 system was that the flight directors had to be followed closely at all times. Since there is virtually no translational damping in hover, preoccupation with one of the degrees of freedom soon resulted in significant errors in the other two. Furthermore, once the flight directors got too far from their null positions, a period of very high pilot activity was required to recover to the desired status.

The pilots also found it difficult to select a good time to press the button to start the scheduled descent command of the vertical flight director. The scheduled descent took about 15 sec, and the pilots were not able to predict the ship motion that far in advance. The technique finally adopted was to follow the vertical flight director down to a point about 2 to 3 m (6.6 to 9.8 ft) above where the mean deck height was judged to be and then to use the deck height indicator to make the final touchdown. Considering that the vertical control was unaugmented, this task was quite demanding in high sea states.

#### Task Performance Parameters

*Transition-* A comparison of the transition times for the AV-8A with the Type 1 system and the AV-8A with the Type 2 system is shown in figure 27. In almost all cases the transition time exceeds that which would be obtained if the reference velocity schedule were followed exactly. The additional time was needed by the pilots to make final corrections to acquire the initial station-keeping point. With the Type 1 system this additional time was about 20 to 30 sec and was independent of turbulence level. With the Type 2 system, the additional time was again about 20 to 30 sec up to a turbulence level of about 1.5 m/sec (5 ft/sec) after which it increased quite rapidly (fig. 27). This rapid increase of time was a result of the progressively greater effort required to follow the flight directors (vertical longitudinal and lateral), and this is reflected in the pilot rating results shown in figure 23.

The maximum and rms longitudinal velocity errors are shown in figure 28. These errors are only mildly influenced by turbulence level. The errors with the Type 2 system were several times larger than those with the Type 1 system, principally because the parameters of the Type 2 system longitudinal flight director were set so that the pilot workload would be low; however, this could be done only at the expense of speed control accuracy. It should be noted that the maximum velocity errors shown in figure 28 all occurred in the first

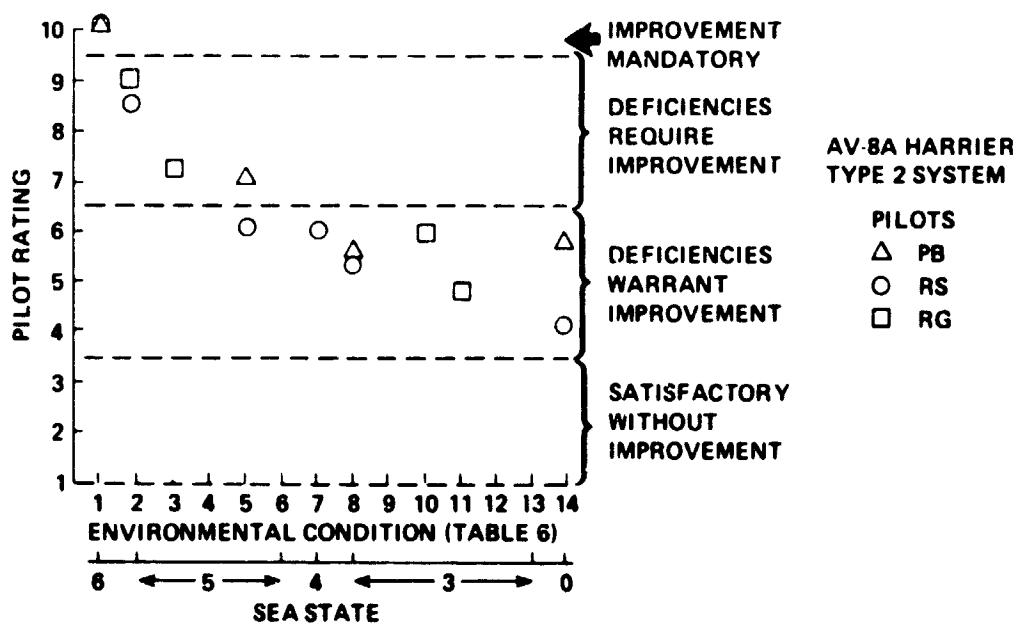


Figure 26.- Pilot ratings for landing from initial station-keeping point.  
 AV-8A Harrier; Type 2 system.

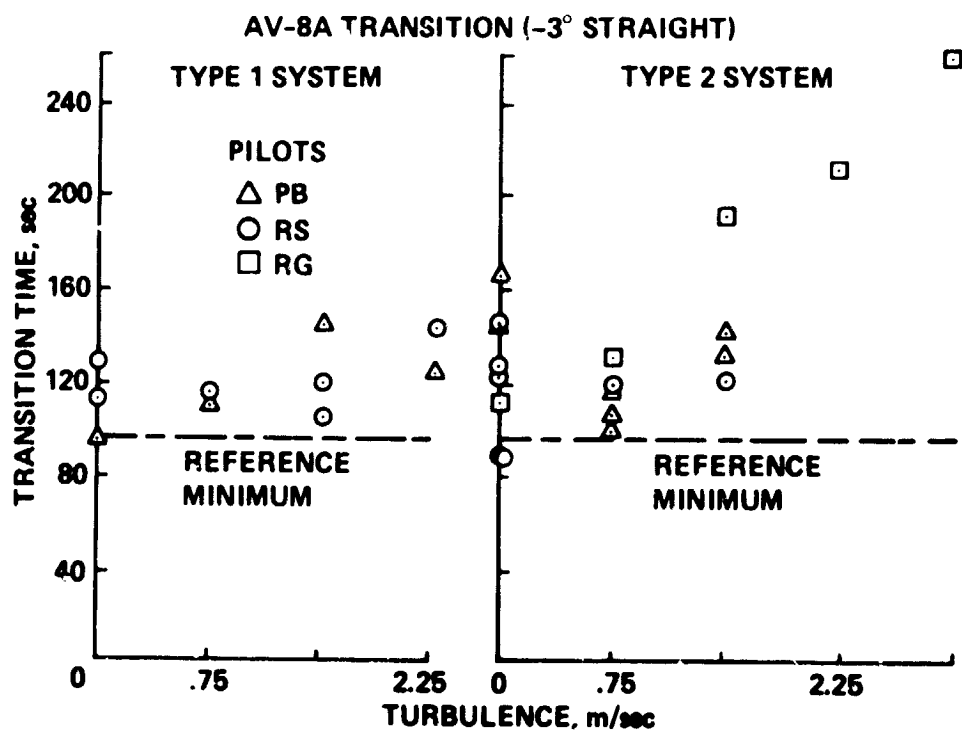


Figure 27.- Transition times.

AV-8A TRANSITION  
(-3° STRAIGHT)

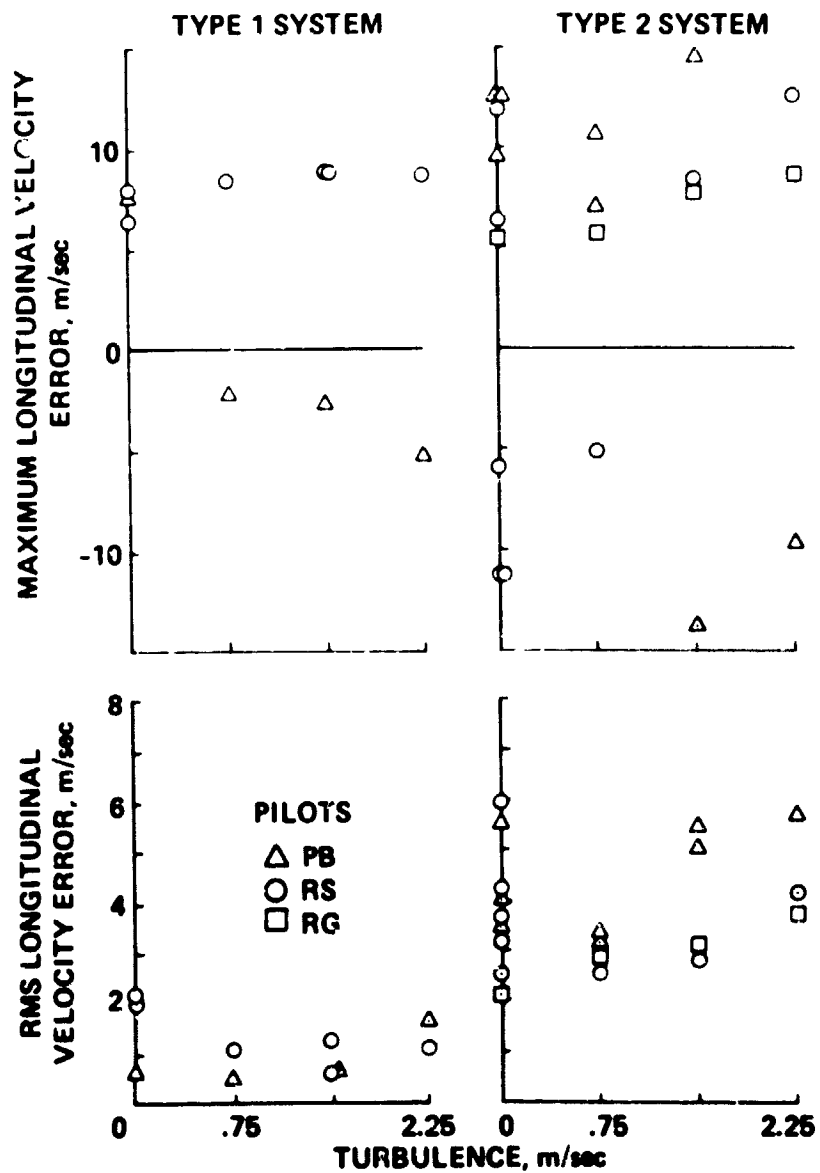


Figure 28.- Velocity errors in transition.

two-thirds of the transition. With either type of system the velocity errors when the aircraft was close to the initial station-keeping point were small (less than 2 m/sec (6.6 ft/sec)) and caused the pilot no problems in acquiring the initial station-keeping point. However, as noted earlier in this report, it was found late in the tests that under some conditions, with the Type 2 system, velocity errors close to the initial station-keeping point can be as large as 5 m/sec (16 ft/sec) (see the following subsection, Evaluation of the Flight Directors).

On the question of speed control during transition, it is important to recognize that the magnitude of speed errors is largely of academic interest. Pilots expressed no concern about large speed errors, because they recognized that the reference speed schedule adopted was arbitrary. Indeed, a good case can be made for adopting a speed schedule tailored to the drag characteristics of the particular aircraft, since such a speed schedule would minimize the number of thrust-vector-angle changes needed during transition. All that matters to the pilots is that the workload be low, that adequate safety margins be maintained, and that the speed error at the end of transition be sufficiently low to permit capture of the initial station-keeping point without making large thrust-vector-angle or pitch-angle changes.

The maximum and rms altitude errors are shown in figure 29. Again, these errors are only weakly dependent on turbulence level, and again the errors are several times greater with the Type 2 system than with the Type 1 system. Altitude errors when using the Type 1 system are introduced when the pilot does not exactly match the desired rate of descent indicated by the flight director. In these tests the mismatches were usually less than 1 m/sec (197 ft/min) and were corrected by the pilot within 5 sec. It follows that the altitude errors were never greater than about 5 m (16 ft), as shown in figure 29. On the other hand, with the Type 2 system, the pilots were generally slow to follow the vertical flight director during the deceleration. At the start of the deceleration the pilot increases the thrust vector angle, using the TVRS, and the vertical flight director responds by indicating a need to reduce power to prevent "ballooning" above the flightpath (fig. 12). Slow pilot reaction to this flight director signal was responsible for the large positive altitude errors shown in figure 29. When the deceleration is fully established, the dynamic pressure falls rapidly and the vertical flight director indicates a need to increase power to compensate for the loss of wing lift (fig. 12). Slow pilot reaction to this flight director signal was responsible for the large negative altitude errors. These latter errors are, of course, the most dangerous, particularly since they occur at relatively low altitudes.

*Landing-* A comparison of the times taken from the initial station-keeping point to touchdown for the three major configurations tested is shown in figure 30. As might be anticipated, the time required to make the landing increases as the complexity of the control/display system decreases. The progression of average times is 69 sec for the lift-fan transport with the Type 1 system, 89 sec for the AV-8A with the Type 1 system, and 113 sec for the AV-8A with the Type 2 system. Note, however, that the time required is independent of sea state for the Type 1 system, but increases with increasing sea state for the Type 2 system (reaching 170 sec for sea state 6). These results show

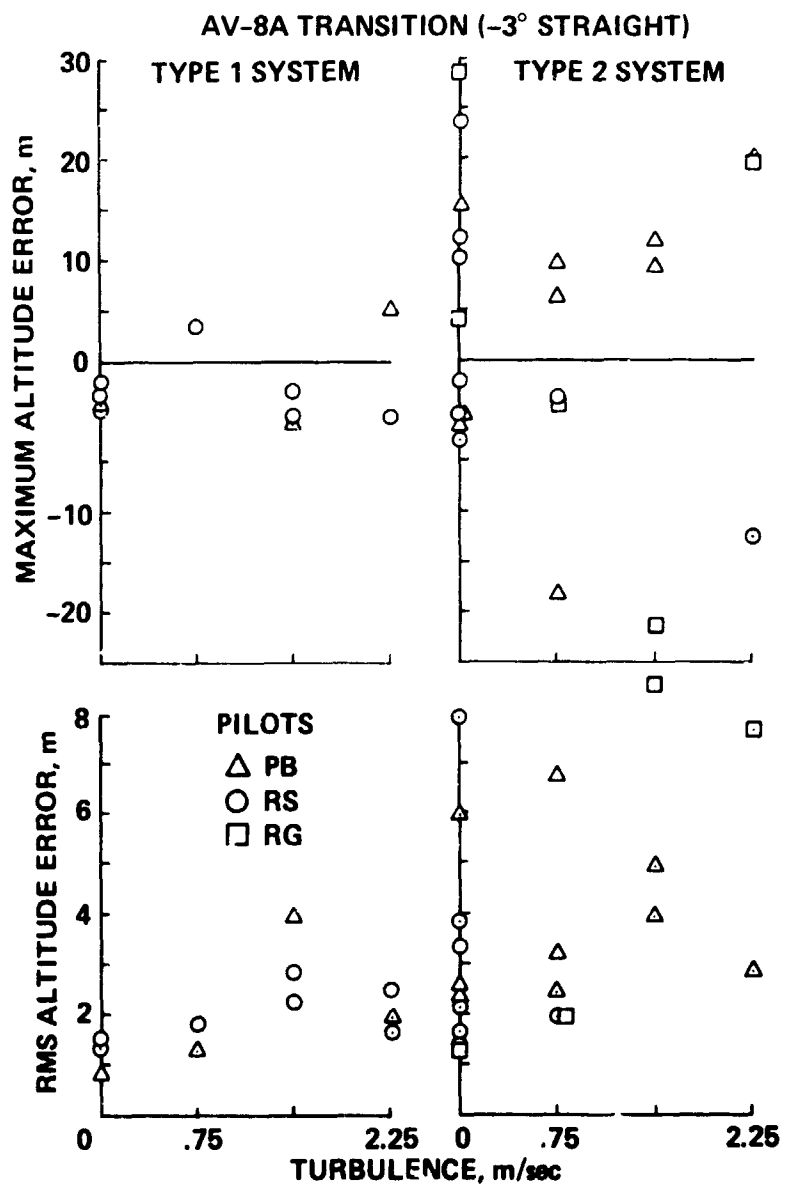


Figure 29.- Altitude errors in transition.



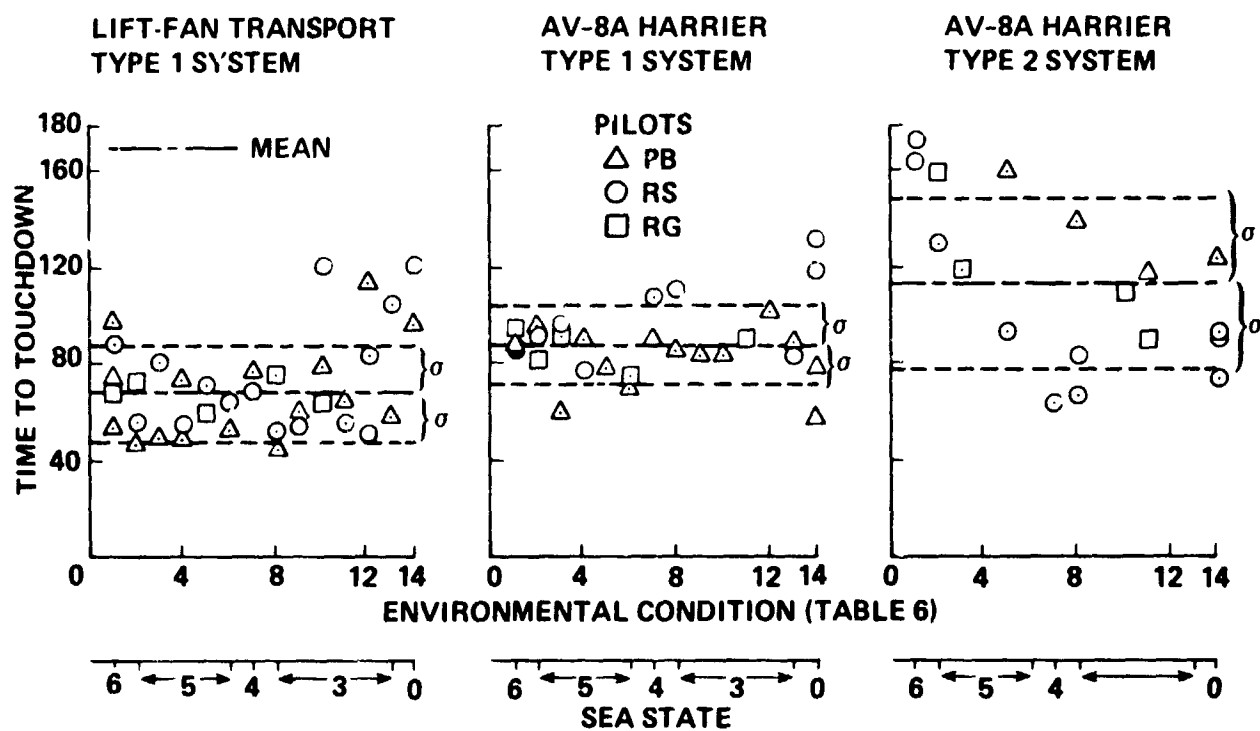


Figure 30.- Time from initial station-keeping point to touchdown.

that although the provision of lateral-velocity command through lateral-thrust deflection does not seem to yield great benefits in pilot rating (compare figs. 24 and 25), it can save a significant amount of time (20 sec) and fuel during the high-power phase of the landing. This result shows that considerable performance benefits can accrue from the use of sophisticated control systems, even though these benefits may not be reflected in the pilot ratings.

The effect of the type of control/display system on horizontal position error and maximum wheel vertical velocities at touchdown is shown in figures 31 and 32, respectively. (The "wheel vertical velocity" is the velocity of the wheel relative to the ship's deck measured along the oleo axis.) With the Type 1 system, position error and wheel vertical velocity follow landing time in being independent of sea state. With the Type 2 system, both parameters again follow landing time by trending upwards with increasing sea state. It can be seen from figure 31 that the average position error for the AV-8A using the Type 1 system is higher than for the lift-fan transport. This difference is due to the greater lateral errors for the AV-8A, and reflects the difficulty of precise control using bank-angle command rather than lateral-velocity command. With the Type 1 system, touchdowns were always within a 2-m (6.5-ft) radius of the desired point. Touchdown position errors increased dramatically using the Type 2 system and were as high as 5.5 m (18 ft), with the distribution of longitudinal and lateral errors being roughly equal. Considering that the landing pad of the DD964 is only about 12 m (40 ft) square, errors of this magnitude would preclude operation in high sea state with a Type 2 system. This conclusion merely reinforces that which is already evident from figure 26.

With only two exceptions, the highest wheel vertical velocities were within the landing gear limits. Landing gear limits were exceeded once (5.2 m/sec (17 ft/sec)) with the lift-fan transport and the Type 1 system. That particular flight was made early in the tests, when pilot experience in the tests was low, and is not supported by the general trend shown in figure 32. The gear limit was exceeded a second time in tests with the AV-8A and the Type 2 system; that flight was made later in the tests and is supported by the general trend.

It should be noted that the highest wheel vertical velocity is a much more reliable measure of a landing than the vertical velocity of the aircraft's center of gravity. As an illustration, for the unsatisfactory landing that resulted in a maximum vertical wheel speed of 5.2 m/sec (17 ft/sec), the vertical speed of the center of gravity was only 1.68 m/sec (5.5 ft/sec); therefore, based on vertical velocity of the center of gravity, the landing would have been judged satisfactory.

#### Evaluation of the HUD Format

All HUD formats are compromises resulting from the attempt to pack as much useful information as possible into the simplest display. Pilot reaction to a HUD is necessarily highly subjective. The value of the pilot's criticism depends strongly on his experience in performing the kind of task for which

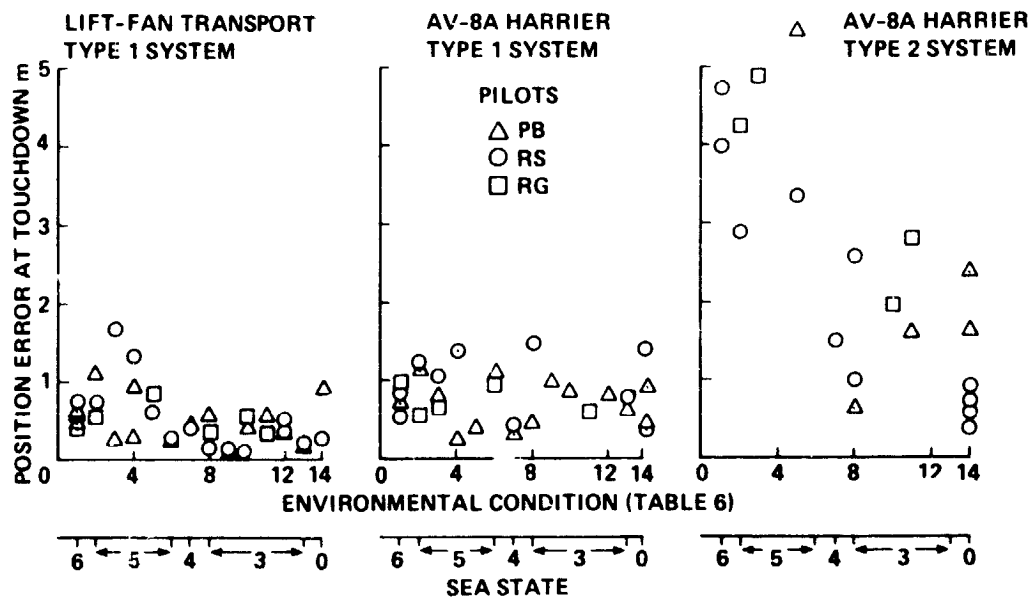


Figure 31.- Position errors at touchdown.

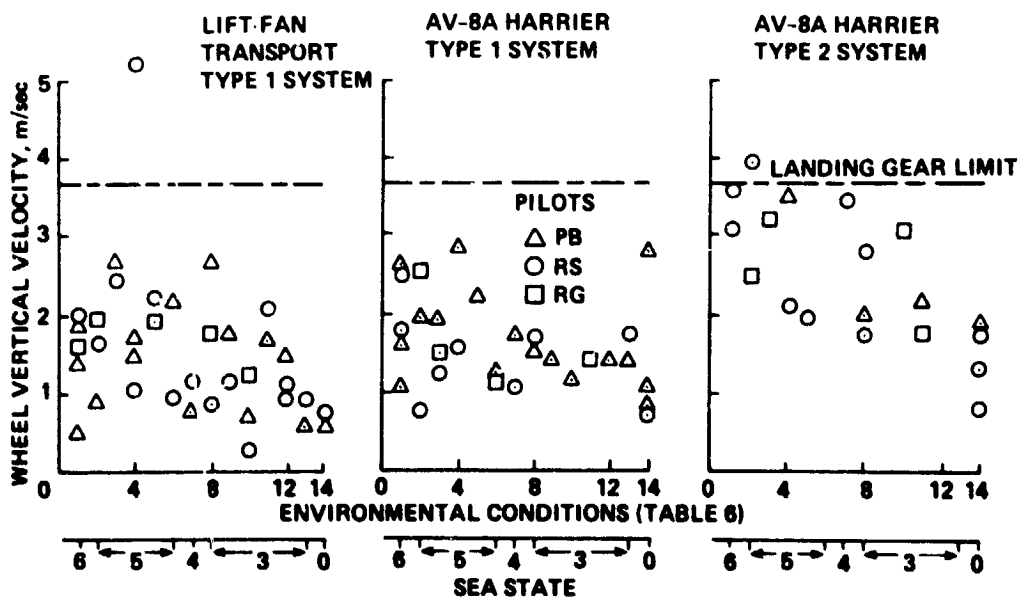


Figure 32.- Highest wheel vertical velocities at touchdown.

the HUD is designed. The HUD formats for both the Type 1 and Type 2 systems proved to be adequate in the sense that the tasks could be performed using them; however, many deficiencies were noted by the pilots. Pilot PB, who had the greatest experience with the VTOL shipboard landing task, was the principal identifier of HUD format deficiencies.

*Attitudes-* The pitch ladder used in both the Type 1 and Type 2 displays was unsatisfactory because there was no distinction between positive and negative attitudes. The  $3^\circ$  interval was satisfactory and provided a useful visual approach slope indicator for  $-3^\circ$  straight approaches. The pitch trim indicator was well received.

The aircraft symbol was unsatisfactory for judging bank angle. The symbol wings were too short for judging small bank-angle discrepancies, and even larger bank angles were difficult to judge accurately. The digital bank-angle display used for the Type 1 system (fig. 3) partially compensated for this deficiency but was difficult to assimilate because of the clutter in the center of the display.

Angle of attack was not displayed on the Type 1 HUD. This was unsatisfactory, since the control system did not include any form of angle-of-attack limiting. An audible warning of excessive angle of attack may be an acceptable alternative to displaying angle of attack on the HUD.

*Position-* The lateral flight director symbol was satisfactory, but the pilot occasionally misread it and started to roll the wrong way. This error was immediately apparent and easily corrected. The reason for the problem was not clear. Initially, the fin on the aircraft symbol was taller than the lateral flight director bar. Later, the fin was reduced in size and this change seemed to help.

Lateral, vertical, and longitudinal position information was available, in digital form only, at the bottom of the display. In this form this information was difficult to include in the scan pattern and to assimilate. Since lateral and longitudinal position information are not critical to flight safety, the method used to display these quantities was acceptable. However, altitude information is vital to flight safety and should be given a much more prominent position on the display. On several approaches, using the Type 2 system, the pilot became mesmerized by the three flight directors clustered in the center of the HUD and failed to notice that the altitude had fallen below the desired 25 m (82 ft) of the initial station-keeping point.

The display of horizontal situation information superimposed on the vertical attitude display was only acceptable if the pitch attitude was held more or less constant. Lateral positioning caused no problem, for left bank caused movement to the left and vice versa. With the originally conceived Type 2 system, however, longitudinal positioning caused confusion: a pitch-down maneuver caused forward motion of the aircraft but caused the pitch ladder to translate upward on the display. In other words, it is unsatisfactory to superimpose horizontal and vertical information, if the method of control causes these two parts of the display to give confusing signals to the pilot.

The pitch flight director bar used in the Type 2 system added to the mental confusion. In a conventional aircraft, an upward movement of the pitch director bar is a command to the pilot to pitch up to climb. In the VTOL case, an upward movement of the pitch director is a command to pitch down to move forward. The conflict arises, of course, because in conventional flight, pitch angle controls vertical motion whereas in hover it controls horizontal motion. It is clearly not good practice to devise a control/display system that conflicts with the pilot's previous experience. As mentioned earlier, the problem was resolved by using the thrust vector angle to control longitudinal position, while maintaining pitch attitude constant.

On two occasions during tests with the Type 2 system, the pilot allowed the aircraft to drift into a position where it would have contacted the ship's superstructure. In reality this would be an unlikely occurrence because the field of view would be less restricted. However, some indication of the proximity of the superstructure should be added to the HUD.

The pilots also would like the HUD to indicate the proximity of the wheels to the edge of the deck. Their judgment of that distance was difficult because the size of the ship symbol increased with decreasing altitude, whereas the aircraft symbol remained fixed in size. Since the variation of ship symbol size did not add much to the pilot's impression of altitude, it was suggested that a ship symbol of constant size would be better.

*Velocity and acceleration-* The velocity indication in the Type 1 system HUD, and acceleration indication in the Type 2 system HUD, were too far out of the normal scan pattern and could easily be missed. Scanning problems were also evident because of the wide separation of the flight director symbols of the Type 1 system. On several occasions, the initial movement of the longitudinal flight director symbol, indicating the required deceleration, was missed by the pilot, as was its final return to zero when the aircraft was close to the initial station-keeping point. When these important events were missed, the pilot had to work hard to regain the scheduled longitudinal speed. On other occasions, the pilot, while concentrating on the longitudinal flight director toward the end of transition, would fail to realize that the vertical flight director was calling for a reduced rate of sink, and would end up at the initial station-keeping point somewhat below the required 25-m (82-ft) altitude. Clearly, the solution to these problems is to avoid large scanning angles in the pilot's primary scan pattern, and to provide commanding elements of HUD symbology that both alert the pilot of dangerously large errors and of the impending need for large control inputs.

#### Evaluation of Pilot Control Modes

All the attitude modes shown in table 1 were satisfactory and the blending from one mode to the next as speed changed passed without comment. The Type 1 system translational control modes, shown in table 2, were satisfactory for general flying in the powered-lift flight envelope, but two problems were noted during the approach and landing tests. When flying a straight approach transition, the pilot must gradually reduce the commanded rate of descent in

order to maintain the glide slope during the deceleration. Although the workload for the task was not excessive, it could clearly have been reduced if the vertical flight controller mode were flightpath-angle command rather than velocity command. Then the pilot would need to move the lever once to establish the desired approach path angle. However, such a mode would clearly be less satisfactory in hover. Therefore, a mode switch would be required to maintain the current vertical control mode in hover. The problem here is that when the mode switch is made, the height control lever would not be in the detent and in fact would be in a position corresponding to a large commanded downward velocity. This problem would be avoided if the pilot remembered to set the lever in the detent just prior to pressing the mode-change switch, but that solution would place a dangerous reliance on the pilot's memory. A possible solution to this problem is to servo the lever so that when the pilot presses the mode change switch the lever is automatically returned to the detent (zero vertical velocity) position. An alternative solution is to use separate pilot controls for the two modes.

The other problem with the Type 1 system translational control modes was that during the hover maneuvers, in turbulence, the aircraft tended to lose altitude. This problem, which was mentioned previously (Pilots' Evaluations), was due to limitations in the thrust available. The pilots were of the opinion that in hover conditions an altitude-hold feature is desirable.

Although the pitch and roll attitude command modes in hover had satisfactory dynamic characteristics, it was clear that even with a flight director precision IMC hover maneuvers, using the Type 2 system, were difficult, especially in high turbulence. The problem is due to low translational damping. Translational rate command modes, through attitude, for both longitudinal and lateral positioning would clearly be far superior. Furthermore, the additional control system complexity would be small, and there is the strong possibility that a hover flight director would be unnecessary.

#### Evaluation of the Flight Directors

HUD format aspects of the flight directors have already been mentioned (see Evaluation of the HUD Format). A general criticism of the directors was that they took no account of the aircraft performance or flight envelope limitations, and if followed blindly could lead the aircraft into the ship superstructure.

The dynamic characteristics of the Type 1 system flight directors were satisfactory, but those of the Type 2 system were decidedly unsatisfactory for several reasons.

The Type 2 system vertical flight director was too sensitive to turbulence at the higher speeds (60 to 120 knots) and too insensitive to altitude errors in hover. The sensitivity to turbulence at the higher speeds was due to the higher-than-normal bandwidth designed into the director. The high bandwidth was provided to overcome the effects of the rapidly varying aerodynamic lift during the deceleration. A better approach to the vertical

flight director design may be to omit the vertical acceleration feedback (fig. 11), reduce the bandwidth, and apply open-loop signals to allow for the varying aerodynamic lift. The problem of insensitivity to altitude in hover can be alleviated by increasing the altitude error gain, while adjusting the velocity gain to obtain suitable damping characteristics.

The Type 2 hover flight directors were too sensitive to turbulence and too insensitive to longitudinal or lateral position errors. Both of these problems can be alleviated by omitting the acceleration feedbacks and by adjusting the flight director gains and the sensitivity of the flight director bars on the HUD (fig. 5(c)).

The major problem with the longitudinal (thrust-vector-angle) flight director was that under some conditions substantial residual velocities and accelerations existed at the end of transition, making it difficult for the pilot to acquire the initial station-keeping point. The reason for this problem is clear from figure 7, which shows that the end of the phase-plane locus (point H) can be anywhere between the two switching lines and can be some distance from the origin. For most of the tests, the initial conditions for the approach were set so that the final point H of figure 7 was close to the origin, and no problems were encountered. Later, the initial conditions were changed and the point H had phase-plane coordinates of up to 3 m/sec and 1 m/sec<sup>2</sup> (9.8 ft/sec and 3.3 ft/sec<sup>2</sup>). With errors of this magnitude, it was difficult for the pilot to acquire the initial station-keeping point. It should be noted, however, that part of the difficulty may have been due to the scaling adopted for the horizontal situation display part of the HUD.

There are at least two ways to improve the longitudinal flight director. One is to reshape the switching lines to reduce the effective dead band. This technique has the disadvantage of increasing the number of times the pilot must press the TVRS. The other is to automatically switch to another set of switching lines defined on the phase plane of velocity and acceleration errors relative to the initial station-keeping point. The switch to the new phase plane could be operated when the longitudinal distance to the initial station-keeping point is less than some preset value (say 15 m). The switching lines on the new phase plane could be arranged so that the final dead-band errors in velocity and acceleration relative to the initial station-keeping point are small (say 0.3 m/sec and 0.1 m/sec<sup>2</sup> (1 ft/sec and 0.3 ft/sec<sup>2</sup>), respectively).

#### Evaluation of the Pilot's Controls

The pilots noted that when using the Type 1 system the control actions required were not well-balanced between the two hands. The left hand must operate the thumb wheel, thumb button, and vertical velocity lever; the right hand operates the stick only. Furthermore, since pitch attitude remains constant, no longitudinal stick inputs are required, and lateral stick inputs are only required to acquire and hold the localizer during transition. It was suggested that a better balance could be achieved if the thumb wheel (longitudinal acceleration control) was transferred from the vertical velocity lever to the stick.

When operating either of the two control/display systems, pilot PB did not like the required changeover from thumb wheel (Type 1) or thumb switch (Type 2) to thumb button (figs. 2 and 4) at the end of transition. Provided lateral thrust deflection is not a control feature of the aircraft, the two controls for either system could be integrated into a single control, with the control mode change made when the pilot presses the hover switch on the stick (switch No. 1, fig. 15).

The force-proportional thumb buttons were not entirely satisfactory. All the pilots would have preferred a button with more compliance and less force required for full control. Also, the convex shape of the button was uncomfortable, especially when applying rearward thumb pressure. The pilots were of the opinion that a concave button fitting the shape of the thumb would have been better.

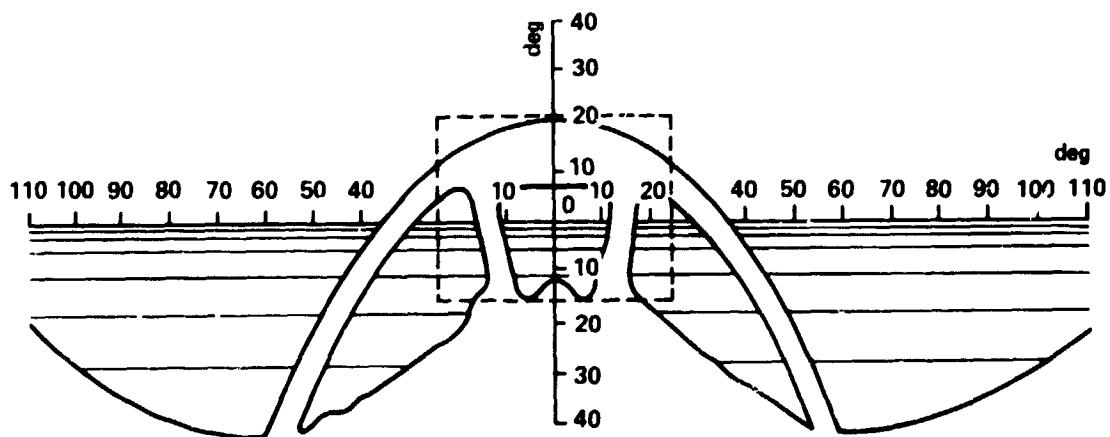
The detents in the vertical velocity lever and thumb wheel were regarded by the pilots as being not positive enough. Occasionally, the pilots had to "jiggle" these controls to assure themselves that the controls were in their detents. In addition, the thumb wheel had a slight springiness in its motion, which influenced the job of precisely commanding the desired acceleration. Also, the thumb-wheel scaling, although satisfactory for low-deceleration transitions ( $1 \text{ m/sec}^2$  ( $3.3 \text{ ft/sec}^2$ )), was not suitable for high-deceleration transitions, because two thumb movements were required to rotate the thumb wheel to the correct position. This latter problem indicates a possible need for a nonlinear scaling of the thumb wheel.

#### Simulation Equipment Limitations

The equipment limitation judged to be the most serious for landing on a ship was the small field of view of the visual attachment. A comparison of the fields of view from the pilot stations in the FSAA and the AV-8A is shown in figure 33. The problem caused by the restricted field of view is evident from figures 19 and 20, which clearly show the lack of peripheral visual information. An extreme situation is shown in figure 19(c), where the aircraft is directly above the touchdown point and no part of the ship is visible to the pilot. In fact, with the aircraft heading shown in figure 19, the ship could not be seen for a substantial part of the hover maneuvers and during final descent. If, in addition, the horizon had been obscured, the view would have been of no value to the pilot. The situation would have been vastly different had the field of view been comparable to that from the cockpit of the AV-8A, as is evident from figures 34 and 35.

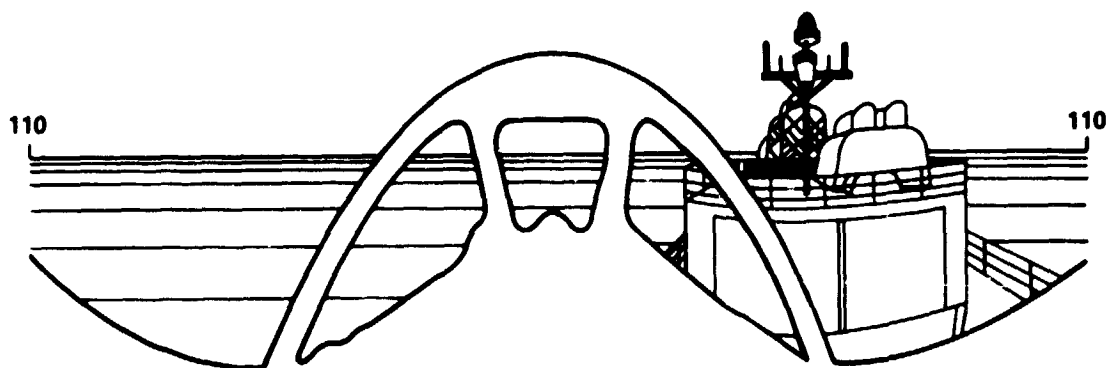
With the restricted field of view and without the information displayed on the HUD, landing would have been possible only for a restricted range of aircraft headings, similar to that of figure 20, and only using the Type 1 system, including lateral velocity command (lift-fan transport aircraft). However, even with the restricted field of view some useful information was provided. The pilots stated that they used the view of the ship's superstructure as confirmation of the information given on the HUD and, in some cases,





NOTE: LANDING ATTITUDE ( $6.5^\circ$ )

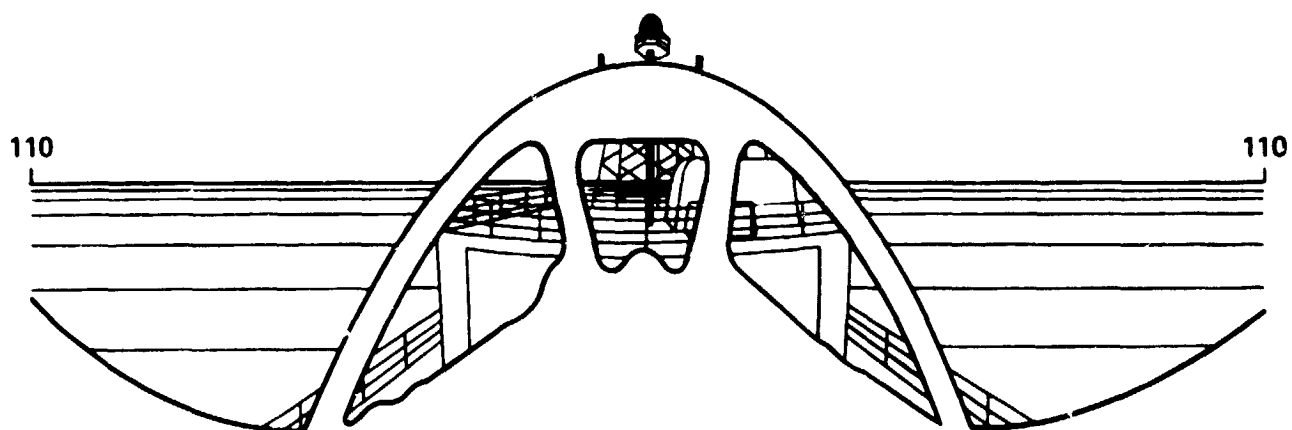
Figure 33.- Comparison of AV-8A (Harrier) and FSAA fields of view.



NOTE: LANDING ATTITUDE ( $6.5^\circ$ )

PILOT'S EYE 7.62 m (25 ft) ABOVE DECK  
3.66 m (12 ft) FORWARD OF TOUCHDOWN POINT  
AIRCRAFT  $45^\circ$  TO SHIP AXIS

Figure 34.- View of ship (DD963) from AV-8A Harrier.



**NOTE: LANDING ATTITUDE (6.5°)**

**PILOT'S EYE 7.62 m (25 ft) ABOVE DECK  
3.66 m (12 ft) FORWARD OF TOUCHDOWN POINT  
(9.1 m (30 ft) FROM HANGAR)**

**Figure 35.- View of ship (DD963) from AV-8A Harrier.**

even adopted a descent technique that used some elements of the visual scene (see Pilots' Evaluations, Landing).

It is clear from figures 34 and 35 that a wider field of view would make the landing task easier, although the greatest effect would be on an aircraft equipped with a Type 2 system. The principal problem in using the Type 2 system, with its attitude command, is that the pilot must provide the required translational damping and, as has been noted, precision hovering implies high workload, using HUD information and the small amount of visual scene information available with the FSAA. This situation could change dramatically with the provision of a wide field of view, because the pilot would be able to distinguish between the various types of motion quicker; thus, it would be easier for him to provide translational damping. It is even possible that the hover flight directors may be made unnecessary. Confirmation of these speculations must await the completion of a wide-angle visual attachment. This piece of equipment should permit a reasonable approximation to the field of view shown in figures 34 and 35.

Another equipment limitation was that the ship-motion device did not provide surge and sway, relative to the ship's center of gravity, or yaw. Some idea of the relative importance of the omitted degrees of freedom can be obtained from figures 36-38. These three figures show the pitch, roll, and yaw of the ship and the translational motion of the nominal touchdown point, in sea state 6; these motions are shown first with all degrees of freedom active, then with surge and sway suppressed, and finally with surge, sway, and yaw suppressed. It is clear that surge (of the ship's center of gravity) has an insignificant effect on the overall motion of the touchdown point. On the other hand, both yaw and sway have a significant effect on the lateral motion of the touchdown point. With all degrees of freedom active (fig. 36), the maximum lateral movement is about 2.5 m (8.2 ft). With sway suppressed (fig. 37) lateral movement is reduced to about 2 m (6.6 ft), and with both sway and yaw suppressed (fig. 38) to about 1.5 m (5 ft). Since the landing pad is only 12 m (40 ft) wide, it is feasible that the inclusion of sway and yaw could influence the landing task significantly. An evaluation of the effects of the missing degrees of freedom must await the completion of a full six-degree-of-freedom ship-motion device.

Finally, in all the transition tests, the speed of the aircraft exceeded the capability of the visual attachment. At the selected scale of 250:1 the maximum full-scale speed that could be represented was 100 knots, whereas all the transitions started at 120 knots. For most of the tests the speed limit presented no problem since, with the fog ceiling and RVR set at 30 m and 213 m (100 ft and 700 ft), respectively, the visual attachment had time to catch up with the true aircraft position before the pilot could see the ship. However, at the highest scheduled deceleration of  $2.74 \text{ m/sec}^2$  ( $9 \text{ ft/sec}^2$ ), the visual attachment did not have time to catch up, and the pilot received the visual impression of excessive closure speeds and decelerations. Had time been available during the tests the problem could have been overcome by starting the longitudinal drive of the visual attachment at any point along the trajectory where the aircraft speed was less than 100 knots.

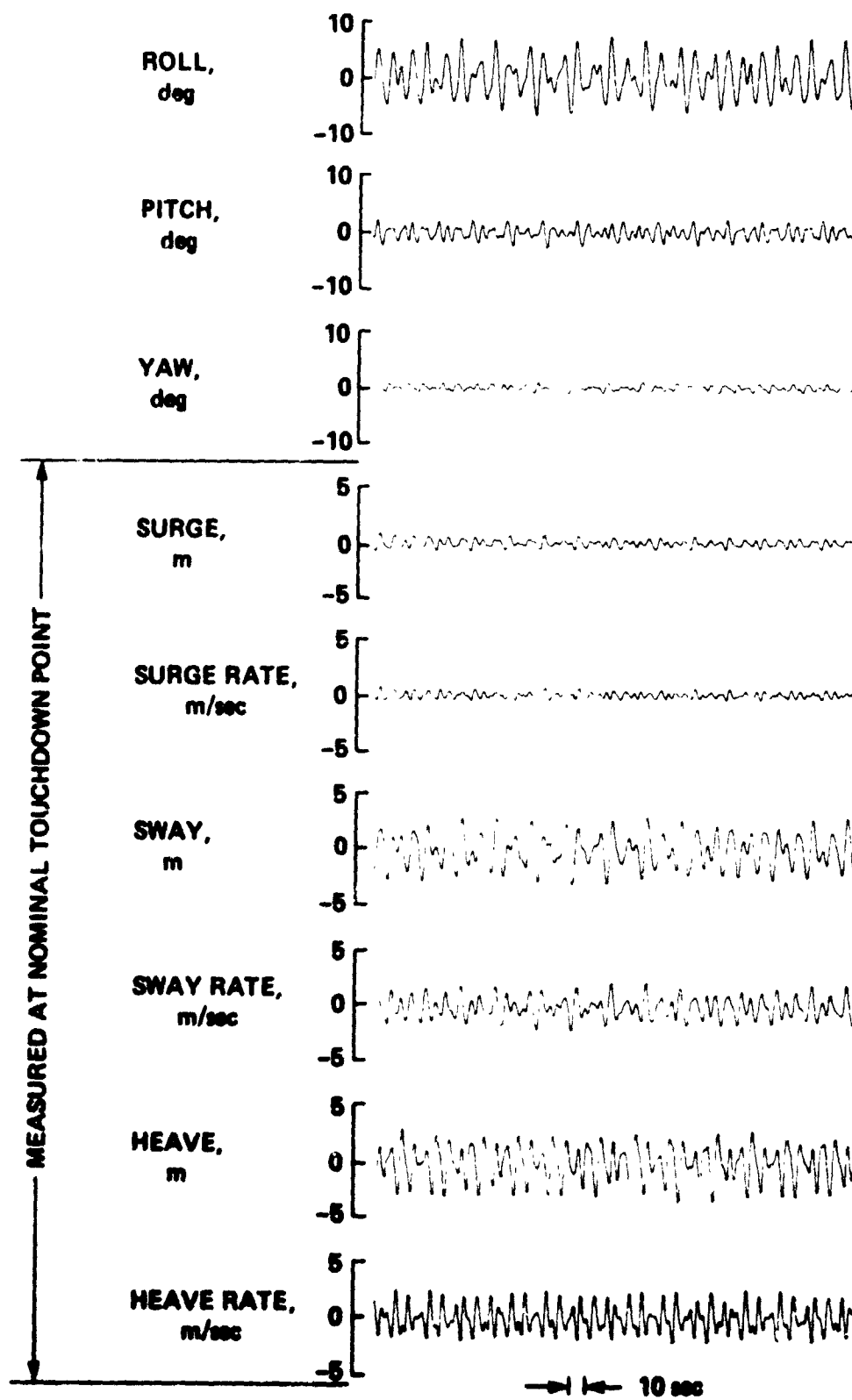


Figure 36.- Ship motion in sea state 6 (all degrees of freedom active).

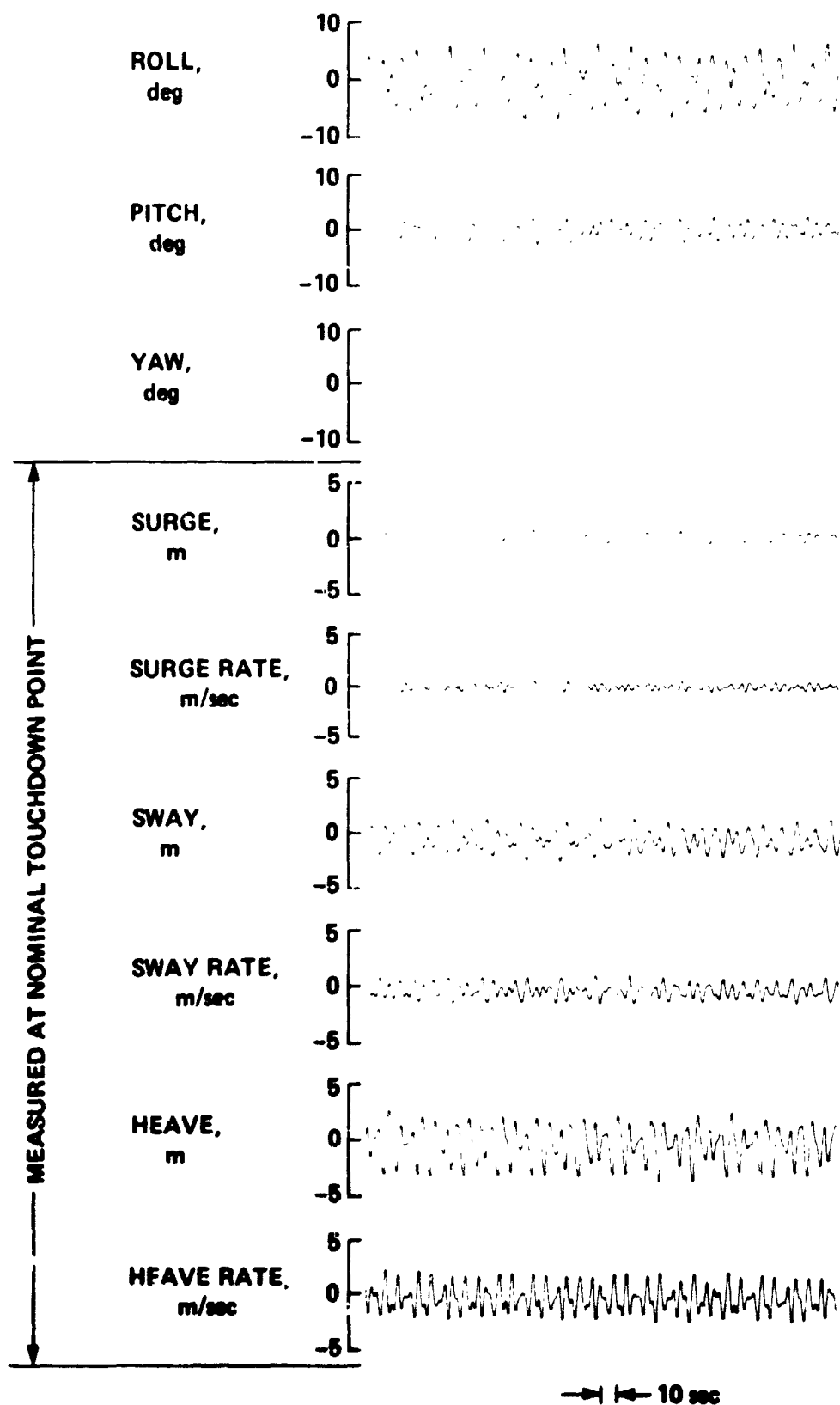


Figure 37.- Ship motion in sea state 6 (surge and sway degrees of freedom inactive).

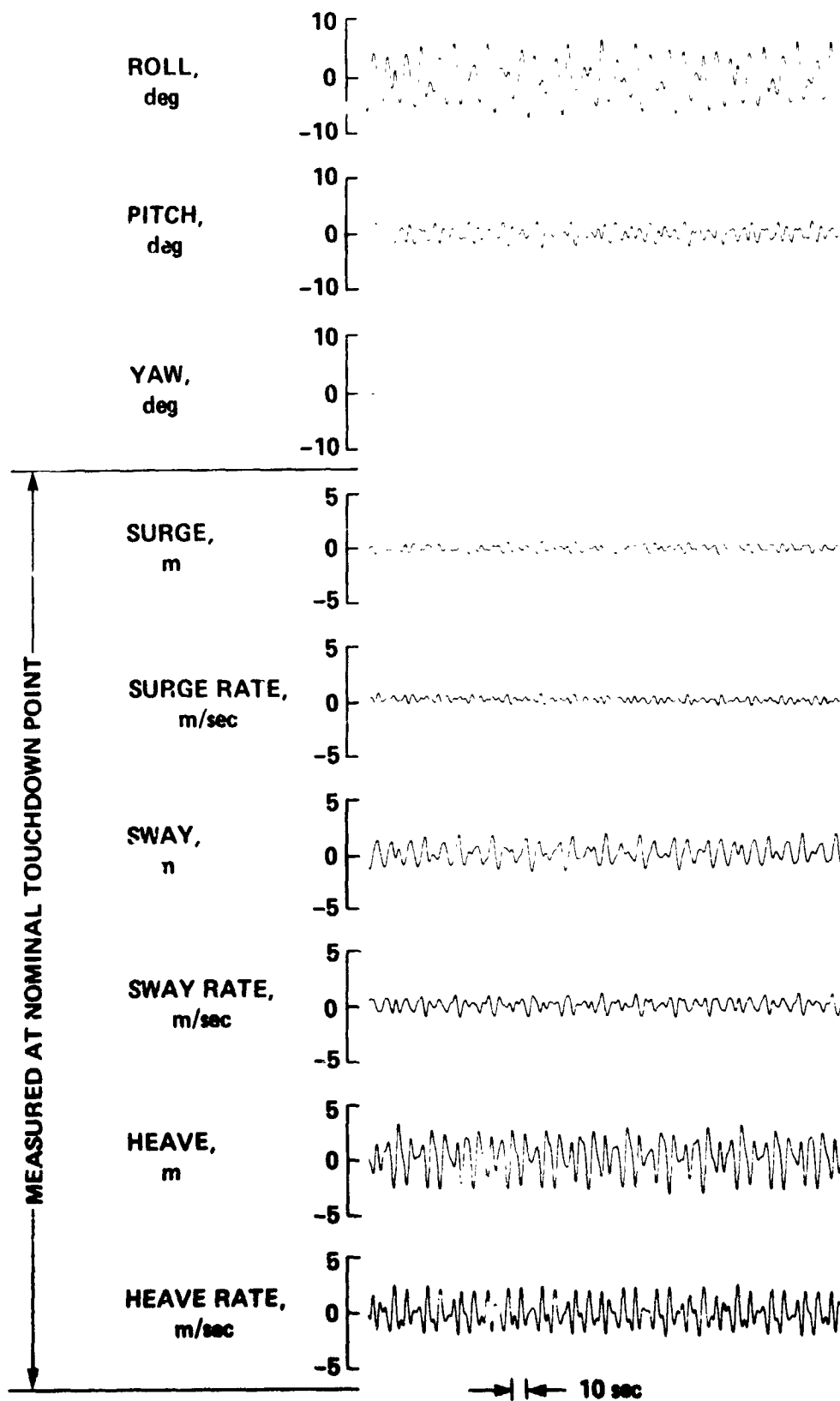


Figure 38.- Ship motion in sea state 6 (surge, sway, and yaw degrees of freedom inactive).

## Modeling Fidelity

A major deficiency in the models of the lift-fan transport and the AV-8A was the lack of ground effects on both the airframe and propulsion system. However, it should be recalled that the hover maneuvers took place 15 m (50 ft) above the deck and the WOD was never less than 15 knots. Under these conditions, ground effects would be expected to be significant only during the last stages of the final descent to touchdown. The results of reference 3 seem to support the conjecture that ground effects are minimal. However, ground effects are very configuration- and environment-dependent, and much more work is required before any general conclusion can be stated.

It was not possible to evaluate the fidelity of the lift-fan transport model, since the actual aircraft does not exist. But such a comparison could be made with the AV-8A. Several deficiencies of the basic AV-8A aircraft model were noted by the pilots. These included errors in stabilizer and thrust vector angle to trim, especially at speeds above 100 knots, and directional stability was excessive. But these kinds of errors are not too important in the type of tests reported here, since the basic airframe and propulsion characteristics are overwhelmed by the action of the flight controller. A more important problem, which was stressed by the pilots, was the lack of a jet pipe temperature (JPT) limiter in the propulsion system model. This device automatically reduces engine power to prevent excessive engine temperature and could have important implications during the final stages of descent, especially at high aircraft weights.

## CONCLUSIONS

Two control/display systems, differing in overall complexity but both designed expressly for VTOL approaches to and landings on ships in IMC were evaluated using Ames Research Center's FSAA. The Type 1 system had both an attitude-command and a translational-velocity-command control system; the Type 2 system had the Type 1 attitude-command system, but relied on direct pilot control of thrust and thrust vector angle for translation. The control systems were applied to existing models of a VTOL lift-fan transport and an AV-8A Harrier. The landings were made on a moving model of the DD963 destroyer. The principal conclusions from the simulation are as follows:

1. Acceptable transitions can be performed with an AV-8A with a Type 1 system in free-air turbulence up to at least 2.25 m/sec (7.4 ft/sec) rms.
2. Acceptable transitions can be performed with an AV-8A with a Type 2 system in free-air turbulence up to 1.5 m/sec (5 ft/sec) rms.
3. Acceptable landings can be performed with both the lift-fan transport and AV-8A, each with a Type 1 system, up to sea state 6. However, pilots preferred the lateral-velocity command feature of the lift-fan transport to the bank-angle command of the AV-8A for lateral positioning. The lateral-velocity command also reduced the time required to land by 20 sec.

4. The dynamic characteristics of the Type 1 system flight directors were acceptable.

5. The Type 2 system vertical, longitudinal, and hover flight directors exhibited dynamic deficiencies. The vertical flight director was too sensitive to turbulence and too insensitive to altitude errors. The longitudinal flight director could produce excessive velocity errors at the end of transition. The hover flight directors were overly sensitive to turbulence (ship air wake) and too insensitive to horizontal position errors.

6. Several deficiencies were noted in both the pilot controls and the HUD formats for both systems.

7. It was clear that the Type 1 system was at a higher state of development than the Type 2 system, and that further work on the control modes and flight directors of the Type 2 system could make its performance closer to that of the Type 1 system.

8. A visual scene with a more representative field of view could significantly ease the landing task, especially when using the Type 2 system in high sea states.



## APPENDIX A

### REFERENCE HOVER POINT EQUATIONS

After the pilot has completed the transition phase of the approach and is ready to start the hover-maneuvers phase, he presses a button on the stick; this is to alert the flight control/display computer that he is ready to begin the maneuvers phase. If the Type 2 system is being used, a translating reference hover point is activated and is used in the hover flight director. The equations defining the motion of the reference hover point are given below, in nondimensional form.

$$\bar{x}_h \text{ or } \bar{y}_h = \frac{\sin(2\pi\bar{t}_h)}{2\pi} - \bar{t}_h + 1 \quad (A1)$$

$$\bar{\dot{x}}_h \text{ or } \bar{\dot{y}}_h = \cos(2\pi\bar{t}_h) - 1 \quad (A2)$$

$$\bar{\ddot{x}}_h \text{ or } \bar{\ddot{y}}_h = -\sin(2\pi\bar{t}_h) \quad (A3)$$

where

- $t_h$             time from start of the hover maneuvers,  $t_h/t_{h_f}$
- $\bar{t}_h$             dimensionless time
- $t_{h_f}$           time to complete the reference hover point translation
- $x_h, y_h$       distances of the reference hover point from the final station-keeping point
- $\bar{x}_h, \bar{y}_h$       dimensionless distances of the reference hover point relative to the final station-keeping point,  $x_h/x_{h_1}, y_h/y_{h_1}$
- $\dot{x}_h, \dot{y}_h$       velocities of the reference hover point relative to the final station-keeping point
- $\bar{\dot{x}}_h, \bar{\dot{y}}_h$     dimensionless velocities of the reference hover point relative to the final station-keeping point,  $\dot{x}_h t_{h_f}/2x_{h_1}, \dot{y}_h t_{h_f}/2y_{h_1}$
- $\ddot{x}_h, \ddot{y}_h$     accelerations of the reference hover point relative to the final station-keeping point
- $\bar{\ddot{x}}_h, \bar{\ddot{y}}_h$    dimensionless accelerations of the reference hover point relative to the final station-keeping point,  $\ddot{x}_h t_{h_f}^2/2\pi x_{h_1}, \ddot{y}_h t_{h_f}^2/2\pi y_{h_1}$
- $x_{h_1}, y_{h_1}$    distances of the initial station-keeping point from the final station-keeping point

Graphs of equations (A1), (A2), and (A3) are shown in figure 39. It follows from equations (A2) and (A3) that the maximum total velocities and accelerations of the reference hover point are given by the following equations,

$$\text{max velocity} = \frac{2}{t_{hf}} \left( x_{hi}^2 + y_{hi}^2 \right)^{1/2} \quad (A4)$$

$$\text{max acceleration} = \frac{2\pi}{t_{hf}^2} \left( x_{hi}^2 + y_{hi}^2 \right)^{1/2} \quad (A5)$$

When the pilot has completed the hover-maneuvers phase and is ready to start the final descent phase, he presses the button on the stick once more to alert the flight control/display computer. If the Type 2 system is being used, a descending reference hover point is activated in the vertical flight director. The equations defining the motion of the hover point are given below in non-dimensional form.

when  $\bar{t}_d \leq 1$ :

$$\bar{h}_r = -\frac{\sin(\pi\bar{t}_d)}{2\pi} + \frac{\bar{t}_d^2}{2} + \bar{h}_h \quad (A6)$$

$$\dot{\bar{h}}_r = \frac{1 - \cos(\pi\bar{t}_d)}{2} \quad (A7)$$

$$\ddot{\bar{h}}_r = \sin(\pi\bar{t}_d) \quad (A8)$$

and when  $\bar{t}_d > 1$ :

$$\bar{h}_r = \bar{t}_d - \frac{1}{2} \quad (A9)$$

$$\dot{\bar{h}}_r = 1 \quad (A10)$$

$$\ddot{\bar{h}}_r = 0 \quad (A11)$$

where

$t_d$  time from the start of the final descent

$\bar{t}_d$  dimensionless time

$t_{df}$  time to reach the steady rate of descent

$h_h$  initial reference altitude

$\bar{h}_h$  dimensionless initial reference altitude,  $h_h/\dot{h}_r t_{df}$

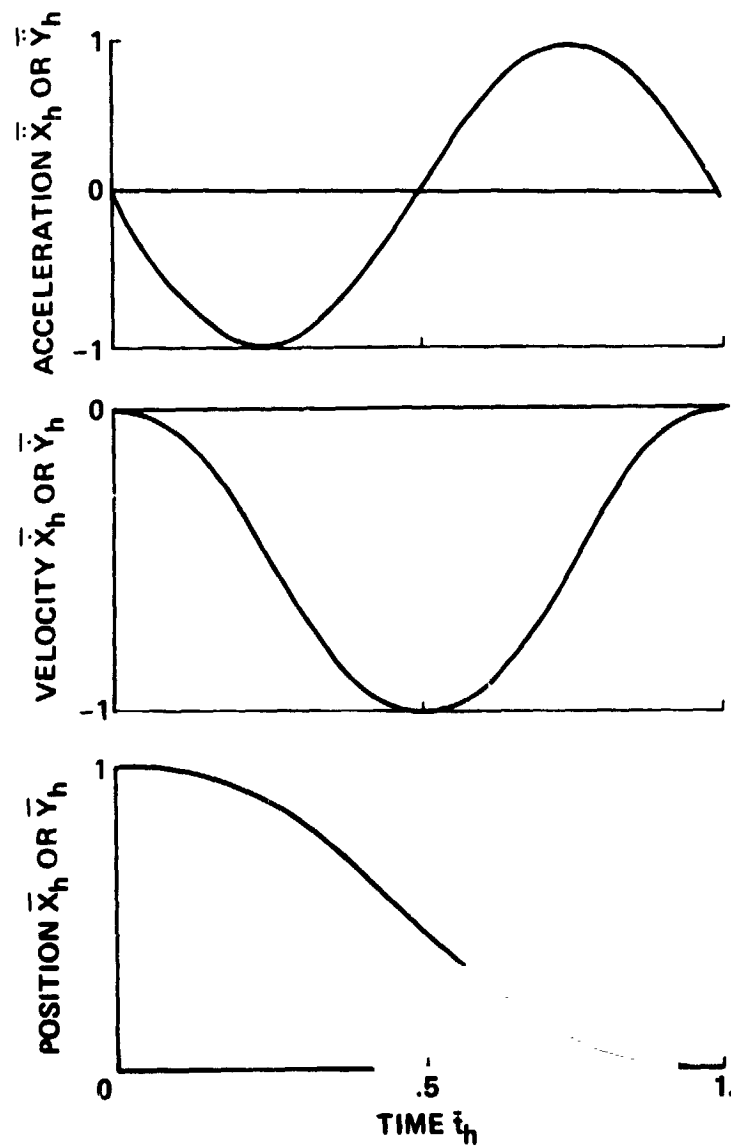


Figure 39.- Reference hover point kinematics in translation.

$h_r$  reference altitude

$\bar{h}_r$  dimensionless reference altitude,  $h_r/\dot{h}_{r_f} t_{d_f}$

$\dot{h}_r$  reference climb rate

$\bar{\dot{h}}_r$  dimensionless reference climb rate,  $\dot{h}_r/\dot{h}_{r_f}$

$\ddot{h}_r$  reference vertical acceleration

$\bar{\ddot{h}}_r$  dimensionless reference vertical acceleration,  $2\ddot{h}_r t_{d_f}/\pi \dot{h}_{r_f}$

$\dot{h}_{r_f}$  final steady-state climb rate

Graphs of equations (A6) to (A11) are shown in figure 40.

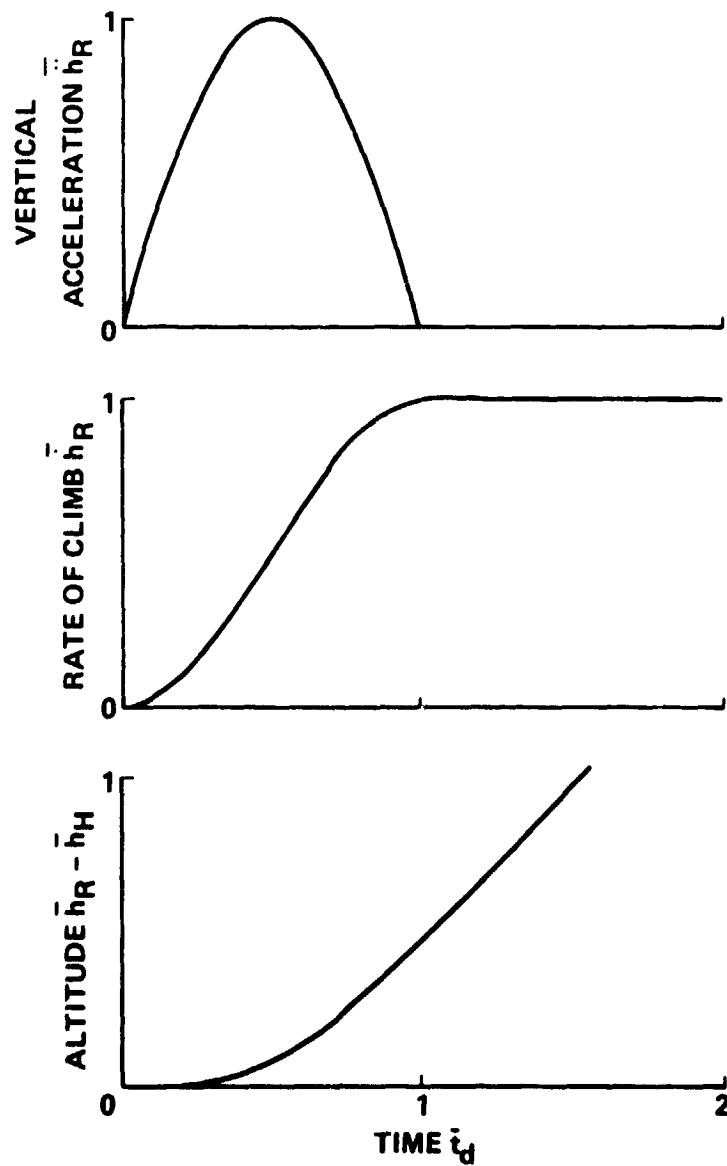


Figure 40.- Reference hover point kinematics in final descent.

## APPENDIX B

### AV-8A HARRIER CONTROL SYSTEM MODIFICATIONS

The advanced flight controller (Type 1), added to the AV-8A mathematical model of reference 6, is described in reference 1. It is assumed that with the advanced controller in operation, the pilot's stick and rudder pedals are detached from the existing AV-8A mechanical control system and are fitted with electrical transducers to provide the input signals to the advanced flight controller computer. The output from the advanced flight controller is used to drive the existing mechanical control system by means of suitable servo actuators. A schematic diagram of this arrangement is shown in figure 41 for pitch attitude control, and in figure 42 for vertical translation control. When the IQADVC switch in figure 41 is unity, the pitch-control system represents the basic AV-8A mechanical system. The IQDAMP switch activates the existing low-authority stability augmentation system. When the IQADVC switch is zero, pitch control (including trim) is through the advanced controller and is full authority. It should be noted from figure 41 that with the advanced controller in operation, both the front and rear reaction control jets are powered, the front jet being activated directly by the advanced controller servo through the existing mechanical linkage. Because of the high effectiveness of the advanced controller, the aircraft's overall dynamic characteristics (with IQADVC = 0) are independent of the ON/OFF status of the basic SAS. Roll and yaw control mechanizations are similar to those shown in figure 41; horizontal axis control (through thrust vector angle) is similar to that shown in figure 42. The flight controller logic for the attitude degrees of freedom is shown in figure 14 of reference 1; for the translational degrees of freedom it is shown in figure 15 of reference 1.

The numerical values of the flight controller parameters for the AV-8A are given in tables 8-12. These parameter values make the dynamic characteristics of the AV-8A similar to those of the lift-fan transport described in reference 1. The nomenclature used in tables 8-12 of this report corresponds to that of reference 1. Also, tables 8-10 (this report) correspond to tables 14-16 of appendix A in reference 1, and tables 11 and 12 (this report) correspond to tables 19 and 20 of appendix A in reference 1. Any parameters undefined in tables 8-12 (this report) have the values given in reference 1.

To create a more nearly linear relationship between the vertical controller output  $i_v$  and the engine thrust  $T_G$ , a nonlinear gearing was added (fig. 43). It is envisioned that the flight controller is coupled to the existing AV-8A control system by means of electric servo-actuators. Frequency response calculations show that the break frequency of the combined servo and mechanical control system elements exceeds 8 Hz. Such high-frequency dynamics cannot be represented with the 55-msec cycle time used for the simulation. The servo and mechanical control elements were, therefore, not represented.

TABLE 8.- PITCH-ATTITUDE CONTROLLER PARAMETERS

Parameter	Symbol	Value
Basic feedforward gain	$K_{100}$	21.07 rad/sec <sup>2</sup> -m (0.5352 rad/sec <sup>2</sup> -in.)
Controller feedforward gain	$K_{200}$	-6.41 rad/sec <sup>2</sup> -m (-0.1629 rad/sec <sup>2</sup> -in.)
Controller coupling gain	$K_{300}$	0.0475 sec <sup>2</sup> -m/rad (1.8685 sec <sup>2</sup> -in./rad)
Controller time constant	$\tau_g$	0.833 sec
Longitudinal stick dead band	$DB_{\delta_{I_\theta}}$	0.0013 m (0.05 in.)
Longitudinal stick upper limit	$LMU_{\delta_{I_\theta}}$	0.1905 m (7.5 in.)
Longitudinal stick lower limit	$LML_{\delta_{I_\theta}}$	-0.0953 m (-3.75 in.)
Controller upper coupling limit	$LMU_{\theta c}$	2.0872 rad/sec <sup>2</sup>
Controller lower coupling limit	$LML_{\theta c}$	-1.7661 rad/sec <sup>2</sup>

TABLE 9.- ROLL-ATTITUDE CONTROLLER PARAMETERS

Parameter	Symbol	Value
Basic feedforward gain	$K_1$	40.984 rad/sec <sup>2</sup> -m (1.0411 rad/sec <sup>2</sup> -in.)
Controller attitude feedforward gain	$K_2$	-11.890 rad/sec <sup>2</sup> -m (-0.302 rad/sec <sup>2</sup> -in.)
Controller rate feedforward gain	$K_3$	-14.548 rad/sec <sup>2</sup> -m (-0.3695 rad/sec <sup>2</sup> -in.)
Controller coupling gain	$K_4$	0.0244 sec <sup>2</sup> -m/rad (0.9605 sec <sup>2</sup> -in./rad)
Roll attitude hold stick integrator gain	$K_{\phi H}$	19.402 rad/sec <sup>3</sup> -m (0.4928 rad/sec <sup>3</sup> -in.)
Controller time constant	$\tau_\theta$	0.04 sec
Controller coupling limit	$LM_{\phi c}$	4.425 rad/sec <sup>2</sup>
Lateral stick dead band	$DB_{\delta_{I_\phi}}$	0.0013 m (0.05 in.)
Lateral stick limit	$LM_{\delta_{I_\phi}}$	0.1156 m (4.55 in.)

TABLE 10.- YAW-ATTITUDE CONTROLLER PARAMETERS

Parameter	Symbol	Value
Basic feedforward gain	$K_{10}$	15.542 rad/sec <sup>2</sup> -m (0.3948 rad/sec <sup>2</sup> -in.)
Controller rate feedforward gain	$K_{20}$	-47.37 rad/sec <sup>2</sup> -m (-1.203 rad/sec <sup>2</sup> -in.)
Controller coupling gain	$K_{30}$	0.0643 sec <sup>2</sup> -m/rad (2.533 sec <sup>2</sup> -in./rad)
Yaw rate feedback gain	$K_{\dot{\psi}}$	4.0 1/sec
Heading hold stick integrator gain	$K_{\psi H}$	13.087 rad/sec-m (0.3324 rad/sec-in.)
Controller time constant	$\tau_7$	0.05 sec
Rudder pedal integrator dead band	$DB_{\psi H}$	0
Rudder pedal dead band	$DB_{\delta I_{\psi}}$	0.0013 m (0.05 in.)
Rudder pedal limits	$LM_{\delta I_{\psi}}$	0.0838 m (3.3 in.)
Controller coupling limiter	$LM_{\psi c}$	0.8291 rad/sec

TABLE 11.- VERTICAL-AXIS CONTROLLER PARAMETERS

Parameter	Symbol	Value
Controller time constant	$\tau_w$	0.25 sec
Controller coupling gain	$K_{3w}$	-32.81 sec <sup>2</sup> -Z/m (-10.0 sec <sup>2</sup> -Z/ft)
Controller coupling upper limit	$LM_{VC_1}$	-0.116 m/sec <sup>2</sup> (-0.38 ft/sec <sup>2</sup> )
Controller coupling lower limit	$LM_{VC_2}$	-3.194 m/sec <sup>2</sup> (-10.48 ft/sec <sup>2</sup> )

TABLE 12.- HORIZONTAL (LONGITUDINAL) AXIS CONTROLLER PARAMETER

Parameter	Symbol	Value
Controller time constant	$\tau_u$	0.05 sec



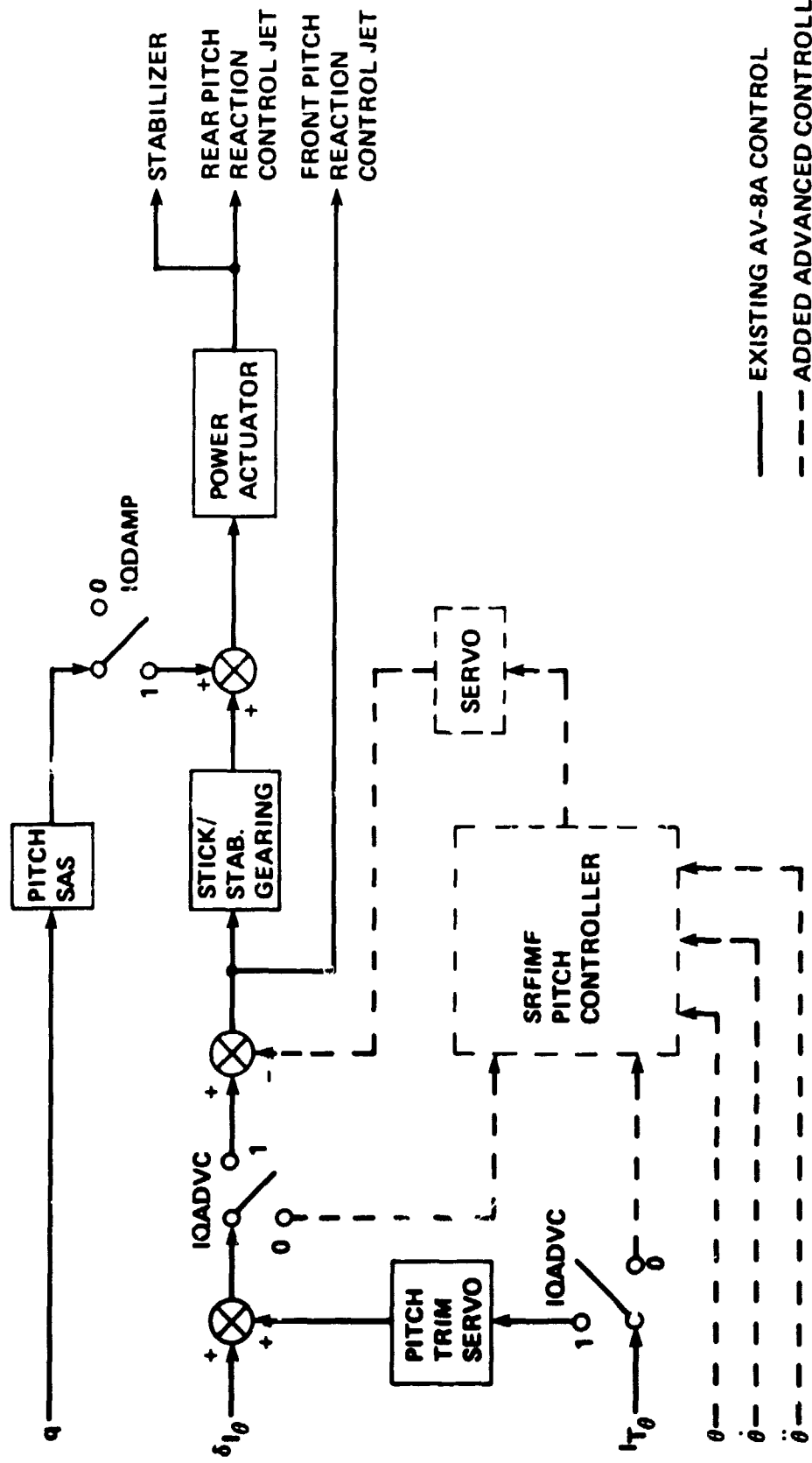


Figure 41.- AV-8A pitch control system with added advanced controller.

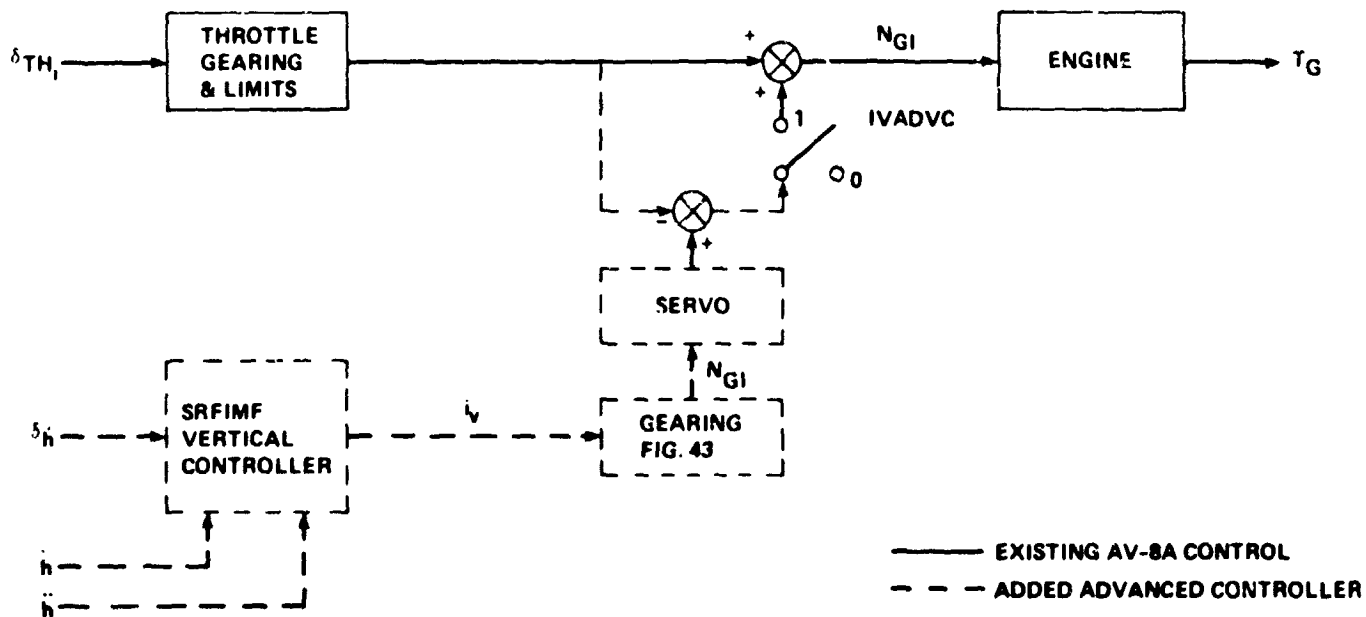


Figure 42.- AV-8A engine control system with added advanced vertical controller.

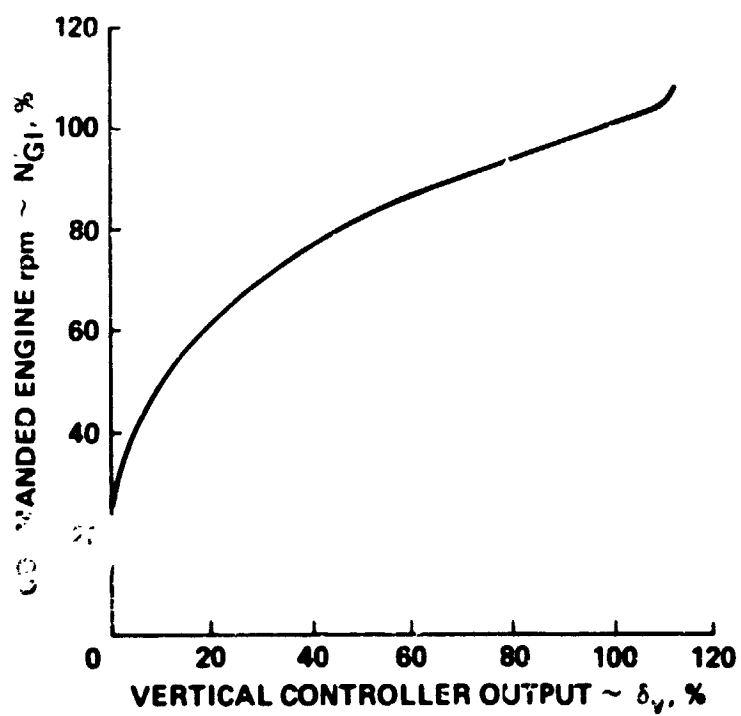


Figure 43.- Vertical flight controller gearing.

## APPENDIX C

### FSAA MOTION DRIVE LOGIC

The motion drive logic system given in figure 5.2.2-1 of reference 10 has been superseded. A block diagram of the logic used for the simulation described in this report is shown in figure 44. Values of the parameters shown in figure 44 are given in table 13.

Several of the washout gains and filter frequencies are functions of the aircraft's ground speed  $V_G$  (m/sec) and are governed by the equation

$$G_i = (GMX_i - GMN_i) \frac{(0.18 V_G - 15.24)}{45.72} - GMN_i$$

where  $i = 1, \dots, 2i$ , and the correspondence between the  $G_i$  and the washout parameters shown in figure 44 is given in table 13. The parameters  $A_p$ ,  $B_p$ ,  $C_p$ , and  $D_p$  of figure 44 are related to the parameters  $\omega_{1p}$ ,  $\omega_{2p}$ ,  $\omega_{3p}$ , and  $\zeta_{3p}$  of table 13 by the following equations:

$$A_p = \omega_{1p} \omega_{2p} \omega_{3p}^2$$

$$B_p = \omega_{3p} [\omega_{2p} (2\zeta_{3p} \omega_{1p} + \omega_{3p}) + \omega_{1p} \omega_{3p}]$$

$$C_p = 2\zeta_{3p} \omega_{3p} + \omega_{1p} + \omega_{2p}$$

$$D_p = \omega_{3p} [2\zeta_{3p} (\omega_{1p} + \omega_{2p}) + \omega_{3p}] + \omega_{1p} \omega_{2p}$$

with similar expressions in the  $q$  and  $r$  subscripts.

TABLE 13.- VALUES OF MOTION DRIVE PARAMETERS [see fig. 44]

Parameter	Value	Units
Gains		
$K_p$	$G_1$	—
$K_q$	$G_2$	—
$K_r$	$G_3$	—
$K_x$	$G_4$	—
$K_y$	$G_5$	—
$K_z$	$G_6$	—
$K_{NX}$	0	—
$K_{NY}$	1.0	—
$K_{NZ}$	1.0	—
$K_{HX}$	1.0	—
$K_{HY}$	1.0	—
$K_{HZ}$	1.0	—
$K_{XL}$	1.0	—
$K_{YL}$	1.0	—
$K_{AP}$	0.5	1/sec
$K_{AQ}$	0.5	1/sec
$K_{AR}$	0.5	1/sec
$K_{AX}$	0.2	1/sec
$K_{AY}$	0.1	1/sec
$K_{AZ}$	0.1	1/sec
$K_{FM}$	0.3048	m/ft
$K_{MF}$	3.2809	ft/m
$GMX_1, GMX_2, GMX_3$	0.5	—
$GMX_4$	0.1	—
$GMX_5$	0.5	—
$GMX_6$	0.1	—
$GMN_1, GMN_2, GMN_3$	0.8	—
$GMN_4$	0.3	—
$GMN_5$	0.8	—
$GMN_6$	0.1	—

TABLE 13.- CONTINUED

Parameter	Value	Units
Filter parameters		
$\omega_p$	$G_7$	rad/sec
$\omega_q$	$G_8$	
$\omega_r$	$G_9$	
$\omega_x$	$G_{10}$	
$\omega_y$	$G_{11}$	
$\omega_z$	$G_{12}$	
$\omega_{1p}$	$G_{13}$	
$\omega_{1q}$	$G_{14}$	
$\omega_{1r}$	$G_{15}$	
$\omega_{2p}$	$G_{16}$	
$\omega_{2q}$	$G_{17}$	
$\omega_{2r}$	$G_{18}$	
$\omega_{3p}$	$G_{19}$	
$\omega_{3q}$	$G_{20}$	
$\omega_{3r}$	$G_{21}$	
$\omega_{EX}$	0.2	
$\omega_{EY}$	0.05	
$\omega_{EZ}$	0.2	
$\omega_{E\phi}$	0.05	
$\omega_{E\theta}$	0.05	
$\omega_{E\psi}$	0.05	
$\zeta_p, \zeta_q, \zeta_r, \zeta_x, \zeta_y, \zeta_z$ $\zeta_{E\phi}, \zeta_{E\theta}, \zeta_{E\psi}, \zeta_{EX}, \zeta_{EY}, \zeta_{EZ}$ $\zeta_{3p}, \zeta_{3q}, \zeta_{3r}$	0.707	—
$GMX_7, GMX_8, GMX_9$	0.7	rad/sec
$GMX_{10}$	2.0	
$GMX_{11}$	0.7	
$GMX_{12}$	1.5	

TABLE 13.- CONCLUDED

Parameter	Value	Units
Filter parameters (continued)		
GMX <sub>13</sub> , GMX <sub>14</sub> , GMX <sub>15</sub>	4.0	rad/sec
GMX <sub>16</sub> , GMX <sub>17</sub> , GMX <sub>18</sub>	2.7	
GMX <sub>19</sub> , GMX <sub>20</sub> , GMX <sub>21</sub>	2.0	
GMN <sub>7</sub> , GMN <sub>8</sub> , GMN <sub>9</sub>	0.3	
GMN <sub>10</sub>	1.6	
GMN <sub>11</sub>	0.3	
GMN <sub>12</sub>	1.0	
GMN <sub>13</sub> , GMN <sub>14</sub> , GMN <sub>15</sub>	3.0	
GMN <sub>16</sub> , GMN <sub>17</sub> , GMN <sub>18</sub>	2.0	
GMN <sub>19</sub> , GMN <sub>20</sub> , GMN <sub>21</sub>	1.5	
Limits		
$\phi_{MAX}$	0.6283	rad
$\theta_{MAX}$	0.3141	rad
$\psi_{MAX}$	0.4189	rad
$X_{MAX}$	0.8534	m
$Y_{MAX}$	11.278	m
$Z_{MAX}$	1.189	m
$AL_{\phi}$	3.2	rad/sec <sup>2</sup>
$AL_{\theta}$	1.6	rad/sec <sup>2</sup>
$AL_{\psi}$	1.6	rad/sec <sup>2</sup>
$AL_X$	2.4384	m/sec <sup>2</sup>
$AL_Y$	2.0	m/sec <sup>2</sup>
$AL_Z$	3.3528	m/sec <sup>2</sup>
$\ddot{X}_{MAX}$	2.438	m/sec <sup>2</sup>
$\ddot{Y}_{MAX}$	2.7432	m/sec <sup>2</sup>
$\ddot{Z}_{MAX}$	3.3528	m/sec <sup>2</sup>

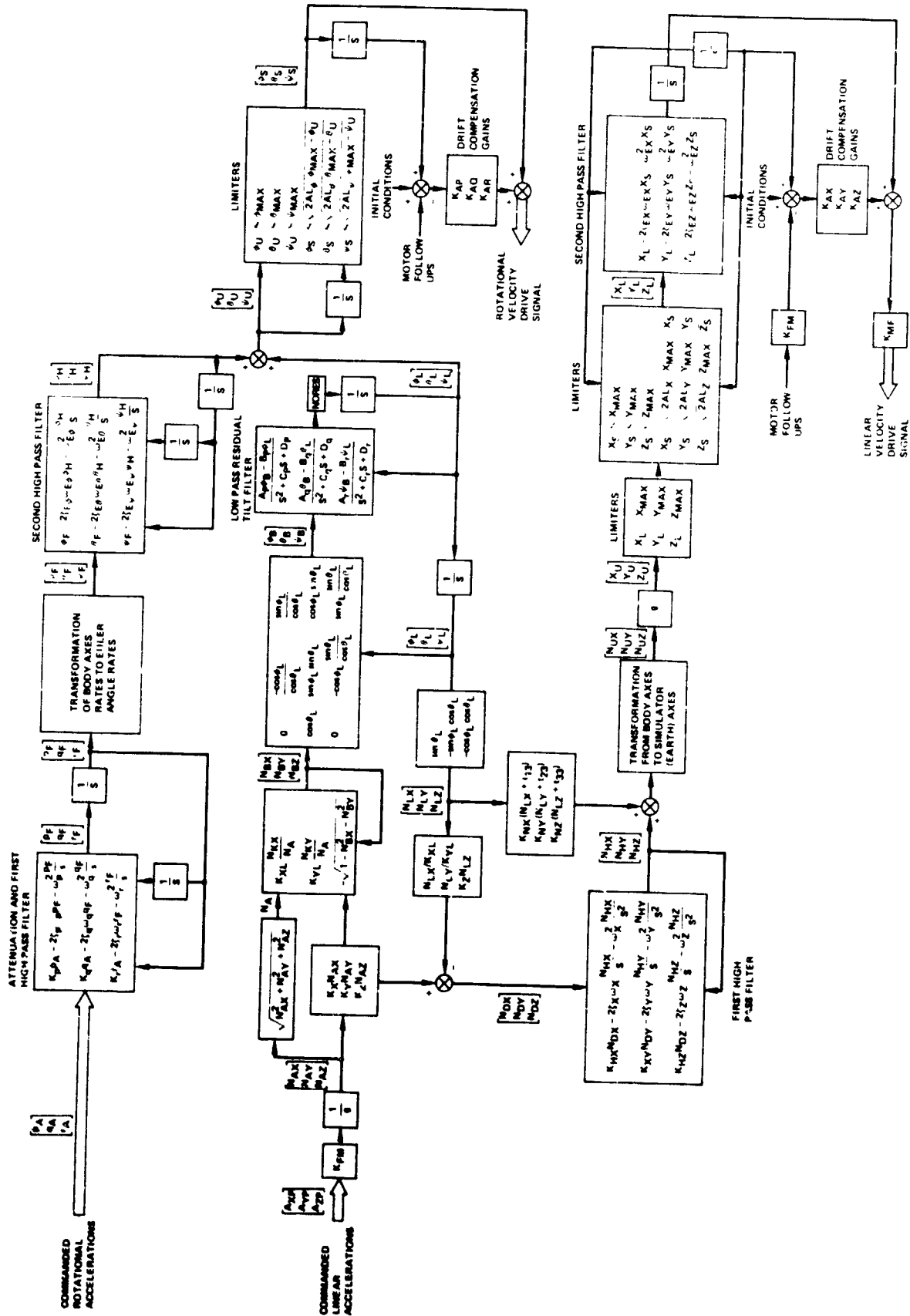


Figure 44.- FSA motion drive logic.



## REFERENCE

1. Merrick, V. K.: Study of the Application of an Implicit Model Following Flight Controller to Lift-Fan VTOL Aircraft. NASA TP-1040, 1977.
2. Merrick, V. K.; and Gerdes, R. M.: Design and Piloted Simulation of a VTOL Flight-Control System. Journal of Guidance and Control, vol. 1, no. 3, May-June 1978, pp. 209-216.
3. Stapleford, R. L. et al.: Flight Control/Flying Qualities Investigation for Lift/Cruise Fan V/STOL. COMNAVAIRDEVCON Report NADC-77143-30, vols. I, II, III, Aug. 1979.
4. Lebacqz, J. V.; and Aiken, E. W.: Experimental Investigation of Control/Display Requirements for VTOL Instrument Transition. Journal of Guidance and Control, vol. 1, July-Aug. 1978, pp. 261-268.
5. Lebacqz, J. V.; and Radford, R. C.: Experimental Investigation of Control-Display Requirements for a Jet-Lift-VTOL Aircraft. Journal of Guidance and Control, vol. 2, no. 6, Nov.-Dec. 1979, pp. 479-485.
6. Nave, R. L.: A Computerized VSTOL/Small Platform Landing Dynamics Investigation Model. NADC-77024-30, Sept. 1977.
7. Brown, R. G.; and Camaratta, F. A.: NAVAIRENGCEN Ship Motion Computer Program. NAEC MISC-903-8, 1978.
8. Fortenbaugh, R. L.: Progress in Mathematical Modeling of the Aircraft Operational Environment of DD 963 Class Ships. AIAA Paper 79-1677, Boulder, Colo., 1979.
9. Chalk, C. R. et al.: Background Information and User Guide for MIL-F-8785B (ASG) Military Specification Flying Qualities for Piloted Airplanes. AFFDL-TR-69-72, Aug. 1969.
10. Sinacori, J. B. et al.: Researchers Guide to the NASA Ames Flight Simulator for Advanced Aircraft (FSAA). NASA CR-2875, 1977.
11. Nicholas, O. P.; Bennett, P. J.; and Hall, J. R.: Simulation Study of Controls and Displays for VTOL Instrument Approach and Landing - NASA Ames, October, 1979. RAE Technical Memorandum FS 360, 1981.